UNIVERSITY OF SALERNO

Department of Civil Engineering

Ph.D.

in

"Risk and Sustainability in Civil Engineering, Construction and Environmental Systems"

XXX Cycle (2014-2017)

HIDDEN ARCHITECTURES. HISTORY AND DRAWING OF "UNSEEN" TOWERS IN THE PROVINCE OF SALERNO

Sara Morena

Tutor
Prof. Simona Talenti

Cotutor
Prof. Salvatore Barba

The Coordinators
Prof. Ciro Faella
Prof. Fernando Fraternali

Evaluators
Prof. Petros Patias
Prof. Elena Merino Gómez

To my grandparents

Index

ABSTRACT

The interest in the protection and conservation of Cultural Heritage and the growing role that it plays in the development of the national policies, represents a valid reason to focus the attention of the research in this field and transmitting the uniqueness and the identity of own territory is a first and fundamental step to guarantee its sustainability. Above all, in an era of globalization, cultural heritage helps us to remember our history and diversity, and its understanding develops the respect and the dialogue amongst different cultures.

However, despite our nation preserves lesser-known architectures of great value, often it pours into a state of abandonment and, in some case, is not even notorious by the majority of the community. The technological diffusion and the great improvement of digitalization, could positively contribute to broadening the tools of knowledge and favouring greater disclosure and accessibility. Hence, the purpose of my PhD doctoral thesis consists in the development of an innovative methodology of protection and conservation of architectural heritage. Through a multidisciplinary approach, that inextricably links the history and new technology in the field of surveying, the aim is the identification of original systems of cataloguing and archiving of data, useful for the interpretation of the built, as well as the generation of infographics models to analyse, preserve and divulge. The innovativeness of the following work consist in the implementation of low-cost technologies in order to mainly focus our attention on that vast little-known heritage; recognizing value to architectures often considered less important. The case studied will focus on the defensive system of the coastal towers of the province of Salerno, which has always been a territory rich in history and a crossroads of people and civilization; a good example on which to experiment with new digital methods for the representation and protection of cultural heritage.

A first part of the research, through a historical-architectural approach, is focused on the morphological and evolutionary knowledge of the coastal territory and of the defensive system through the analysis and the study of direct sources. The coastal towers, in fact, are representative of an architecture developed over time considering both the need to defend the city but also, and above all, the orographic characteristics of the place. In this case, it was necessary not only to study the individual buildings but also to focus attention on the strategies that underpinned this project, the "intangible" heritage part that is fundamental to fully understand the plan of defence. The second part of the thesis involves the use of new survey technologies useful both for the knowledge and conservation of the heritage. In the first case, in fact, a *virtual*

Figure 1: Rosselli F., Tavola Strozzi, (1472), National Museum of San Martino, Naples. (Russo F., 2009).

tour of the defensive system was reproduced to restore the network of gazes that once existed, guaranteeing iterative actions between a fortress and another, as well as enriching it with further historical and informative links. In the second case, while, it is a documental-engineering approach through the implementation of low-cost photogrammetry for the generation of data and three-dimensional models which having a certain scientific rigor; in order to estimate the reliability and accuracy of that obtained the *error theory* has been employed, already used for some time by the Drawing group of the Department of Civil Engineering of Salerno. Subsequently, the "predictive value of tests" has been involved to evaluate the probability of errors that can be made in the use of the method previously chosen for our verification.
Hence, through this work we want to illustrate an integrated framework for the protection and management of the building heritage, integrating to the historical documentary studies, a *virtual tour* and technical drawing useful for the divulgation of the information and a careful phase of architecture survey; presuppositions, these, fundamental for any type of intervention and knowledge of the built.
If historical events have often delete part of the past of this towers and the time has contributed to make events forget our history, the implementation of digital technologies will help to rediscover them and assured a new accessibility. In addition, the new survey methodologies represent a base to incentivize the understanding of its evolution over the time and the protection of own patrimony, eliminating the distances between the present and the past.
Cultural Heritage, as defined by UNESCO, is the legacy of physical artefacts and intangible attributes of a group or society that are inherited from past generations, maintained in the present and bestowed for the benefit of future generations. They are, therefore, fundamental elements for the study of human history and their preservation is essential to know as well as to draw people in and give them a literal way of touching the past.

ABSTRACT

L'attenzione manifestata oggi giorno nella protezione e nella conservazione del Cultural Heritage, così come il crescente ruolo che riveste nelle politiche di sviluppo di una nazione, rappresentano dei validi motivi per orientare la ricerca e investire maggiormente in tale campo.
Riconoscere e trasmettere l'unicità e l'identità del proprio territorio è il primo e fondamentale passo al fine di garantirne la sostenibilità. Soprattutto in un'era di globalizzazione, il patrimonio culturale ci aiuta a ricordare la nostra storia e la diversità e la sua comprensione accresce il rispetto e il dialogo tra culture differenti. Tuttavia, nonostante l'Italia conservi un patrimonio diffuso di grandissimo valore, spesso lo stesso versa in uno stato di abbandono e, in alcuni casi, risulta quasi o del tutto sconosciuto alla popolazione di quei luoghi. La diffusione tecnologica e il grande progresso della digitalizzazione potrebbero contribuire positivamente diffondendo adeguati strumenti di supporto per la conoscenza e favorendone, in tal modo, una loro maggiore accessibilità. Lo scopo di questa tesi di dottorato, quindi, consiste nel contribuire ulteriormente alla sperimentazione e sviluppo di una metodologia originale di protezione e conservazione del patrimonio architettonico. Attraverso un approccio multidisciplinare, che lega in modo inestricabile la storia e le nuove tecnologie nel campo del rilievo, l'obiettivo è l'identificazione di sistemi innovativi di catalogazione e archiviazione dei dati, utili per l'interpretazione del costruito, nonché la generazione di modelli infografici per analizzare, preservare e divulgare. L'aspetto più innovativo consiste nell'implementazione di tecnologie low-cost al fine di focalizzare l'attenzione principalmente su un vasto e poco conosciuto patrimonio storico, riconoscendo il giusto valore a quelle architetture spesso considerate minori. Il caso studio si concentrerà sul sistema difensivo delle torri costiere della provincia di Salerno, da sempre territorio ricco di storia e crocevia di popolazioni e civiltà; un valido esempio su cui sperimentare nuovi metodi digitali per la rappresentazione e lo studio del patrimonio culturale.
Quindi, una prima parte della ricerca, attraverso un approccio storico-architettonico, si centra sulla conoscenza morfologica ed evolutiva del territorio costiero e del sistema difensivo attraverso l'analisi e lo studio delle fonti dirette. Le torri costiere, infatti, sono rappresentative di un'architettura sviluppatasi nel tempo, considerando sia la necessità di difendere la città ma anche, e soprattutto, le caratteristiche orografiche del luogo. Pertanto, è stato necessario non solo studiare i singoli edifici ma anche focalizzare l'attenzione sulle strategie che sottendevano tale progetto, parte "intangibile" di un patrimonio che rappresenta uno degli aspetti fondamentali per

Figure 1: Rosselli F., Tavola Strozzi, (1472), Museo nazionale di San Martino, Napoli. (Russo F., 2009).

comprendere appieno questo sistema difensivo. La seconda parte della tesi ha previsto l'utilizzo di nuove tecnologie di rilievo utili sia per la conoscenza sia per la conservazione. Nel primo caso, infatti, è stato riprodotto un *virtual tour* del sistema difensivo al fine di ripristinarne la rete di sguardi un tempo esistente, garantendo azioni interattive tra una fortezza e l'altra, oltre ad arricchirla con ulteriori link di carattere storico e informativo. Nel secondo caso, invece, si è proceduto con un approccio di tipo documentale-ingegneristico attraverso l'implementazione di fotogrammetria low-cost per la generazione di dati e modelli tridimensionali caratterizzati da rigore scientifico; a tal fine, e per stimarne l'affidabilità e la precisione di quanto restituito, è stato sviluppato un innovativo ricorso alla teoria degli errori, nel solco del filone di ricerca trattato da tempo dal gruppo di Disegno del Dipartimento di Ingegneria Civile di Salerno. Successivamente, un "test dei valori predittivi" è stato applicato per valutare la probabilità di errori che possono essere commessi nell'uso del metodo oggetto di verifica.

Attraverso il progetto di tesi si propone un quadro integrato per la tutela e la gestione del patrimonio edilizio, corredando gli studi storici con un tour virtuale ed elaborati grafici utili sia per l'analisi più architettonica sia per la divulgazione delle informazioni: presupposti fondamentali per ogni tipo di intervento futuro e/o per la conoscenza del costruito.

Se gli eventi storici hanno spesso cancellato parte del passato di queste torri e il tempo ha contribuito a far dimenticare gli eventi della nostra storia, l'implementazione delle tecnologie digitali contribuirà a riscoprirle e ad assicurare una nuova 'accessibilità'. Inoltre, le nuove metodologie di rilievo rappresenteranno un presupposto fondamentale per comprendere le evoluzioni subite nel tempo e per la protezione del proprio patrimonio, minimizzando le distanze tra presente e passato.

Il Cultural Heritage, come definito dall'UNESCO, rappresenta l'eredità di beni materiali e immateriali di un gruppo o di una società tramandati dalle generazioni

passate, conservate nel presente e conferiti a beneficio delle generazioni future: gli elementi affrontati, quindi, risultano fondamentali per lo studio della storia umana e la loro salvaguardia, operazione essenziale per conoscere oltre che per affascinare le persone e dare loro la possibilità di toccare il passato.

Introduction

Overview

The multidisciplinary approach – historical and engineering – represents one of the fundamental aspect of my PhD thesis. The use of new technologies in the field of conservation of historical and architectural heritage, in fact, represents an important and fundamental step the analysis, conservation and dissemination of entire sites or a single building. In this context, one of the objectives of this research is to investigate new multimedia fruition techniques of archaeological and monumental heritage. The aim is to guarantee accessibility at any time and in any place to a wide range of heterogeneous information. In addition, the use of user-friendly interfaces for the consultation and management of data would increase the interest and knowledge of a growing number of people.
The study of the coastal towers of the province of Salerno requires an analysis that is not only punctual on the single building but interests the whole system. The intention is to restore and spread the plan strategies and visual connections between one tower and another; it is also interesting to enrich these connections with further historical or technical information of various kinds. To pursue this goal, it was assumed to test the technology of the *virtual tour*, in this way, in fact, it could be possible to navigate from one site to another and, through the various panoramic, to explore the place where the single tower is located. At the simple visualization of the place, you could add additional information panels to query, according to your needs, for the virtual visit. Only by operating in this way, it could be possible to understand and transmit the defensive strategy of the system, which is certainly one of the most interesting aspects of the plan.
Another technology, which we will use in this research, is the close-range photogrammetry, in particular, we will try to purpose our goal through the implementation of low-cost instruments. The generation of three-dimensional photogrammetric models would be the basis for further infographics representations such as the generation of BIM models to analyse and enrich with additional data the individual models of the towers, not only geometric and volumetric. The use of this new method of representation, in fact, would guarantee the realization of models

from which to extract various types of information. Beyond the structural and technical data, certainly fundamental for possible tower recovery interventions, these representations could also report data on the various addition that the building has undergone in order to make understandable the changes and evolutions over time. The validity of the realized three-dimensional model, finally, will be analysed with the *error theory*; in this way it will be possible to verify or not the strategy used and to understand the potentials offered today by these new technology. The idea is to ensure the generation of 3D models with not only visualization purposes but also will be the basis for extrapolation of measurements or further information for eventual future interventions of maintenance and recovery of the building.
The questions that arise are many and varied; nowadays the new survey techniques are efficient tools for the dissemination and conservation of cultural heritage, and in the last few year with the increasing capabilities of standard personal computers have ensured advanced technologies such as the possibility to view in real time via the internet of places of cultural interest; often adding multimedia content such as audio, text, video, etc. Beyond the purely visual communication of these sites, in the case in question, we are asked the question of how such innovative technologies, as in the case of the virtual tour, can be effective for transferring information that could hardly be transmitted with simple graphic representations - the network of looks of the towers for example - and what impact they can have in the dissemination of the cultural and territorial heritage that surrounds us.
The goal, then, is the possibility to codify a multidisciplinary approach that links the new technologies of architectural survey to so-called humanistic areas, ie social and anthropological studies, for a better knowledge, analysis, evolution and future enhancement of the territory. As repeatedly stressed, often, we overlook the importance of the lesser-known architecture of our heritage. The identification of a digital database would represent a powerful tool of protection and conservation to preserve and disseminate the archaeological-architectural assets, even those “minors”, to current and future generations.
A second aspect of the research, instead, has been directed to close-range photogrammetry, in particular to low-cost technologies. In this part of the thesis work, in fact we are asked about the possibilities - software and hardware - today on the market trying to estimate the accuracy achievable. As known, photogrammetric technology is an efficient tool to derive geometrical information from digital imagery in a fast and economic way. The derived models can provide the basis for real measurements as well as for the generation of virtual reality and/or BIM models enriched with important information that go beyond the simple morphological characteristics of the product.

The novelty of this research consists in the identification of an innovative verification technique for the validation of the results obtained; as previously anticipated, based on the *error theory*, already widely used in the survey field, a comparison was made between the different methodologies and technologies used. In a first application, we are based on the deviation of the available measurements (i.e. the x and y coordinates of 73 points identified on the different orthophotos obtained) with respect to the relative *average value*, estimating the *tolerance* and identifying which of the various applications was more accurate.
This comparison, subsequently, was further validated through the *predictive value of tests*, which is a nominal dichotomous qualitative type and is necessary to evaluate the quality of a comparison and not its amplitude. One of the first times that this type of test is transferred in the field of architectural survey with the aim of proving the criterion used for comparison and to guarantee with greater precision what has been analysed.
The uncertainty and possible inaccuracies that are committed in a check, in fact, do not always allow to obtain reliable results and certain reliability. Hence, the use of this test could be of great use to document and confirm the validity of the results, estimating the quality of the method used for comparing and calculating the percentage of errors (in probabilistic terms) possible in the implementation of a given methodology. An original three-dimensional comparison (thus evaluating also results of depth), finally, has been tested on three-dimensional models generated both by the different applications and by the various instruments.
The achievement of these objectives and the multidisciplinary nature of the thesis foresee an organization of it in two parts. The first, with an historical archival approach, is mainly developed in the first three chapters. In particular, the *Chapter 1* provides a brief analysis of how the defensive system has evolved over the time, with particular reference to the defence system of *Torreggiamento.* The chapter ends with the cataloguing of the towers located along the coast of the province of Salerno. *Chapter 2* focuses on the defensive strategies and, above all, on the network of "gazes" that existed between the towers of the plan. It includes the comparison between an ancient cartographic representation and the situation that exists today.
The visual connection, however, despite being one of the key aspect of the system, is at the same time one of the less known aspect, as well as one of the most difficult to transmit. In this regards the *Chapter 3* deals to analyse the generation of a virtual tour to highlight this characteristic. After an introduction to basic concept on 360° photogrammetry, in this unit, therefore, it is descripted the workflow: the instruments and the software used.
The second part of the thesis, while, concerns the possibility of making acquisitions and useful data for purpose not only of visualization but also has scientific utility. Hence, *Chapter 4* is an overview on the basic of photography. After an historical

review of this tool, the unit quickly describes the main elements and some tips in order to obtain a quality shoots.
Chapter 5, instead, discusses about the close range-photogrammetry. This includes the definition of some important coordinate systems and the indication about the orientation phase of the camera. In addition, there are two case studies to demonstrate the use of photogrammetry in the field of architecture and heritage conservation.
Chapter 6 is concerned with photogrammetric image acquisition for close range application and the software use to data processing.
Finally, in the *Chapter 7* comparison are made, with the use of *error theory*, in order to prove the accuracy of the data obtained. The results were then further validated with the *predictive value of tests.*

1. Coastal defence system of the province of Salerno

1.1 Brief historical background and main defence plans

Enchanting landscape and custodian of surprising naturalistic views, the Salerno coast, which extends from Positano to Sapri, has seen flourishing cities developed during its history. However, just its nature that characterizes and distinguishes it with briefly stretches of sea that are easily navigable and the presence of jagged coastline, has contributed to generate favourable conditions for attack by the enemy.[1]
The origin of piracy emerged along with navigation and it at the beginning was not so different from the merchant traffic. The problem began to emerge only after the formation of the first large States, because this practice undermined the safety of the territories, so the populations began to construct, already in Roman times, a series of towers located on the territory to monitor the coast. The situation ceased only when the Roman Empire surrounded the entire Mediterranean, destroying the enemy bases, re-established the social equilibriums. Around 500A.D. with the downfall of the Roman Empire, the endemic scourge of piracy returned. The hostility from the sea worsened around the middle of the VII century with the death of Mohammed

Figure 1.1: 18th century print of pirate raid. (Russo F., 2009)

Figure 1.2: A.L.R. Ducros, Ship being fitted out in Porto Carello, Castellamare, 1759. (Russo F., 2009)

that generated the sudden Islamic expansion and then the incursion from the Saracen enemies intensified more and more and the sea became a treacherous theatre of fight between the Christian and Muslims (Figure 1.1). Furthermore, pirate attack increased and became institutionalized, around the XVI century, with the name *Privateering*, a practice that will run rampant for the next three centuries. The gravity of the situation inevitably involved the planning of adequate signal system (sound of the bells or warnings of fire and smoke visible to sailors along the coast) and defence plans; however, at the beginning only punctual towers were built with alarm function and in the inhabited areas. It was only in the Angevin era, around the end of XIII century, that it is possible to speak of the first defensive plan with the building of a chain of cylindrical towers for anticorsair sighting and signalling, but always along limited section of maritime frontier. [2] During this era, moreover, there was the spread of firearms that allowed coastal defence to improve, thanks to the new cannons of French conception. In fact, these weapons allowed them to do something that had been so far impossible like repel the enemy before they landed.[3]

This kind of cannons, very slim and relatively light that could be moved on specific mountings and capable of firing balls of iron, therefore influenced the construction of the new buildings. During this period a small fleet was also launched that should contributed, together with the tower system, to the guard of the cost (Figure 1.2).

And so between victories and defeats thanks to this first and simple system of zonal alarm the time passes with the illusion that the Islamic momentum may have been contained within stable limitations.

1.1.1 Defence system *Torreggiamento*

On 29 May 1453, the Turkish artillery crossed the walls of Constantinople; it was the confirmation of the new Turkish threat also in the Western world, long underestimated (Figure 1.3). This danger also afflicted the Kingdom of Naples, at that time under the Aragon dynasty, and it is the reason why the previous defensive system was increased further by building new towers and incorporating some of those already existing adapting to new needs and in particular to new defence techniques, it was called *Torreggiamento*[4]. For the defence of the coast during the second half of the XV century Alfonso of Aragon taxed the *university*[5] for the arming of the galleys and, also, entrusted the surveillance and defence to the garrisons of the towers as well as to improve groups of citizens. It must be specified that the towers were always under the control of the crown and it was forbidden to possess them, even if in the history there were some attempts by the nobles.[6] On 6 January 1492 the Aragon family conquered Granada, the last Muslim stronghold in Spain, but

Figure 1.3: View of Constantinople, XVII century print. (Russo F., 2009)

despite this event the Moor were still a concern to the crown. The excessive exposure of the coastal sites became a nightmare for them, for this reason the attempt by Spain to remove the North-African coast from Muslim domination was born.
In the XVI the coast of Salerno had large stretch of coastline without towers and also with the absence of adequate Spanish military presence along the coast to avoid looting by enemy ships. Tragic episodes happen in different areas of Cilento, memorable was the sack of the fortified city of Policastro in the 1532.[7] In the 1528, in addition, the corsairs had the support from the French, because the latter was in war against the Spanish crown, making the situation more fearful. While the Spanish army fought against the French army in the centre of Europe, along the Mediterranean coast rage the Turkish fleet. From this moment, therefore, the universities had the deliberation to organize the defence of their territory, also building fortifications and towers at their own expense.[8]
Recapping, at the beginning of the XVI century, despite the presence of some towers located on the coasts, the Salerno territory was without an efficient sighting system. The necessary control was not guaranteed and there was not a real communication between the buildings in order to have a global vision of the whole territory.
On 4 September 1532, with a series of pragmatics, the settlement plan began. One of the main objectives of the project was the possibility of hindering the approaching ships, before that they landed. However, for the extension of the southern coasts and the unavoidable economic difficulties, the first sighting places were also situated in

Figure 1.4: Tiziano Vecelli, Pedro Álvarez de Toledo, Viceroy of Naples, 1540. Neue Pinakothek, Monk

Figure 1.5: Ribalta Francisco, Don Para Arafan de Ribera, 1616

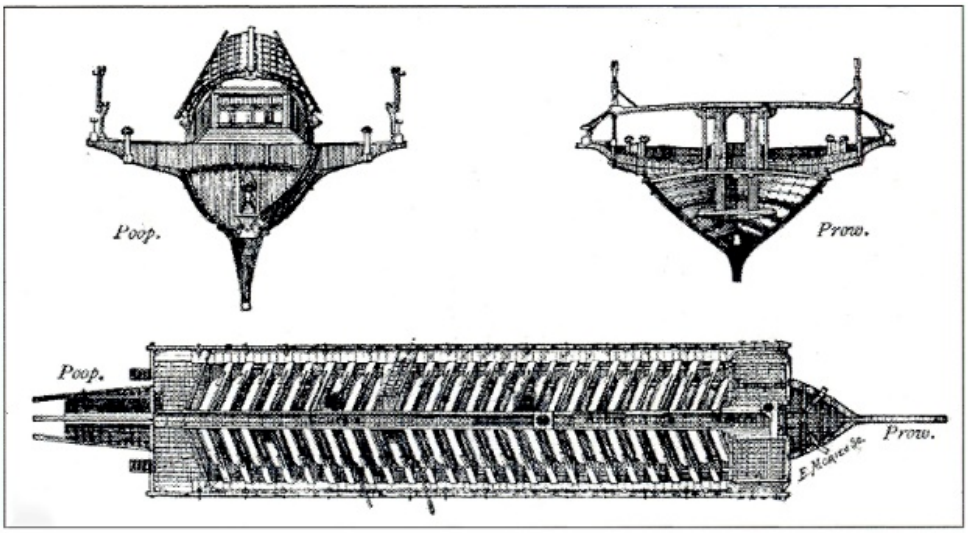

Figure 1.6: Orthogonal drawings of galley. (Russo F., 2009)

old fortresses or simple promontories. The absence of an adequate Spanish naval military presence and the need to defend themselves from enemies' attacks led the viceroy Don Pedro de Toledo (Figure 1.4) to design a well-planned barrier system along the coast of the Kingdom. [9]

The first ordinances sent by the viceroy foresaw that directly the universities taken care of the realization of adequate fortifications along their coasts. Nevertheless, the economic impossibilities of them, made the complete implementation of the plan impossible, the intentions of the ruler were clear but not the identification of the lenders.[10] It was decided, therefore, to build the towers only near the most exposed areas, in order that visibility between each other was sure. In any case, the looting continued probably also due to considerable defensive deficits at sea; once again a problem of the State of not being able to sustain the expenses necessary for the maintenance of the numerous warships (Figure 1.6). During these years, the coastal cities suffered several attacks that caused the loss of many human lives, in addition to the destruction due to the devastating looting of urban areas.

On 22 February 1553, Don Pedro de Toledo died and the realization of the defence system was entrusted to successor Don Parafan de Ribera (Figure 1.5). Among the reason that led to a rapid implementation of the defensive system there is the scary looting on the night of 13 June 1558 an Massalubrense and Sorrento, where about 5000 inhabitants were deported. Another assault, instead, took place on the night of 28 May 1563 when hundreds of barbarians landed in Naples, a few hundred meters from the palace of Viceroy Pedro Afan de Ribera. Although in this case there were

not so many prisoners, the attack debunked the myth of city immune to any assault, especially because it happened near the royal residence, endangering the life of the official government. It should not be surprising, therefore, that after only a few weeks the realization of the towers of the Kingdom had begun, favoured by a project hypothesis already completed for some time and ready to be put into operation.
Viceroy entrusted the realization of the plan directly to his technicians and to the administration, but at the payments had to provide for the individual universities. The enormous orographic variety of the territory entailed a careful study of characteristics of the site before proceeding with the construction of the building, so that a specific technical service of engineers was established. Their tasks were about not only the planning but also the direction of the works and the maintenance of the same. The construction of the towers involved a careful study both of geology of the place but also the type of towers to be built in relation to the type of defence to be guaranteed and the type of artillery to be supported. As reported by Russo[11] in each critical point of the coast the officer proffered his opinion on the vulnerability of the sea, the artilleryman on the calibre of the weapons require, the engineer the size of the tower in relation to the weapons and the contractor the relative cost. The whole were compiled on cards, which reported information about architectural drawing of the tower and a topography reference as well as the estimated cost. The last step was the executive project during which checks were carried out to verify what had been done (Figure 1.7 and 1.8). After about six years the coastal defence system was active even if it was never really completed, but despite the less number of towers compared to the planned ones, it was possible to monitor the entire coastal perimeter. In the most hostile stretches, when the visual connection was much more difficult, the passing of information was guaranteed by horsemen, called *cavallari.* According to

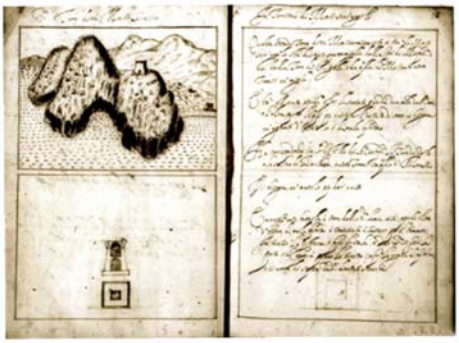

Figure 1.7: Survey of the Torre Monte Sant'Angelo by Gambacorta around the end of 1500s. (Russo F., 2009)

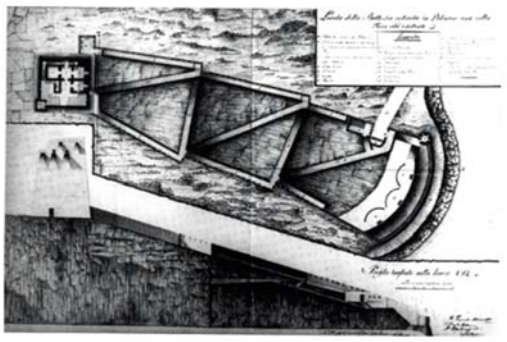

Figure 1.8: Plan of the battery constructed behind the Torre di Palinuro. (Russo F., 2009)

Pasanini[12] in the 1590 the number of the towers were 339, not enough to ensure planned coast coverage,[13] which of 111 along the coast of the Principality of Citra.
One of the main problem was for the armaments of the towers above all for the few specialized factories in the area and, consequently, at the economic difficulties and the high taxes paid by the population. Another difficulty was the staff to be assigned to the towers; in fact, the men required a minimum of military training, such as handling guns and gunpowder, but also knowing how to read and write, and above all, it had to be of absolute loyalty to the empire.
This happened because during the period of viceroyal the Spanish treasuries were used to finance the war and to support other objectives of the crown, in this state, therefore, less attention was given to the defence on the sea.

1.2 Construction and building materials of the towers

During the executive project of the defensive system in viceroyal era was used a basic module of tower that incorporated the principal requirements of solidity, flexibility of use and economy; from this standard archetype lend to a several variants in relation with the territorial characteristic. Several factors, in fact, condition dimension and high of the tower in order to ensure the visual connection, the resistance to attack and the position near the sea or in some particular ground.
Mainly are distinguishable two types of traditional planimetries for the costal towers: circular and square. Usually, the round tower is typically of the Angevin period (XII century); although, this rigid schematization has led to some problems in the dating of the towers for which the date of realization did not coincide with the morphology of the towers.[14] According to directive of the 1563 by the governor of the Principality of Citra, in fact, were realized seven circular towers from Salerno to Agropoli, they

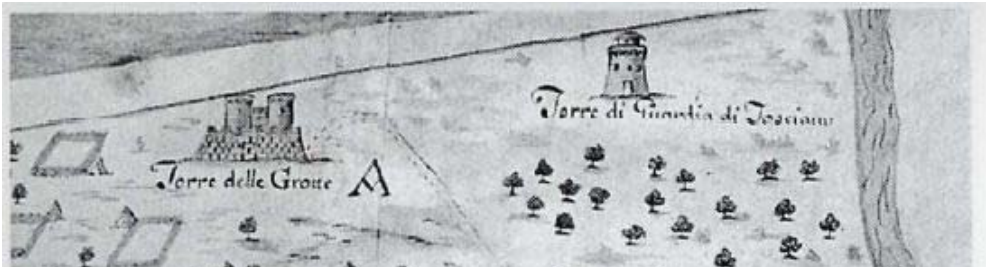

Figure 1.9: Particular of the Platea of the 1722, the Torre di Guardia di Tusciano. (Mastrolonardo, 1995)

had to have a square with 12 handbreadths[15], even if the tower near the river mouth Sele is 20 handbreadths [16]. Of this circular type are still visible along the coast of Province of Salerno the following towers: *Picentina* (Salerno), *Tusciano* (Battipaglia), *Sele* and *Paestum* (Capaccio), *San Marco* (Agropoli).

The advantages of this typology was not only easier and cheaper construction but also had greater resistance to environmental and warfare offences. Its shape is certainly related to the artillery of the time, it was able to deviate al lot of shots without extensive damage. However, the absence of any predetermined direction it was not suitable for the installation of the cannons, also because initially it was not designed to this finality.

Subsequently, with the evolution of the artillery, also changed the building characteristics of the towers. Initially it was proceeded to reinforce existing ones, but subsequently it was necessary to redesign the whole structure of the towers according to the new requirements. The square plan, in fact, was the only one that would allow for a battery of several cannons, but related to the previous one needs superior constructive skills and costs. Some authors like Pasanisi and Cisternino[17] presume that the choice of aforementioned square plan was also done to give shelter at the population. Generally, the first towers to be erected were those with larger dimensions. Some instruction specified that they had to have large wall thicknesses and a square not less than 24 handbreadths and foundation and parapet of 8 handbreadths.[18]

These towers, moreover, had inclined walls probably for two different reasons; statics and bellicose. The geometric characteristics, in fact, improve the towers resistance above all decreasing the unit pressure of the structure on the ground by enlarging their base. In addition, this solution increased the neutralization of the thrust by artillery fire; their performance was not so different from that of the buttresses. Furthermore, the escarpment of viveroyal towers, maybe to intensify their vantages, was extended to the entire height giving them an unmistakable pyramid-

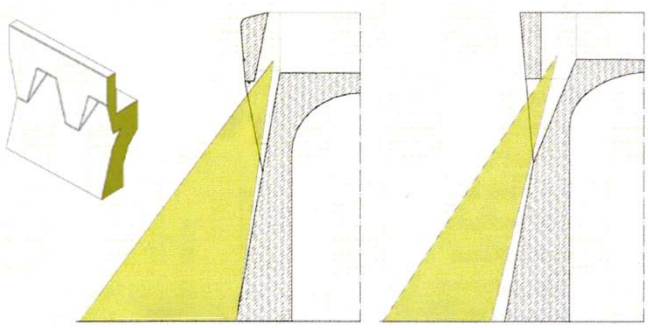

Figure 1.10: Different typologies of embrasures. (Bixio A. 2008)

trunk shape and great solidity. The second reason, while, was the need to keep any attackers away from the towers base in order that they were more easily in the target area of their weapons (Figure 1.10). Important was also the orientation of each tower that was placed in function of edges, which are the areas where it was not possible to attack the enemies.
Defending this weak points was difficult, which is why at the top of the walls of the towers were decided to superimpose a protruding structure, the embrasures. Along the perimeter of the crowning, were also holes that guaranteed protection to the defenders and, at the same time, the possibility to attack the enemies. This battlements over time became a symbolic elements of the fortifications, so much so that they were often used only for decorative purposes.[19]
Moreover, besides the role of defence all the towers carried out the task of sight, there were two methods: *direct* and *indirect*. In the first case, the alert was given directly to the population in the same instant in which the suspicious vessel was seen. In the second case, while, it was a message transmitted from one tower to another, also guaranteeing noteworthy warnings. Furthermore, the type of signalling could be *optics* and *acoustics*. The first consisted of smoke signals at daytime and fire at night; this mode, however, was used only by tower to tower and not directly for citizens. The direct warning, while, took place in acoustic mode through the rumbling of the petrary.

1.2.1 Towers interiors

Usually, the interiors were very simple and were developed on two large spaces covered with vaults organized orthogonal to each other in order to give more compactness to the building and better resist to the stresses due to shooting. In this way, in fact, the loads acting on the structure were spread out uniformly onto all the four walls. The type of vault most used in the tower with square plan was the barrel one, but no shortage of exception like towers of *Vettica* in Amalfi or *Chitamonte* in Vietri where the last level was covered with a pavilion vault cut with a horizontal plane. In the tower with circular plan, while, often there was a dome placed onto some pendentives.
The ground floor, most of the time, had the only function of cistern for collecting rainwater, while, the upper floors was used respectively as soldiers' billet and magazine. Usually, the second level was accessible only from an external staircase and in relation to the size of the tower, it was divided in two or more rooms and often with the presence of a chimney. The last level, instead, was used as food or

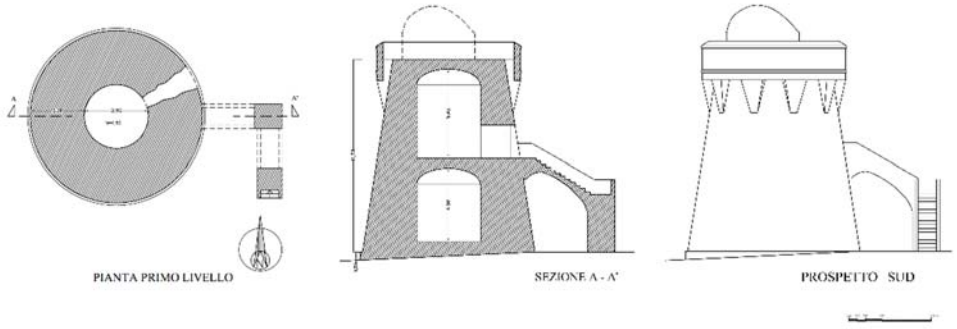

Figure 1.11: Survey of the Torre di Paestum by Superintendence

ammunition depot and was connected with the previous floor and the upper square through an inner staircase built in the thickness of the wall. This is the typical interior organization, although, as always happens, there were some exceptions like the *Torre Mingardo* in Cemerota and *Torre di Cetara* that had three floors.
On the roof plan of the tower, there was the square where the artillery pieces were arranged; the numbers of cannons were various in relation with the size of the space. It was delimited by a protruding parapet respect with the walls underlying and with holes along its perimeter in order to use the weapons. On the side of the mountain, in addition, often was located the *bartizans*, that is the room for the territory guard.

1.2.2 The walls

The category of building of the towers, as easily deductible, was the load bearing masonry and the thickness changed varied with the variation of the kind of tower. The round ones erected during the XVI century and surveyed in the province of Salerno, usually had values around 3,5m (Figure 1.11). In the case of the towers with square plan, while, the thickness were greater; from a minimum of 2,5m to a maximum of 4,5m like in the case of the towers of *Vietri* or *Angellara* in Salerno.
In addition, different wall sizes also depended on the role assigned to the tower. The watchtowers are higher but had thin walls because they must guarantee only the visual connection and rarely were subjected to assaults for their position. Differently was the case of the defensive towers, more easily subject to clashes with enemies. To resist such attacks the external walls were realised with large stones and above all a good mortar.

The masonries were constructed with local stone; so in the Amalfi coast were used the limestones type, while in the Cilento above all the sandstone. Particular attention was given in some part of the building; in fact the external walls were realized with smooth stones and, in the corner, they were larger, while, in the interior part of the building the walls were less refined.
Moreover, usually, the rows of stones were larger in size at the base and were decreasing in size towards the higher parts, finally the two facades were unit with a mixture of brick or cut stone and mortar. As was usual at the time, every three or four courses of stones, about 70cm, the masonry was levelled with a layer of mortar, usually of 2,5cm thickness.[20] In addition, in some cases it is possible to see the presence of holes arranged horizontally on the wall, they were used during the construction phase to support the scaffoldings, but they are not always visible due to the presence of the plaster. Despite a series of orders about the good building practices, several were the problems encountered in the time, above all the economic restrictions that entail fallacious choices during the execution phase. Among these certainly the use of rounded shape river pebbles or use of poor quality mortars, that many times caused the collapse of the building (Figure 1.12). The most common inconvenience was the use of seawater or improper aggregate in the mixture.

Figure 1.12: Torre Caleo, it is possible to see the use of larger stones at the base and the presence of rounded shape river

1.3 The main operational functions

The viceroyal towers performed various kind of functions in order to actively defend the coast and the sea. Mainly they were: *offensive*, *defensive*, *sighting* and *lodging*. It is easy to understand that in general, the towers performed more than one task at the same time, but some of them prevailed over others in a tower.
Offensive function. This task was intrinsic to the installation of cannons which number and calibre varied according to the size of the tower. The arrangement of the armaments of the tower was designed simultaneously with that of the building; consequently, it also influenced the orientation of the fortress with respect to the sea. On a square platform, in fact for reasons of static, in the corner the weapons could not fire, it was possible only in perpendicular direction of the walls. Therefore, the range of the cannons was not able to cover the whole area, but there were dead parts in correspondence with the corners. For these reason, this sector were made to coincide with those areas of the coast where there were less possibility of attacks. As visible in the figure 1.13 the direction of the tower along a littoral without any inlets was one side facing the sea, two toward the coast and the last with the entrance toward the rear (the same disposition was used for the tower on the promontories). In the case, instead, of buildings that were on inlets or small ports, they are placed with the corner directed toward the sea.
Other structural elements that identified the offensive aspect of the towers were the presence of a reserve of ammunition near the weapons and a small storage area (like a small bartizan) placed in the corner, on the ground of the building, to limit damage if it collapse in case of explosion.

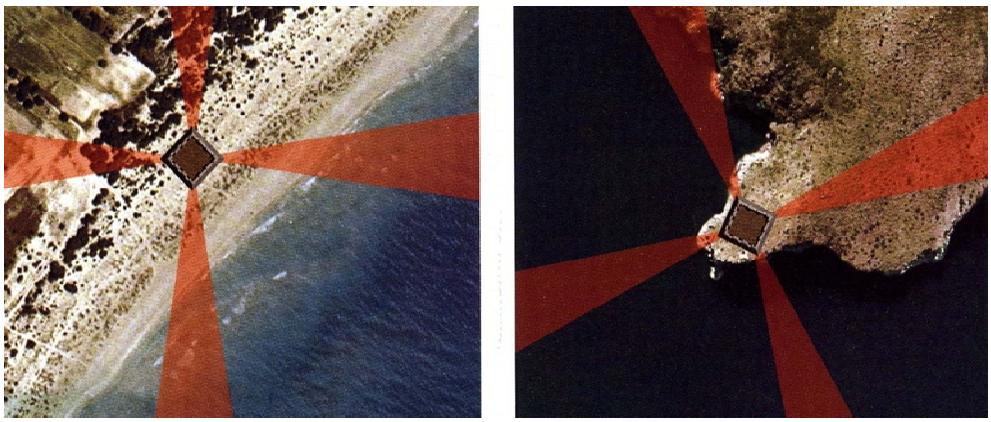

Figure 1.13: Orientation of the towers, the side is perpendicular to the sea on the flat beach and with a corner facing the sea on the cliff. (Russo F., 2009)

Defensive function. Function performed by all the buildings of the system through some architectural expedient. In fact, the inviolability of the tower was possible placing its only access on the upper levels, generally not lesser to 6m above ground and reachable through the use of a retractable stair or with a small drawbridge (in the case of fixed ramp). Another important and visible aspect were the typical and characteristic *buttafochi* (as called in the specification of the 1570) or *gettarole di fuoco.*

They are different from the medieval *canditoie* because the latter were used to hurl stones or fire downward, but in this case it was impracticable because of the inclination of the walls. Generally, they were dissimilar in each towers, and as the square became larger, it required a great number of embrasure to cover the entire perimeters.

Sighting and signal function. Different from the previous ones, in this case it is more difficult to identify architectural elements representative of this function. It would seem logical that exists a correlation between sighting and height. In this way, it is assumed that the alarm and the signalling of the enemy ships would have been faster as well as the width of the horizon that could be seen. Another element useful for recognizing the sighting task was the *bartizan*, a small box placed in the square of the tower and where the guard was kept.

Lodging function. So that the towers could be protected, surely they had to carry out the function of lodging. Usually three men lodged inside it, two adjutants and a corporal commander, called *castellano* or *chatelaine*. During the season of the constant threat and incursions, called *suspicion* or *scandal,* they have to guard the tower for considerable period (sometimes for months) without ever abandoning it.

During the other part of the year only the caporal remained in it, with one adjutant at most, while the other component returned to his normal life. It was not tolerated any departure from the tower or interruption of the watch, also briefly.

The mainly difficulty it was the scarcity of potable water, above all near the sea (problem not found near the rivers). This is the reason for which large cisterns were installed on the ground floor of the buildings. A clay pipe insert into the cistern brought in rain water collected from the upper square during the winter and from a small inner cavaedium it was possible to draw the water without leaving the place. In addition, the walls have some recesses as furnishings, complemented by a couple of rudimental straw pallets table and stools. There was also a simple fireplace used to cook and warm up.

From the second floor, while, accessible through a staircase built into the wall, the guardian watch, receive and transmit signals. These towers, hence, had been carefully studied, they are so accurate and so functional that in the time they required very few variations if not reinforcement.[21]

1.4 Classification and typology of the towers

Cataloguing the towers according basic schemes is only a simplification, they may help to understand and study the main characteristics of them. However, we must specify that the towers of the defensive system differ from one to another and that each of them stands out for its particularities. Below is the classification made by the Russo author in his book.[22]

Modified medieval coastal towers. These are towers that existed before the Ribera plan was designed; most of these were included in the sequence of towers and carry out only a linking function. The main constructive adaptations were shortening by lopping off the top, adding the embrasures and counterscarp crowing; all changes necessary to use the new artillery technologies. In the province of Salerno, there are different testaments of this typology like the famous tower of Praiano, called *Assiola* and also *Trasita* and *Sponda* towers, built respectively in Positano and Fornillo place. One of the most interesting, although, is the *Torre di S. Francesco* or of *Capo d'Atrani*, near Amalfi and constructed around the XII century. This has a conical trunk base surmounted by a short cylindrical body, with an interposed toric section beam.

Circular based towers. Generally, these kinds of building were typical in the Angevin era, although there are some exception during the viceroyal plan; that is, four between Sele and Agropoli (already mentioned). The reason, maybe, depends about the soft soil of the location, which implicated the construction of smaller and lighter buildings. Despite the form, the interior subdivisions were the same and identical also was the entrance caesura and the *bartizan* on the square; the only problem, as we know, were the not enough space to place the cannons. Hence, the

Figure 1.14: Tower with circular and no embrasures. (Russo F., 2009)

absence artillery involves that these towers were used exclusively as *semaphoric repeaters* to guaranty optical continuity of the signals (Figure 1.14). A perfect example is the *Torre di Paestum* that was constructed using the materials of the walls of the ancient city and that today is located around hundred meters from the sea, inside a small square and marred only by a garish room of crushed stone located near the cistern.

Towers with no gun embrasure. These kinds of towers are not so numerous. They have a squat pyramidal trunk on a square base and have not any embrasure. Nowadays it is not known why they were constructed, maybe the reason were some economic problems or an improbable superfluosness of the coping in relation to the location. Probably they are the product of rapid reconstruction; in fact, being the coping the most delicate and costly part of the tower, during the several reconstruction they opted simply to demolish it. For the previous reason, this kind of tower cannot be considered as one typology of the defence system but only as a subsequent adaptation (Figure 1.14).

Towers with single embrasures. In this case, as the previous one, there are very few of these kinds and it is assumed that some of them were originally constructed as such while, the majority, must be considered as having undergone the same simplification process. The presence of only a single gun embrasure imply no so much self defence power, reason for which they were located in not so dangerous areas (Figure 1.15); an example is the *Torre Paradiso* in Minori. The main entrance was originally elevated and it was surmounted by a rudimentary gun embrasure. Maybe, originally it was a double height tower that was altered at a later date due to partial cave in the building.

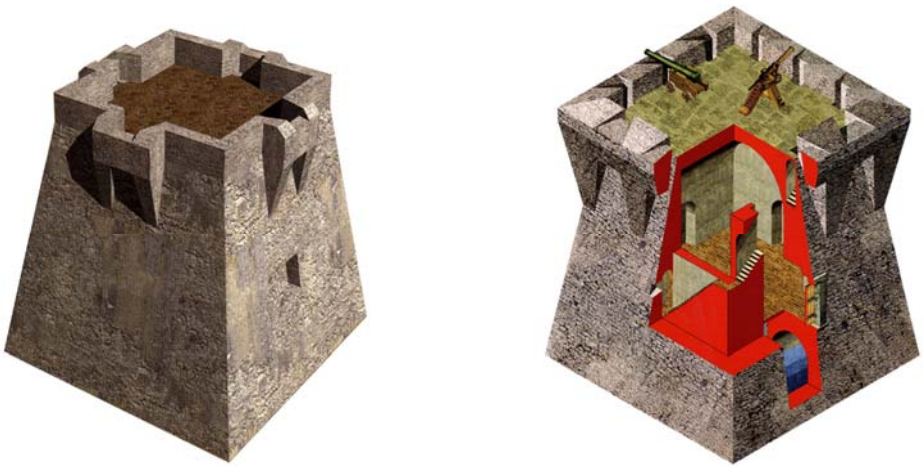

Figure 1.15: Tower with one and three embrasures. (Russo F., 2009)

Towers with three embrasures. These towers are the most numerous of the entire system and they are further divided according to their size in small, medium and large (with the measure of the size from 10m to 16m). The Principality of Citra has a large number of these type of towers. One of the most suggestive, as suggested by the author Russo, is the *Torre di Capo Conca*, near Conca dei Marini. It is perfectly integrated with the natural context and placed upon high calcareous plate that overlooking the sea (Figure 1.15).
Towers with four embrasures. It can be considered as an improvement of the previous larger towers and, for this reason, they were interchangeable with the building that had three embrasures. Some example of these towers are *Crestarella* in Vietri sul Mare despite the changes made in the years or *Erchie* in Maiori. The latter better preserve its originally characteristic, even if half of the square was used as lodging and the holes of the ancient structure were transformed into anachronistic windows; also the staircase was modified with a style totally different from the originally simplicity of the tower (Figure 1.16).
Towers with five embrasures. These type represent the major towers and were realized to carry out active defence. For their interdiction activities they were built in place considered hazardous that generally coincided with populated area or near port with significant traffic. Often they housed the mounted guard, called *cavallari*, consequently in the buildings there were some small stable for the horses. As previously written one way to sight is indirect way, the role of these figures were to alert the areas more difficult to be controlled (Figure 1.16). One of the best example is the *Torre Vito Bianchi* in Vietri sul Mare despite a series of additions over the years (a more detailed description of the changes over time is in the paragraph 5.5.2).

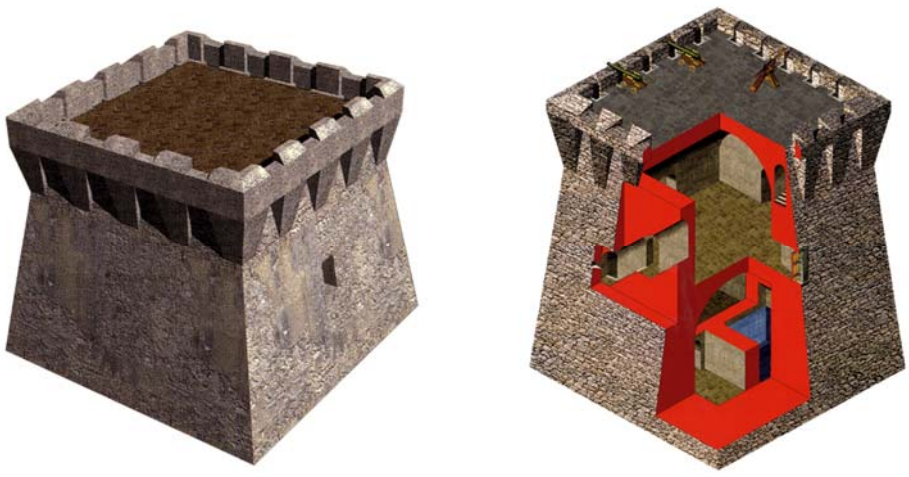

Figure 1.16: Tower with four and five embrasures. (Russo F., 2009)

Double height towers. It is supposed that these kinds of towers, with variables levels, were useful to protect the guardians in some dangerous areas. These typologies were used only along this coast, there are not similar in the entire kingdom. Maybe these architectural expedient have been built for some technical issues of stability on the ground (Figure 1.17). In the Principality of Citra there are three examples. The first one is the *Torre di Cetara*, it is an extraordinary fusion between the sloped cylindrical (maybe of the Angevin period) and squared tower. In the building it is possible to identify two parts and the mountain side that rises for another 4m respect with the sea side. Although both, the higher and lower part, have counterscarp coping: two embrasures in the upper part and two in the other, while in the side of coast it has five embrasures. Another example is *Torre Albori*, near Vietri. Originally, it was similar to the previous one, even if subsequently it was subjected to restoration in the usual Castilian style with large windows and adding of fake merlons, turrets and hole in the base section. Finally the *Torre dello Scarpariello* in Ravello, the best preserved but also the most difficult to reach due to its location.
Enlarged towers. According the author Russo, more than a type these are sporadic anomalies due to the local opportunities (Figure 1.17). In the defence system, in fact, there are less examples, which one of the best preserved, is the *Torre Normanna* of Maiori. It seems to be the assembly of the double height viceroyal tower with a circular keep. Majestic tower which role in the defence plan is still unknown. Nowadays the internal subdivision of this tower is altered, but it appears to be in a good state of conservation and allows a correct architectural visibility.

Figure 1.17: Tower with double height and enlarged tower. (Russo F., 2009)

1.4.1 Cataloging of the towers of the Salerno coast

N	TOWER	MUNICIPALITY	PERIOD	TYPOLOGY	FUNCTION
1	Li Galli	Positano	1343	historical trace	sighting
2	dell'Isola Lunga de' Li Galli	Positano	1343	4 embrasures	offensive
3	del Castelluccio	Positano	1343	historical trace	unknown
4	del Fornillo o Clavel	Positano	1500	pentagonal plan	offensive
5	Trasita	Positano	1300!	circular plan	offensive
6	Sponda	Positano	1300	circular plan	sighting
7	di Renzo	Positano	1300!	circular plan	offensive
8	del Capo Praiasciene or di Gavitella	Praiano	1567	1 embrasure	offensive
9	di Grado di Vettica	Praiano	1300	circular and square plan	sighting
10	la Torricella or Forte di Praiano	Praiano	1567	no embrasures	sighting
11	di Praiano or Del Capo	Praiano	1278	circular plan	offensive
12	di Santo Stefano	Furore	unknown	historical trace	offensive
13	Capo di Conca	Conca dei Marini	1564	3 embrasures	offensive
14	Capo di Vettica	Amalfi	1567	4 embrasures	sighting
15	Bellosguardo or Revellino di Amalfi	Amalfi	1567	historical trace	offensive
16	Capo D'Atrani or del Tumolo	Amalfi	1300	circular plan	offensive
17	di Pogerola	Amalfi	1300!	no embrasures	sighting
18	di Atrani	Atrani	1567	historical trace	offensive
19	dello Ziro	Scala	1292	circular plan	offensive
20	dello Scarparielloor Ficarola	Ravello	1533	3 embrasures	sighting
21	di Paradiso	Minori	1533	double height	offensive
22	di Minori	Minori	1591!	4 embrasures	offensive
23	Mezzacapo	Minori	1565	3 embrasures	sighting
24	della Trinità or la Rotonda	Maiori	unknown	historical trace	offensive
25	dell'Angelo or Normanna	Maiori	1534!	double height	sighting
26	della Marina or Torrione	Maiori	1565	historical trace	offensive
27	di Cesare or Acquarulo	Maiori	1532	5 embrasures	sighting
28	Badia or Santa Maria d'Ogliara	Maiori	1532	4 embrasures	offensive
29	Lama del Cane	Maiori	1532	4 - 5 embrasures	sighting
30	la Torricella	Maiori	1279	circular plan	sighting
31	Tummolo	Maiori	1565!	double height	sighting
32	di Erchie	Maiori	1532	4 embrasures	offensive
33	di Cetara	Cetara	1567	double height	offensive
34	della Puntadi Fuenti	Vietri sul Mare	1300!	historical trace	offensive
35	di Albori	Vietri sul Mare	1564	double height	offensive
36	di Vietri, della Marina or Vito Bianchi	Vietri sul Mare	1564	5 embrasures	offensive
37	del Chiatamone or Crestarella	Vietri sul Mare	1564	4 embrasures	offensive
38	di Monte San Liberatore	Vietri sul Mare	1534	historical trace	sighting
39	dell'Annunziata	Salerno	1565	historical trace	offensive
40	della Carnale	Salerno	1565	3 embrasures	offensive
41	Angellara	Salerno	1568	4 embrasures	offensive
42	Picentina	Salerno	1563	circular plan	offensive
43	Tusciano	Battipaglia	1563	circular plan	offensive
44	di Laco Piccolo or Aversana	Battipaglia	1563	historical trace	unknown
45	Basiata or Aversana	Eboli	1563	historical trace	unknown
46	del Sele	Capaccio	1563	circular plan	offensive
47	di Paestum	Capaccio	1563	circular plan	offensive
48	di San Marco	Agropoli	1563	circular plan	offensive
49	di San Francesco or di Agropoli	Agropoli	1566	5 embrasures	offensive
50	Rotoli or Mainenti	Agropoli	unknown	no embrasures	sighting

51	del Tresino	Castellabate	1235!	historical trace	sighting
52	di Zappino or di Ripastretta	Castellabate	1563	4 embrasures	sighting
53	della Pagliarola or Perrotti	Castellabate	1400!	5 embrasures	offensive
54	della Torricella or Guardiola	Castellabate	1566	unknown	unknown
55	di Punta Licosa	Castellabate	1565	5 embrasures!	offensive
56	di Cannetiello or di Mezzo	Castellabate	1567	4 embrasures	sighting
57	di Punta Ogliastro	Castellabate	1566	5 embrasures!	offensive
58	dell'Arena or Ripe Rosse	Montecorice	1592	5 embrasures	offensive
59	di Timbarosse or di Ripa	Montecorice	1664	historical trace	sighting
60	di San Nicola	Montecorice	1590!	5 embrasures!	offensive
61	di Agnone	Montecorice	1535	4 embrasures	offensive
62	Mezza or Fiumarola	San Mauro Cilento	1580	no embrasures	offensive
63	di Acciaroli or del Porto	Pollica	1573	3 embrasures	offensive
64	della Macchia	Pollica	1600!	historical trace	unknown
65	Caleo	Pollica	1566	5 embrasures	offensive
66	della Punta or Capo Pollica	Pollica	1568	4 embrasures!	sighting
67	di Capogrosso	Casal Velino	1567	3 embrasures	sighting
68	Dominella or di San Matteo	Casal Velino	1566	3 embrasures	sighting
69	della Bruca or di Castellammare	Ascea	1144	circular plan	sighting
70	della Sciabica	Ascea	1589	3 embrasures	offensive
71	Porticella or Capo di Ascea	Ascea	1566	4 embrasures	sighting
72	Fiumicello	Pisciotta	1566	4 embrasures	offensive
73	dell'Acquabianca	Pisciotta	1554	4 embrasures!	offensive
74	del Passariello	Pisciotta	1566	5 embrasures	offensive
75	Ficaiola	Pisciotta	1554	5 embrasures	offensive
76	Torruta	Pisciotta	1554	historical trace	sighting
77	di Valle di Marco	Pisciotta	1500!	historical trace	offensive
78	delli Caprioli or di Palinuro	Centola	1554	4 embrasures	offensive
79	di Lago	Centola	1718	historical trace	sighting
80	del Porto or Fortino	Centola	1554	4 embrasures!	offensive
81	del Prodese	Centola	1663	unknown	offensive
82	del Capo or della Guardia	Centola	1554	3 embrasures!	sighting
83	Spartivento or del Faro	Centola	1554	circular plan	offensive
84	del Monte	Centola	1554	unknown	offensive
85	del Carillo	Centola	1663	historical trace	sighting
86	di Calafetente	Centola	1554	4 embrasures	sighting
87	del Giudeo or Mozza	Centola	1554	no embrasures	offensive
88	di Molpa or di Leyna	Centola	1554	unknown	offensive
89	dell'Arco	Centola	1664!	historical trace	offensive
90	del Mingardo	Camerota	1532	5 embrasures	offensive
91	Muzza or Spacco della Pietra	Camerota	1594	3 embrasures!	sighting
92	Finosa or Capo delle Gatte	Camerota	1569	3 embrasures	sighting
93	d'Arconte or delle Viole	Camerota	1594	3 embrasures!	offensive
94	dell'Isola	Camerota	1599!	3 embrasures	sighting
95	di Teano or d'Avviso	Camerota	1500!	no embrasures	sighting
96	del Poggio	Camerota	1500!	no embrasures	sighting
97	Lajella	Camerota	1532	no embrasures	offensive
98	Zancale or delle Cale	Camerota	1566	3 embrasures	sighting
99	Cala Bianca or Cenfresca	Camerota	1566	4 embrasures	sighting
100	del Frontone or del Semaforo	Camerota	1566	no embrasures	sighting

101	degli Infreschi or Anforisca	Camerota	1235	5 embrasures	sighting
102	Calamoresca	Camerota	1566	3 embrasures	sighting
103	la Scalella or Trarro	San Giovanni a Piro	1566	3 embrasures	sighting
104	di Spinosa or del Garagliano	San Giovanni a Piro	1566	4 embrasures	sighting
105	di Sant'Anna or di Scario	San Giovanni a Piro	1566	5 embrasures!	offensive
106	Oliva	San Giovanni a Piro	1566	5 embrasures	offensive
107	di Capitello	Ispani	1566	4 embrasures	offensive
108	Petrosa	Vibonati	1566	5 embrasures	offensive
109	del Buondormire	Sapri	1566	historical trace	offensive
110	di Capobianco	Sapri	1566	4 embrasures	offensive
111	Scialandro or di Mezzanotte	Sapri	1300!	circular plan	sighting

[1] Talenti S., Morena S., (2016). Da Positano a Sapri: la rete di "sguardi" del sistema difensivo costiero. In: Verdiani G. (Eds), *Defensive Architecture of the Mediterranean XV to XVIII Centuries. International Conference on Modern Age fortifications of the Mediterranean coast, FORTMED*. Florence (Italy), Didapress, 2016; pp. 169-176.

[2] Russo F., (2009). *Le torri costiere del regno di Napoli. La frontiera marittima e le incursioni corsare tra il XVI ed il XIX secolo*. Naples (Italy), Edizioni Scientifiche e Artistiche, 2009.

[3] Hogg I. V., (1982). *Storia delle fortificazioni*. Novara (Italy), Istituto geografico De Agostini, 1982; p.106.

[4] The term identifies a defensive system born in the 16th century under the Aragon family. to defend the coast of the Kingdom of Naples. The project had to have an elevated number of towers with visual connections in order to protect the entire coast of the Kingdom of Naples.

[5] Municipalities of southern Italy that arose during the Lombard period.

[6] Santoro L., (2012). *Le torri costiere della Provincia di Salerno: paesaggio, storia e conservazione*. Salerno (Italy), Paparo edizioni, 2012; p. 13.

[7] Vassalluzzo M., (1969). *Castelli torri e borghi della costa cilentana*. Salerno (Italy), Pepe, 1969; p.194.

[8] Santoro L., op. cit.; p. 16.

[9] Talenti S., Morena S., op. cit. ; pp.169-176.

[10] Santoro L., op. cit.; p. 19.

[11] Russo F., op. cit.; p. 127.

[12] Pasanini O., (1926). Costruzione generale delle torri marittime ordinata dalla R. Cort di Napoli nel sec. XVI. In: *AA.VV. Studi di storia napoletana in onore di Michelangelo Schipa*. Naples (Italy), I.T.E.A., 1926; p. 436.

[13] Santoro L., op. cit.; p. 33.

[14] Cardone V., (1993). Tipologia e morfologia delle torri in Campania. Studio puntuale sul riuso delle emergenze fortificate. In: *Tipologia e morfologia delle torri in Campania. Studio puntuale sul riuso delle emergenze fortificate. Colloqui internazionali castelli e città fortificate, Palmanova*. Udine (Italy) Università degli Studi di Udine, 1993; p. 363.

[15] It is an ancient unit of linear measure from 6,4 to 10 cm.

[16] Vassalluzzo M., op. cit.; p. 42.

[17] Cisternino R., (1977). *Torri costiere e torrieri del Regno di Napoli: 1521-1806*. Rome (Italy), Istituto italiano dei castelli, 1977; p.108.

[18] Santoro L., op. cit.; p. 90 .

[19] Hogg I. V., op. cit.; p. 47.

[20] Santoro L., op. cit.; p. 93.
[21] Russo F., op. cit.; pp. 198-218.
[22] Russo F., op. cit.; pp. 173-195.

2. The network of “gazes” of the defensive system

2.1 The importance of the visual connection

The aim of the unit is to deepen the cognitive analysis of the coastal *Torreggiamento* during the viceroyal period, focusing not so much on individual towers, but rather on the entire defence system of the coastal territory.
Through the analysis and comparison of ancient maps, got until now, we want focus the attention on the visual communication between the towers, or on the “dialogue” that entertain each other the different artefacts. In particular, there will be a comparison between the original project of dislocation of the towers on the territory, and the situation that exists today on the Amalfi and Cilento coast. In this way, we can start an evaluation between the “looks” from sixteenth-programmed projects and those granted by the remains of the defensive system in the Salerno area.
In this way, we want to bring back to the attention what remains today of the ancient gazes between the different towers; which too often continue to be seen as singles beauties and not as parts of a much more sophisticated plan. At this point, it is possible to understand how the abandonment of such architectures, especially in some areas, inevitably risks to make one of the most ingenious works of all time disappear.

2.1.1 The method of the plan

Born as an ingenious defence project to protect populations from corsair attacks, the network of towers stretching from Positano to Policastro along the coast of Salerno, is today for us, a fascinating testimony of a distant past.
Observing the orography of the Principality of Citra we can see its vast heterogeneity, in particular it is possible to identify two typology of coasts. The first one is the Amalfi coast with its amazing views and a landscapes alternated by high cliffs to less steep parts. The second one, while, is the Cilento coast different from the previous one for its more varied morphology: the coastline appear more plan at north until Pisciotta and more irregular at south. The great variety of territory that

Figure 2.1: Clarkson Stanfield, A View of Vietri in the Gulf of Salerno, 1855; Coll. Ashmolean Museum, Picture Library, Beaumont Street, Oxford

meets along these stretches of coastline has certainly influenced the edification of the individual towers, characterizing them and making them different from each other. Hence, known in depth the typological choices and construction techniques used by our ancestors is certainly duty for an adequate conservation and preservation of these artifacts.

However, in order to understand a population and a territory, it is necessary not to limit ourselves to the study of the single buildings but to question oneself on those careful strategies that often underpinned such projects.

The organizational defensive system was a really network of "gazes" in order to closely observe and monitor the entire coastline (Figure 2.1). The choice of the location, in fact, was not only related to its accessibility or the presence of viable roads; but it was the consequence of careful studies of a group of technical staff. In fact, they did not analyze only the punctual settlement of the tower but the whole plan, and so it is strongly conditioned by a reticular scheme of visual relations existing between them.

The importance of this visual connection is understandable studying the historical cartography in order to underline the relationships and the interaction that exist both between the built and nature and between tower and tower. Even if today seems

apparently without a rule, in reality, it was a defensive system strongly thought out and designed.
The conscious numerical difference (in minority for the Kingdom of Naples) of the marine fleet compared to Barbary pirates focus the attention in a realization of an uninterrupted fortification of the coastline. Think to defend the territory with the military fleet was, and will always remain, a utopian dream.[1] First of all the reason of this gap was the cost for the realization and armament of it, then, another problem no less important, the deficiency of men necessary for the fleet.
In reason of these, they proceeded in the construction of a chain of armed towers in order to provide both the active defense with its cannons that the passive defense of warning residents, the entire system was called *Torreggiamento*.
The strongholds, so, became active with the weapons like cannon fire in order to guarantee not only a degree of security of the population, but also the protection of the coastal ship.

2.2 *Province* of the Kingdom of Naples

Kingdom of Naples represented a part of the south Italian Peninsula between the 1282 and 1816. Its origin is a result of the *War of the Sicilian Vespers* (1282-1302). In fact, following the *Peace of Caltabelotta*, signed on 31 August 1302, the previous Kingdom of Sicily was divided into an island portion, went to Frederick III, and a peninsular portion, went to Charles II. The first was known as *Kingdom of Trinacria* while the latter, passed to the dynasty of the Angevins, was called the *Kingdom of Sicily* and only subsequently, with the modern scholarship, *Kingdom of Naples*.
In the history the Kingdom lived a period of great splendour both under the various dynasties of Angevin (1282-1442), with the Aragon reconquer of Alfonso I (1442-1458) and under the rule of a branch of the house of Aragon (1458-1501). In 1504, the Spanish defeated the French crown and the Kingdom was since then joined dynastically to the Hispanic monarchy with that of Sicily. The juridical unification of both Kingdoms took place only in the 1816 with the foundation of the *Kingdom of the Two Sicilies.* With the term *province* of the Kingdom of Naples are indicated the ancient administrative district in which the Kingdom was divided. The organization of the territory and the definition of boundaries were established with the *giustizierato*[2] during the Norman and Swabian period.
During the time they were subjected to some change and after the *Peace of Caltabelotta* first mentioned the organization in the peninsular was different. In

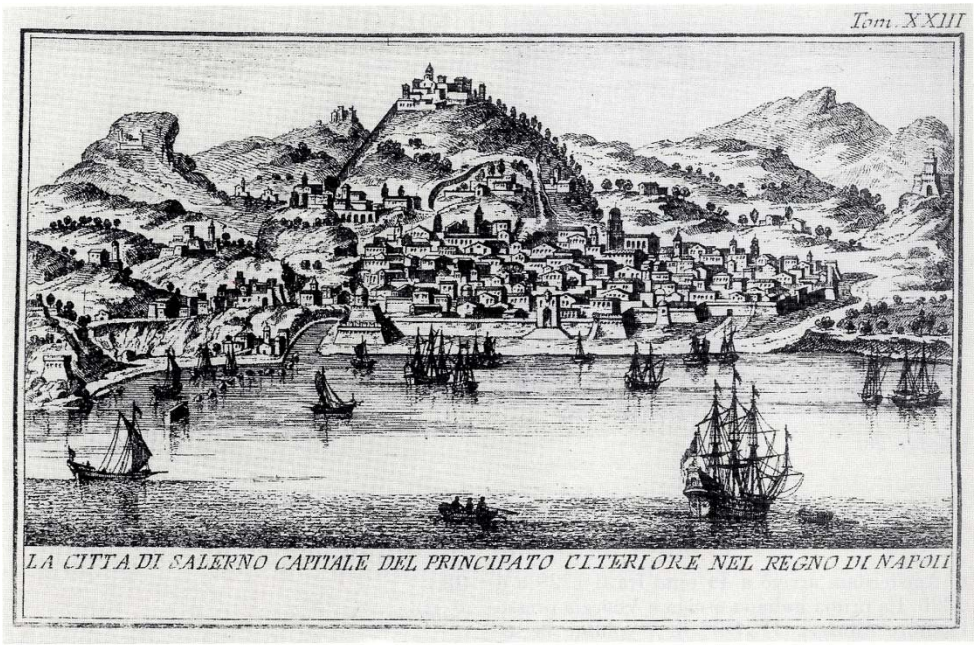

Figure 2.2: Francesco Sesone, La città di Salerno capitale del Principato Citeriore nel Regno di Napoli, 1763; BPS. (Soprintendenza, 1994)

1284, in fact, Charles of Anjou divided the *giustizierato* of *Principato and Terra Beneventana* into two distinct provinces: the *Principatus ultra serras Montorii,* or the *Principality Ultr*a, and the *Principatus citra serras Montorii*, that is the *Principality of Citra* (Salerno was established as the capital, Figure 2.2).
During the Aragon era the figure of the *giustiziere* (representative of the authority of the sovereign at the provincial level) was replaced from another figure the *preside* and the administrative districts were called *province.*
From this period, the second half of the 15th century, the Kingdom was divided into twelve constituencies: *Terra di Lavoro*, *Principality of Citra*, *Principality Ultra*, *Giustizierato of Basilicata*, *Calabria Citeriore*, *Calabria Ulteriore*, *Terra d'Otranto*, *Terra di Bari*, *Capitanata*, *Contado Molise*, *Abruzzo Citra*, *Abruzzo Ultra*. The last changes were doing during the 19th century under Joseph Bonaparte.

2.2.1 Principality of Citra

In the study the focus was mainly on *Principality of Citra*, at the beginning it included Salerno, Sala and Bonati. Successively, around the 1800, there was an administrative and territorial reorganization of the province and finally, with the

admission of the *Kingdom of the Two Sicilies* to the *Kingdom of Italy*, the Principality of Citra was suppressed and the institution was reorganized according to the Savoy institutions, definitively changing its name to the *Province of Salerno* in 1862.
Different are the cartographic representations from the past, one of these is the paper manuscript written by Nicola Antonio Stigliola (1546-1623) and by Mario Cartaro (1540-1620). The Atlas Stigliola-Cartaro reproduces the relief of the different *province* of the Kingdom of Naples. This is a representation in which significant geographic data and toponyms – both internal and external – of the towers are contained (Figure 2.3).
There are several examples of the tables made between 1595 and 1642 as evidence of the importance that this work especially for administrative purposes. Which that we used for the following analysis dates back to 1613. It is more simplified the 16th century copy; in fact the information about the coordinate system, the streets, fortress and forts are not indicated. This is because, given the huge military information contained within the graphical table, was imposed a ban on printing by the Spanish court, which well knew the risks related to the dissemination of information concerning the accessibility of the territory.[3]

Figure 2.3: Principato Citra, N. A. Stigliola, M. Cartaro, 1613. BNN, Coll. private

However, this simplification is convenient for the purpose of our study because offering an easier identification of the same and avoiding an overabundance of data that could have confused their identification.

2.3 The end of the defensive system

Once the defensive system was realized and, above all, became functional the number and frequency of raids decreased and the attention of the Barbary pirates became focused on the capture of merchant ships.
During the time, the towers were subjected to different maintenance interventions due to the continuous natural and human damaging conditions to which they were subjected. Like the walls, also the armament and the artillery had to undergo constant technical inspection and repair. Above those towers, thus, soldiers spent their entire life with no interruption; it was strictly forbidden to leave the building despite being located in remote and isolated areas; any disobedience was severely punished.
An event that changed considerably the situation of the Mediterranean coasts was certainly the great French amphibious operation. In the 1830 at the port of Marseilles,

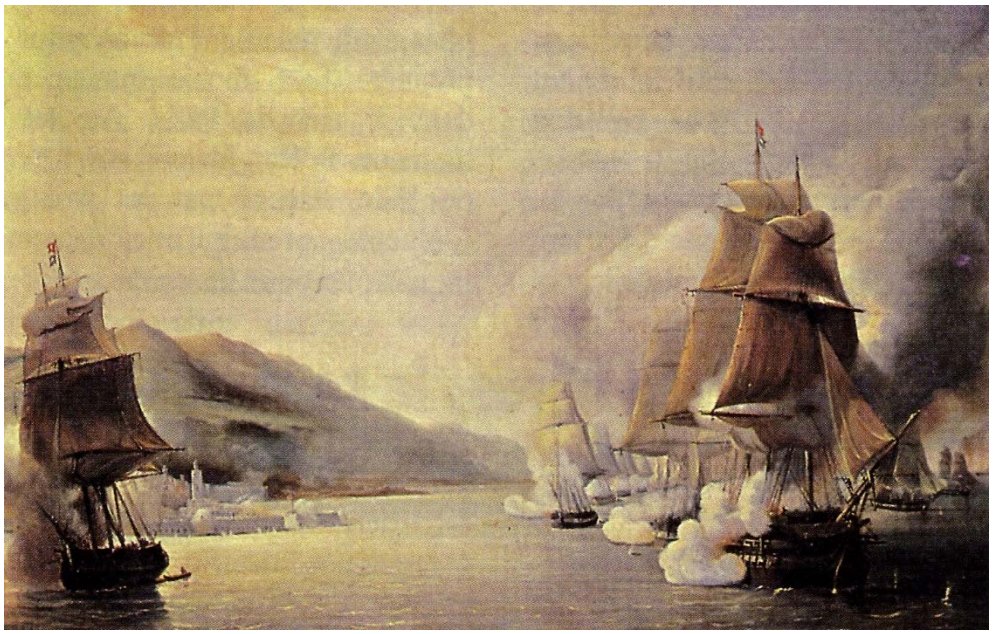

Figure 2.4: Painting of the bombardment of Algiers in 1830, premonitory sign of the French conquest of the city. (Russo F., 2009)

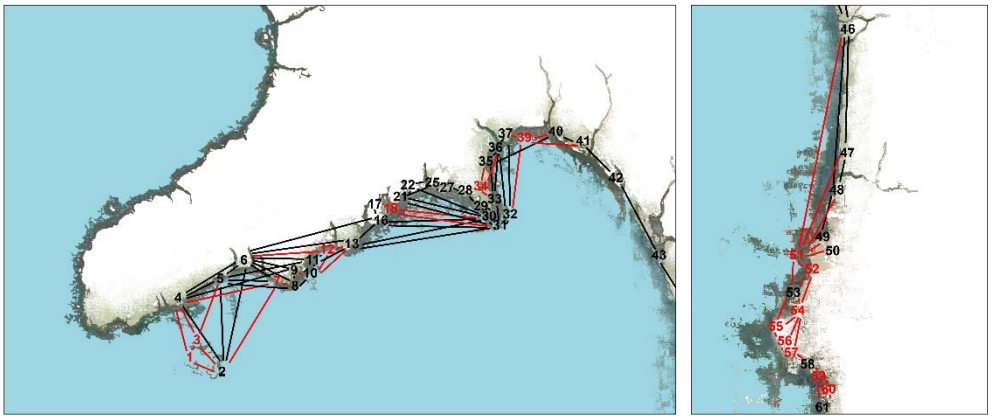

Figure 2.5: Schematization of the network of “gazes” of the towers in Amalfi Coast and Municipality of Castellabate; in black are those still existing in red in the missing ones

.

begun the preparation for the colossal expedition against the capital of the piracy and many volunteers joined from different nations. In the spring of the same year the large naval group headed directly toward Algiers, the attack ended with the collapse of the walls of the city and the possession of it by the French; piracy ended on that day (Figure 2.4).

After this victory, in fact, the raids ceased along the Salernitan coast. Thus began the abandonment of many towers that lost their function as fortifications. In particular, following the edict of Vittorio Emanuele II of 1860, numerous artefacts were auctioned off and purchased by the respective municipal administrations or private individuals.

Several are the interventions and the destiny to which these towers have been destined: the restoration and the consolidation of some of them - even if often questionable - have allowed their conservation, guaranteeing the testimony and safeguarding them from the complete degradation.

2.3.1 Comparison

The study of the current coastal territory and the analysis of what today are the towers still existing have allowed a comparison between the current visual relations and the connections foreseen by the ancient tower reported in the cartography by Stigliola and Cartaro. Hence, we proceeded, to the graphic restoration of the visual connections of the Amalfi and Cilento coastlines. In particular, with the black lines

the visual communications still existent between the towers (or recoverable after redevelopment interventions) have been highlighted; while, in red, those no longer existing due to the disappearance of the building.
Of particular interest is the area related to the territory of Castellabate, in this zone a significant number of towers are collapsed and so, a part of the ancient visual network between the strongholds (Figure 2.5).
Based on this data, then, a table has been drawn up (Figure 2.6) in which the different towers of the province of Salerno have been catalogued. From the analysis, it can be seen how a fairly high number of such buildings has been lost or kept in ruins. In particular, of the 111 towers present along the Salerno coast 34 (highlighted in green) have disappeared or only a few traces are found, 22 (highlighted in grey) are in ruins, while the remaining part is in good condition or completely restored. [4]

N°	TOWER	MUNICIPALITY
1	Torre Li Galli	Positano
2	Torre dell'Isola Lunga de' Li Galli	Positano
3	Torre del Castelluccio	Positano
4	Torre del Fornillo o Clavel	Positano
5	Torre Trasita	Positano
6	Torre Sponda, di Positano o di Mezzo	Positano
7	Torre di Renzo	Positano
8	Torre del Capo Praiasciene, dello Scaricatore o di Gavitella	Praiano
9	Torre di Grado, di Vettica o Grado di Vettica	Praiano
10	Torre la Torricella, Cella o Forte di Praiano	Praiano
11	Torre di Praiano o a Mare, la Sciola o Assola o Del Capo	Praiano
12	Torre di Santo Stefano	Furore
13	Torre Capo di Conca, della Pigna o del Cimitero	Conca dei Marini
14	Torre Capo di Vettica	Amalfi
15	Torre Bellosguardo, Revigliano o Revellino di Amalfi	Amalfi
16	Torre Capo D'Atrani, di San Francesco o del Tumolo	Amalfi
17	Torre di Pogerola	Amalfi
18	Torre di Atrani o della Maddalena Revellino di Atrani	Atrani
19	Torre dello Ziro	Scala
20	Torre dello Scarpariello, di Capo Focardo, Marmorata o Ficarola	Ravello
21	Torre di Paradiso	Minori
22	Torre di Minori	Minori
23	Torre Mezzacapo, di Minori, la Torricella o dell'Annuziata	Minori
24	Torre della Trinità, la Rotonda o di Revigliano	Maiori
25	Torre dell'Angelo, del'Angulo o Normanna, della Formicola	Maiori
26	Torre della Marina o Torrione	Maiori
27	Torre di Cesare o Acquarulo	Maiori
28	Torre Badia, Santa Maria d'Ogliara o Santo Spirito	Maiori
29	Torre Lama del Cane, Americana o del Mortaro	Maiori
30	Torre la Torricella o Torretta di Capo dell'Orso	Maiori
31	Torre Tummolo	Maiori
32	Torre di Erchie	Maiori
33	Torre di Cetara	Cetara
34	Torre della Puntadi Fuenti, di Fuontio di Santa Maria della Catena	Vietri sul Mare
35	Torre di Albori	Vietri sul Mare
36	Torre di Vietri, della Marina o Vito Bianchi	Vietri sul Mare
37	Torre del Chiatamone, de lo Chiatamons o Crestarella	Vietri sul Mare

38	Punto di avvistamento di Monte San Liberatore	Vietri sul Mare
39	Torre dell'Annunziata	Salerno
40	Torre della Carnale, Forte San Giuseppe, Polveriera	Salerno
41	Torre Angellara	Salerno
42	Torre Picentina o Vicentina	Salerno
43	Torre Tusciano	Battipaglia
44	Torre di Laco Piccolo o Aversana	Battipaglia
45	Torre Basiata o Aversana	Battipaglia
46	Torre del Sele	Capaccio
47	Torre di Paestum	Capaccio
48	Torre di San Marco	Agropoli
49	Torre di San Francesco, di Agropoli o Cappucini	Agropoli
50	Torre Rotoli o Mainenti	Agropoli
51	Torre del Tresino o di Trentova	Castellabate
52	Torre di Zappino, della Zappa o di Ripastretta	Castellabate
53	Torre della Pagliarola, della Marina o Perrotti	Castellabate
54	Torre della Torricella, della Ficarolòa o Guardiola	Castellabate
55	Torre di Punta Licosa, di Licosa o della Punta	Castellabate
56	Torre di Cannetiello, di Mezzo o Mezzatorre	Castellabate
57	Torre di punta Ogliastro	Castellabate
58	Torre dell'Arena o Ripe Rosse	Montecorice
59	Torre di Timbarosse o di Ripa	Montecorice
60	Torre di San Nicola	Montecorice
61	Torre di Agnone	Montecorice
62	Torre Mezzatorre, Cala delle Acque o delle Canne o Fiumarola	San Mauro Cilento
63	Torre di Acciaroli, del Porto, della Marina o Bastione	Pollica
64	Torre della Macchia	Pollica
65	Torre Caleo	Pollica
66	Torre della Punta, Capo Pollica o di Cannitiello	Pollica
67	Torre di Capogrosso	Casal Velino
68	Torre Dominella o di San Matteo	Casal Velino
69	Torre della Bruca o di Castellammare	Ascea
70	Torre della Sciabica	Ascea
71	Torre Porticella, Issica, del Telegrafo, di Capo di Acqua o Capo di Ascea	Ascea
72	Torre Fiumicello	Pisciotta
73	Torre dell'Acquabianca	Pisciotta
74	Torre del Passariello o della Marina o di Piano di Mare	Pisciotta
75	Torre Ficaiola	Pisciotta
76	Torre Torruta	Pisciotta
77	Torre di Valle di Marco	Pisciotta
78	Torre delli Caprioli o di Palinuro	Centola
79	Torre di Lago	Centola
80	Torre del Porto, del Forte o Fortino	Centola
81	Torre del Prodese, Batteria della Punta del Fortino o Batteria del Prodese	Centola
82	Torre del Capo, o Tauriello, della Guardia o della Quaglia	Centola
83	Torre Spartivento o del Faro	Centola
84	Torre del Monte, di Palinuro, del Monaco, del Telegrafo, di Costa d'Oro, del Monte d'Oro	Centola
85	Torre del Carillo	Centola
86	Torre di Calafetente	Centola
87	Torre del Giudeo o Torre Mozza, di audio, Calaloiodio e Monaco	Centola
88	Torre di Molpa o di Leyna	Centola
89	Torre dell'Arco	Centola
90	Torre del Mingardo	Camerota
91	Torre Muzza o Spacco della Pietra	Camerota
92	Torre Finosa o Capo delle Gatte	Camerota
93	Torre d'Arconte o delle Viole	Camerota
94	Torre dell'Isola	Camerota
95	Torre di Teano o d'Avviso	Camerota

96	Torre del Poggio o d'Avviso	Camerota
97	Torre Lajella, di Camerota o della Marina	Camerota
98	Torre Zancale o delle Cale	Camerota
99	Torre Cala Bianca o Cenfresca	Camerota
100	Torre del Frontone o Falconara, del Semaforo, degli Iscolelli	Camerota
101	Torre degli Infreschi o Anforisca	Camerota
102	Torre Calamoresca, Maresca, Marcellino	Camerota
103	Torre la Scalella o Trarro	San Giovanni a Piro
104	Torre di Spinosa, del Garagliano o Murice	San Giovanni a Piro
105	Torre di Sant'Anna o di Scario	San Giovanni a Piro
106	Torre Oliva o dell'Olivo	San Giovanni a Piro
107	Torre di Capitello	Ispani
108	Torre Petrosa	Vibonati
109	Torre del Buondormire	Sapri
110	Torre di Capobianco	Sapri
111	Torre Scialandro o di Mezzanotte	Sapri

Table 2.1: Towers of the Province of Salerno; in white are towers in good condition, in grey are the ruins and in green are the ones disappeared

[1] Russo F., (2009). *Le torri costiere del regno di Napoli. La frontiera marittima e le incursioni corsare tra il XVI ed il XIX secolo*. Naples (Italy), Edizioni Scientifiche e Artistiche, 2009; p. 69.

[2] A giustizierato (English: justiciarship; Italian: [dʒustittsjeˈraːto]; plural giustizierati; an alternative term for circoscrizione), refers to a type of country subdivision that was used by several former Italian states in the medieval period. (https://en.wikipedia.org/wiki/Giustizierato).

[3] Soprintendenza ai beni ambientali, architettonici, artistici e storici delle province di Avellino e Salerno. Assessorato ai beni culturali, (1994). T*ra il Castello e il Mare: l'immagine di Salerno capoluogo del Principato*. Naples (Italy), Fausto Fiorentino, 1994; p. 60.

[4] Talenti S., Morena S., (2016). Da Positano a Sapri: la rete di "sguardi" del sistema difensivo costiero. In: Verdiani G. (Eds), *Defensive Architecture of the Mediterranean XV to XVIII Centuries. International Conference on Modern Age fortifications of the Mediterranean coast, FORTMED*. Florence (Italy), Didapress, 2016; pp. 169-176.

3. A first virtual tour of the defensive system

3.1 Technologies for the cultural heritage

In the time, the use of the photography for the knowledge, the documentation and valorisation of cultural heritage has grown increasingly. Constantly evolving it has changed its function over the years from a "simple" tool useful to the representation of the reality, until a true art form.
From the XIX century the use of camera spread widely also in the field of architecture, as a support in the project, above all in the field of survey and restoration. Beside its great use in the field of architectural survey through photogrammetry technology, it can also be used not only for the metrical and geometrical aspects of architectures but also for understanding the spatial relations between them and the surrounding space.
The use of photography, therefore, has proved to be very useful also in the field of knowledge, dissemination and valorisation about the cultural heritage facilitating the public enjoyment of such historical buildings. Virtual tour is an example because makes possible a dynamic view of sites; in this way is possible an interactive tour of the places quite similar to realty.
In addition, the availability online of this virtual tour exceeds the limits of borders and allows for greater spread of our assets, enhancing the interest and possibility encouraging people to visit the site.
The aim of the following work, in fact, is to deepen the cognitive analysis of the coastal *Torreggiamento* of the province of Salerno in the viceroyal era.
As explained in the previous chapter, it is a dense network of towers, located in careful strategic points. In this part of the project, we want to concentrate the

Figure 3.1: Barker's London panorama, from the top of the Albion Mills, 1792

attention on the virtual restoration of the visual connection between the towers.
The idea, therefore, is to restore the ancient gazes through the creation of different panoramas take near the various towers and, subsequently, to guarantee iterative actions between one building and another, in addition to enriching this virtual tour with further historical and informative links.
In short, the whole process aims to promote a different experience of the coast of Salerno helping to spread the knowledge of the defensive system and its strategy by focusing attention on an aspect of the system difficult to understand and often forgotten. Proceeding in this way, it will be possible to contribute at the diffusion of this historical patrimony. The generation of virtual tour would also allow the cataloguing and archiving of historical and technical contents useful for the interpretation of our historical buildings. Furthermore, in order to achieve this purpose it is foreseen the implementation of low-cost technologies. In this way it is possible to generalize the work done and to turn the attention in general to lesser known architectures; recognizing value to them that, unfortunately, often are in a state of complete abandon.

3.2 Basic concepts on 360° photo

A panoramic photography is a technology for the creation of seamless stitching of multiples images with the use of appropriate instruments and software in order to return high quality panoramic images with high number of pixel. The word “panorama” comes back to 18th century when the painter Robert Barker coined this word for his new form of painting, the word derives from the Greek “πᾶς” (all) and “ὅραμα” (view) and it was used to refer to a broad view of setting.
They generally were painted on the wall of some buildings specially designed for such art, called rotundas; the aim is the same of today, create the illusion of being on the place.
With the invention of the camera, the interest in the panoramas was also directed in the field of photography. Already around the 1843 the Australian Joseph Puchberger patented a camera with rotating optical system where the lens was rotate through a manual crank while shooting, the angle of view was 150°. Successively, other photographers continued to improve their cameras following almost of the same concept.
Currently there are some cameras which allow to capture a pictures with high resolution in a single exposure, such as Gigapxl Project (with a negative of 9”x18”

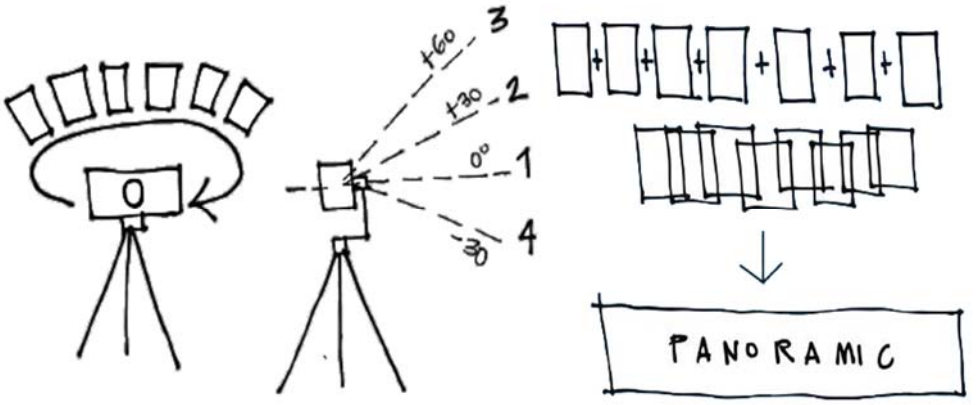

Figure 3.2: Main steps for generation of panoramic photos

which, once scanned, gives a resolution of 4 Gpx) and pan-STARRS (digital that captures 1,4 Gpx and dedicated to astronomic use)[1].

There are, however, more economical ways to get into panoramic photography. In the last few years, indeed, exist special software can marge conventional photos, obviously realized with a certain overlap, in order to create a digital panoramic image. Moreover, on the market also panoramic heads were appeared which are supportive for the acquisition of more images with the camera and that will be stitch later for the realization of one higher resolution photo (Figure 3.2). The last one, after, could be printed out on photo paper or converted to interactive panoramas for viewing on a computer display.

Panoramic images are the typical data necessary for the generation of a virtual tour. The observer can see only a portion of this picture and, through the use of special viewer software, can move with the mouse in different directions. These photos thus obtained can then be linked to each other and enriched with additional information data (video, text or drawing).

In order to present a realistic display of the panorama on the computer screen is necessary a projection, after the stitching of the images, indeed, is necessary to display the curvature of space through projection and generally it is used three different form in the panoramic production process: *Cylindrical, Spherical* and *Cubic* (Figure 3.3).

The *Cylindrical* projection is the most frequently used and it consists in a wrapping of the panoramic image around a cylinder and the observer stay at the centre of this geometric shape. The panoramic filmstrip can move on the right and on the left behind a cut-out window. This projection is better for setting where the down and upper parts of the picture are not very important.

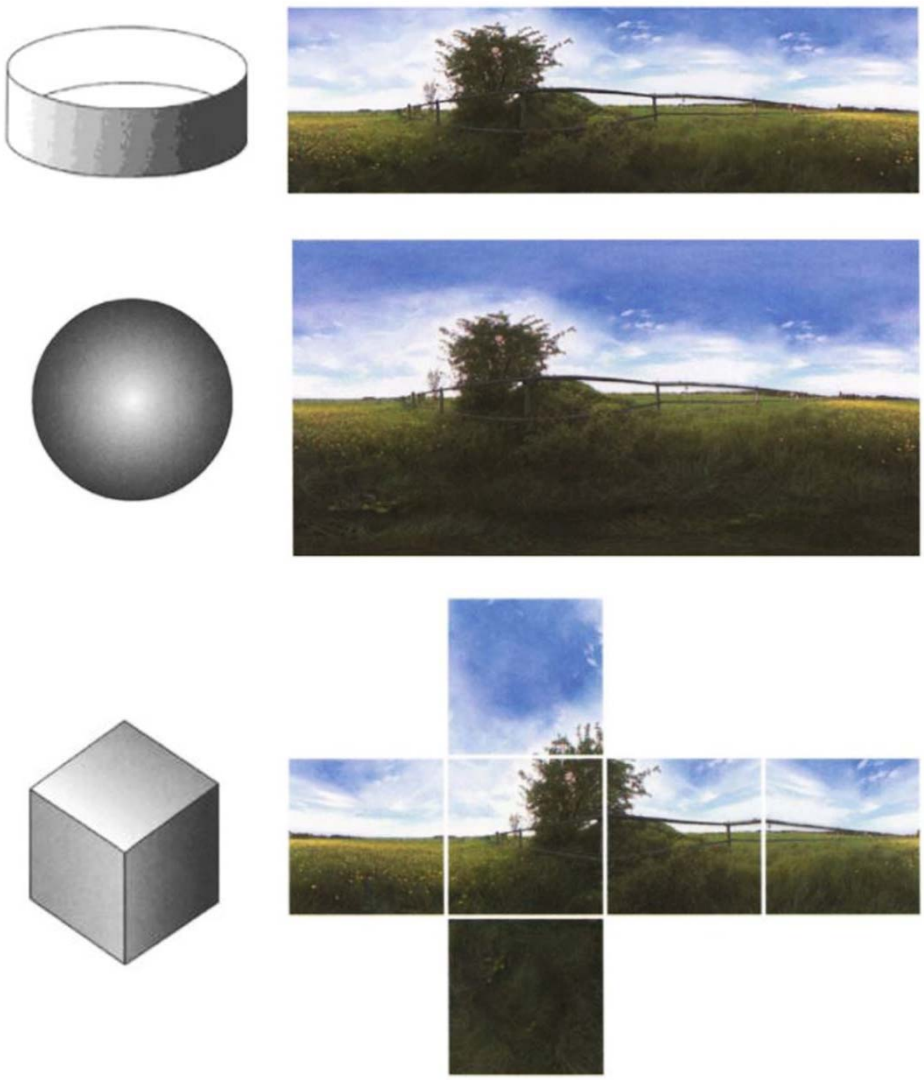

Figure 3.3: Cylindrical projection with limited vertical angle. (Jacobs C., 2004)

The *Spherical* projection, while, is different from the first because its pivoting range is unlimited. The panoramic image, so, envelops a sphere and, also in this case, the point of observation is in the centre. This is a typical panorama to use when emphasizing the top or bottom of the captured space.
As in the previous case, *Cubic* projection does not have limitation on the vertical angle, but the process involved in the cubic projection are less complex than the other. It is composed by eight corner and six sides, so for this format are required

six quadratic pictures. Normally quite difficult is to distinguish the cubic projection from the spherical one, but if the picture is greatly magnified the edges of the cube sometime become visible.[2]
Generally, the creation of a virtual tour consists of three phases: photographic survey, post-processing for the photos stitching and finally the creation of link between the different panoramic photos and add information data. At the end, the work will share on online platform and it is available to everybody.

3.2.1 Stitching algorithms: SIFT

The creation of a satisfying virtual tour surely needs well-made panoramic photos, for this reason, the realization of good images stitching is one of the fundamental steps of this process.
Panoramic image stitching, thus, is a technique to merge a sequence of images into one blended picture and nowadays, modern computer software make possible to do it in automatically way. In the following case we use the software Autopano of the Kolor house; it is an image-stitching application and its operation is based on SIFT algorithm (Scale-Invariant Feature Transform).
Published by David Lowe, it is a feature-based method and works by establishing correspondences between points, lines or other geometrical entities, this means that the result of image stitching will be good if the interest points are found correctly. Generally keypoints are detected using a cascade filtering approach, before are identified some locations that are then examined in further details. In particular, the major steps are the following:
Scale-stage extreme detection: the first stage of computation search over all scales and image locations. It is implemented efficiently by using a difference of Gaussian function to identify potential interest points that are invariant to scale and orientation.
The scale space of an image is defined by the function

$$L(x, y, \sigma) = G(x, y, \sigma) * I(x, y)$$

where $*$ is the convolution operator, $G(x, y, \sigma)$ is a variable-scale Gaussian and $I(x, y)$ is the input image.
Various techniques can then be used to detect stable keypoint locations in the scale-space and *difference of Gaussians* is one of such technique. It is possible using scale-space extreme, $D(x, y, \sigma)$ which computing the difference between two

images, one with scale k times then other.

$$D(x, y, \sigma) = \big(G(x, y, \sigma) - G(x, y, \sigma)\big) * I(x, y)$$
$$= \big(L(x, y, k\sigma) - L(x, y, k\sigma)\big)$$

To detect the local maxima and minima of $D(x, y, \sigma)$ each point is compared to its eight neighbours in the same image and nine in the upper and lower scale (Figure 3.4). It is selected only if the value is larger or smaller than all of these neighbours.
Keypoint localization: In this stage, keypoints selected are based on measures of their stability; generally, the points with low contrast or poorly localized along an edge are rejected. This purpose is obtained by calculating the *Taylor expansion* (up to the quadratic terms) of the scale-space function $D(x, y, \sigma)$, so that the origin is at the sample point:

$$D(x) = D + \frac{\partial D^T}{\partial x} x + \frac{1}{2} x^T \frac{\partial^2 D}{\partial x^2} x$$

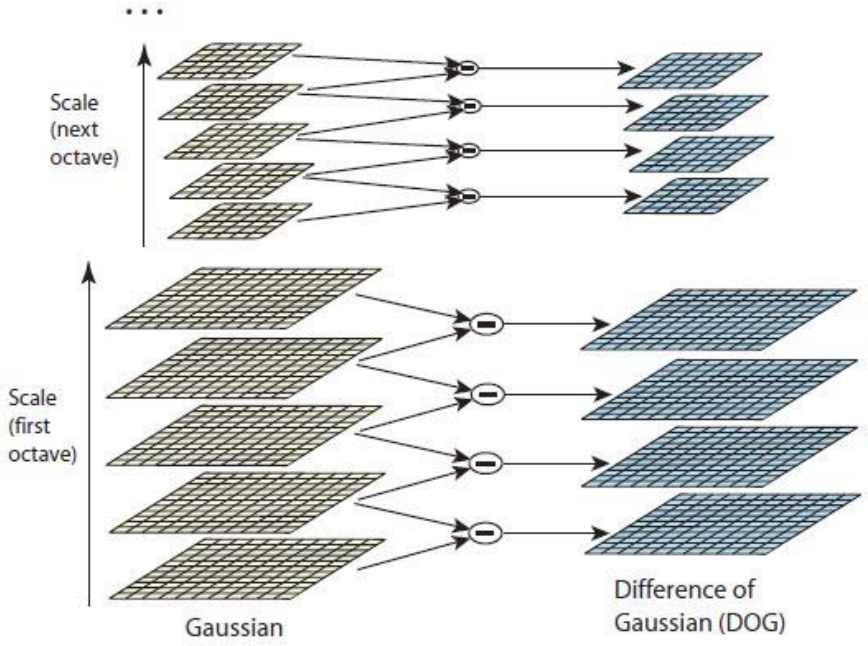

Figure 3.4: For each octave of scale space, the initial image is repeatedly convolved with Gaussians to produce the set of scale space images shown on the left. Adjacent Gaussian images are subtracted to produce the difference-of-Gaussian images on the right. After each octave, the Gaussian image is down-sampled by a factor of 2, and the process repeated. (Lowe D. G., 2004)

where D and its derivatives are evaluated at the sample point and $x(x, y, \sigma)^T$ is the offset from this point. The location of extremum, $\hat{x}$, is given by

$$\hat{x} = \frac{\partial^2 D^{-1}}{\partial x^2} \frac{\partial D}{\partial x}$$

If the offset $\hat{x}$ is larger than threshold value then this point is excluded.
The final offset is used to evaluate the function value at the extremum, and so $D(\hat{x})$, is useful for rejecting unstable extrema with low contrast. This can be obtained by

$$D(\hat{x}) = D + \frac{\partial D^T}{\partial x} \hat{x}$$

therefore sensitive to noise or are poorly localized along an edge.
However, it is not sufficient to remove only keypoints with low contrast. The *difference of Gaussian* function will have strong responses along edges, even if the candidate keypoint is not solid to small quantity of noise.
Therefore, in order to increase stability, we need to eliminate the keypoints that have poorly determined locations but have high edge responses.
For poorly defined peaks in the *different of Gaussian* function, the principal curvature across the edge would be much larger than the principal curvature along it. Finding these principal curvatures amounts to solving for the eigenvalues of the second-order *Hessian matrix*, H:

$$H = \begin{bmatrix} D_{xx} & D_{xy} \\ D_{xy} & D_{yy} \end{bmatrix}$$

The eigenvalues of H are proportional to the principal curvatures of D. Evaluating the trace and the determinant of previous matrix we can compute the sum and the product of the eigenvalues:

$$Tr(H) = D_{xx} + D_{yy} = \alpha + \beta$$

$$Det(H) = D_{xx} D_{yy} - (D_{xy})^2 = \alpha\beta$$

where α and β are respectively the eigenvalue with lager and smaller magnitude.

$$\frac{Tr(H)^2}{Det(H)} = \frac{(\alpha+\beta)^2}{\alpha\beta} = \frac{(r\beta+\beta)^2}{r\beta^2} = \frac{(r+1)^2}{r}$$

where r is the ratio between the largest magnitude eigenvalue and the smallest one; $\alpha = r\beta$.
Looking the formula, it is possible to notice that it depends only on the ratio of the eigenvalues rather than on their individual values.
Therefore, to verify that the ratio of principal curvatures is lower than some threshold, r, just need to check

$$\frac{Tr(H)^2}{Det(H)} < \frac{(r+1)^2}{r}$$

This is very efficient to compute, with less than 20 floating point operations required to test each keypoint.
Orientation assignment: One or more orientations are assigned to each keypoint location based on local image gradient directions. All future operations are performed on image data that has been transformed relative to the assigned orientation, scale, and location for each feature, thereby providing invariance to these transformations.
The approach taken to find an orientation is firstly to use the scale of keypoints to select the Gaussian smoothed image L, with the closest scale, so that all computations are performed in a scale-invariant manner.
Secondly, an orientation histogram is formed from gradient orientations of sample points. At last, according to the histogram, orientation to the keypoints can be assigned.
Peaks in the orientation histogram correspond to dominant directions of local gradients. The highest peak in the histogram is detected, and then any other local peak that is within 80% of the highest peak is used to also create a keypoint with that orientation.
Keypoint descriptor: The previous parameters impose a repeatable local 2D coordinate system in which to describe the local image region, and therefore provide invariance to these parameters.
The next step is to compute a descriptor for the local image region that is highly distinctive yet it is as invariant as possible to remaining variations, such as change in illumination or 3D viewpoint.
The figure 3.5 shows computation of the keypoint used by D. G. Lowe. The first stage is computing the magnitude and orientation at each image sample point

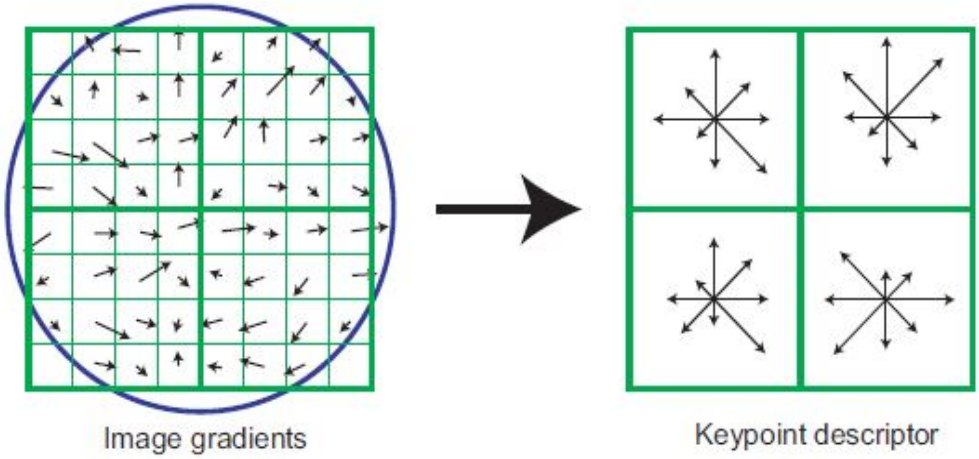

Figure 3.5: Computation of the Keypoints descriptor (Lowe D. G., 2004)

around the keypoint location, using the scale of the keypoint to select the level of Gaussian blur for the image (indicated by the overlaid circle).
The keypoint descriptor is shown on the right side of the figure; it allows for significant shift in gradient positions by creating orientation histograms over 4x4 sample regions.
The figure shows eight directions for each orientation histogram, with the length of each arrow corresponding to the magnitude of that histogram entry. Despite the figure shows a 2x2 array of orientation histograms, the experiments show that the best results are achieved with a 4x4 array of histograms with 8 orientation bins in each.
Finally, the feature vector is modified to reduce the effects of illumination change. First, the vector is normalized to unit length.
A change in image contrast in which each pixel value is multiplied by a constant will multiply gradients by the same constant, so this contrast change will be cancelled by vector normalization. A brightness change in which a constant is added to each image pixel will not affect the gradient values, as they are computed from pixel differences.
In conclusion, this algorithm is very useful for identifing SIFT keypoints, they are characterized by a high distinctiveness, which enables the correct match for a keypoint to be selected from a large database of other keypoints.
Furthermore their computation is efficient, so that many keypoints can be extracted from a typical image without requiring excessive time for processing[3].

3.3 The procedure

There are several tools today on the market and various techniques to follow for the realization of good panoramas and, consequently, interesting virtual tours. Obviously, the choice of the technologies to use depends on the purpose to be achieved.
Therefore, below will be illustrated the instruments we used to recover the ancient network of "gazes" of the defence system of the Coast of Salerno.
For the shoots done in this unit of research, we used two different digital reflex. One of this is the Canon EOS 600D Digital Reflex characterized by a sensor CMOS APS-C 18 Megapixel and used with a lens Canon EF-S 18-200mm. The second one is the Nikon D60 Digital Reflex, it has a sensor Nikon DX 10 Megapixel and we worked with a Sigma EX DG FISHEYE lens with a focal of 8mm (Figure 3.6).
Likewise two panoramic tripod head are been employed, Gigapan Epic Pro and Nodal Ninja 4; they are fundamental to make a high quality panoramic photograph. Mainly their function is to allow a precise placement of the camera in order to facilitate the acquisition phase by ensuring a correct overlap between the photos and, above all, eliminating parallax errors.
Giga Pan EPIC PRO is a robotic panoramic head and it needs an initial programming phase, but once all the parameters are set, the unit will pan and tilt to create proper coverage for intense panoramas. Generally, this kind of tools is suitable for wide-angle lenses, but we worked with the Canon EOS600D and the lens aforementioned. Noda Ninja, while, it is a manual panoramic head and the

Name	Nikon D60
Sensor	CCD 23,6X15,8 mm
Pixel	10,2 megapixel
Pixel size	36,6 μm²
Lens	Sigma EX DG FISHEYE
Focal length	6,4-25,6 mm
ISO	100-1600
File	JPEG, RAW, JPEG+RAW

Name	Canon EOS 600D
Sensor	CMOS da 22,3x14,9 mm
Pixel	18 megapixel
Pixel size	18.4 μm²
Lens	EF/EF-S
Focal length	18-200 mm
ISO	100-12800
File	JPEG, RAW, JPEG+RAW

Figure 3.6: Camera technical specification of the Nikon D60 and Canon EOS600D

hardware designed to work in conjunction with a lot of type of camera and lens (from ultra-wide angles to 100mm telephotos) in that case we worked with a fisheye mounted on the Nikon D60.

3.3.1 Parallax defined

In using an ordinary camera when we do panoramic photos, as it is known, multiple and slightly overlapping shots of the scene are taken by pivoting the tool in one fixed point. Finding the optimal position is very important in order to avoid the so-called *parallax error* and so, keep foreground and background points lined up perfectly in overlapping frames.
This effect occurs because each image shot is actually different from the one before: in fact when we turn the camera on its tripod screw, the front of the lens will move to the right, while the back of the body will move to the left (or vice versa) and at the end things captured in the photos simply won't line up properly (Figure 3.7). In order that the parallax error is avoided, the camera must be rotated around the entrance pupil. It is a floating point located inside the lens and incorrectly referred to by some as nodal point. In a camera there is ordinarily an aperture stop that often is located inside the lens; when we look a lens from the front we see the 'virtual image' of this aperture which is created for us by the lens elements and it is not in real size or distance from us; this virtual image of the aperture stop is called the *entrance pupil* of the lens. Of all the rays of light that depart from a certain point of the subject, those that actually contribute to form the image create a cone of rays of light. This cone has a vertex on the subject's point and the base on the entrance pupil. On the other side of the optics, the light rays come out in the form of a cone whose base is the exit pupil and the vertex is the point on the image plane. The entrance and exit pupils have the same shape as the

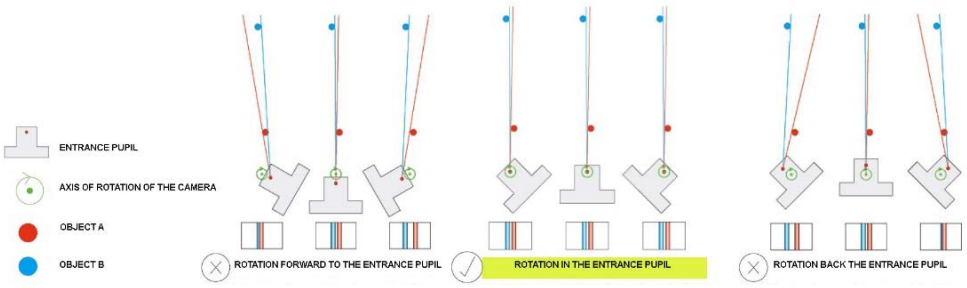

Figure 3.7: Parallax error

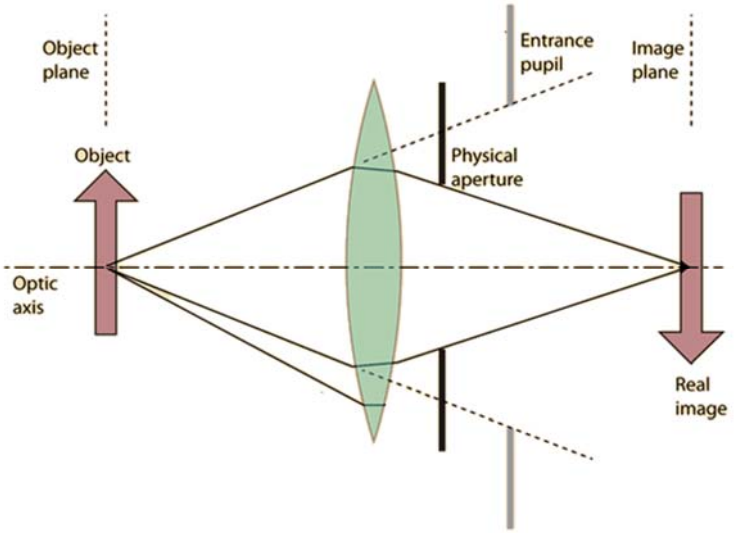

Figure 3.8: Entrance pupil of a lens. (http://230nsc1.phy-astr.gsu.edu/hbase/geoopt/stop.html)

diaphragm and their size is proportional to that of the diaphragm (Figure 3.8). It is to understand that this point is also important for the effect of the lens exposure - f/number of the lens – in fact, it is the ratio between the focal lens and the diameter of the entrance pupil and not the diameter of the physical aperture stop.
Similarly, the centre of perspective lies at the intersection of straight lines between all the points that appear to line up, so the centre of perspective must coincide with the entrance pupil. Based on this, when taking adjacent images you want to rotate the camera around a line that runs through (or very close to) the entrance pupil. By finding the pivot point of the lens, and rotating the camera about this point, you will assure parallax free images.
Furthermore, parallax is more obvious in the viewfinder with objects close to the camera: the more distant the objects, the lesser the parallax. So, if using a lens with zoom capability, the entrance pupil will change in position as the zoom changes. In this case study the location of the entrance pupil was found thanks to the use of the two tools GigaPan and Nodal Ninja. In both the procedure we focus the camera in some scene with two vertical reference elements that overlap and that are located at different distances, one near and the other more distant. Then, from the same position but with different rotation and so different scene, we take another photo which these objects will lie on the other side of the image (Figure 3.9). The last step is to verify if the near and far object features remain in the same alignment. If we see a parallax shift, then we must change the location of the pivot axis and test again. [4]

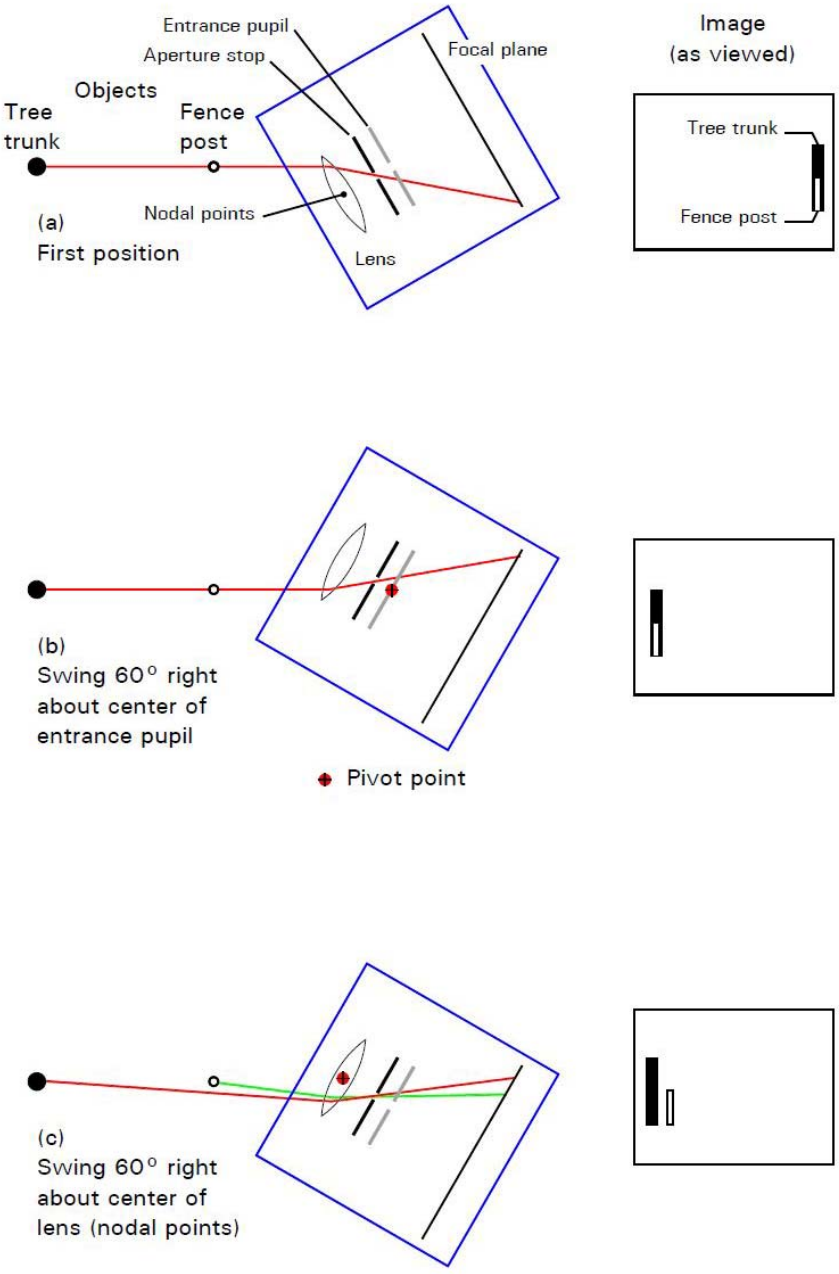

Figure 3.9: Rotation of camera with behind the lens aperture stop. (Douglas A. K., 2008)

3.3.2 Workflow with GigaPan EPIC Pro

As previously mentioned, the tools GigaPan EPIC Pro was used for the realization of a part of the virtual tour (Figure 3.10). Although it is an automated panoramic head, it requires some previous settings in order to find a correct configuration between the camera and the instrument.
Obviously, the first step is the elimination of the parallax error. This is possible by translating the camera horizontally until it is positioned in the precise pivot point. In our case, we had done some attempts in the laboratory in order to try the correct collocation and it is the same for each camera with the same focal.
Successively, one of the most important stages is setting the time required to take a photos in each rotation.
Of course this time is conditioned also by the area to be detected as well as the time needed to take the single picture. Outlining the FOV (Field Of View), therefore, GigaPan EPIC Pro automatically calculates the value of the angle of separation between a shot and the next.
Nevertheless it is the optimal angle, it is possible to increase the value and still to achieve a panoramic to 360° with good quality but decreasing the acquisition time.
Another parameter to set is the area to be covered. Instead of operating at an angle of 90° in the lower transverse direction and 90° in the upper vertical direction, it was decided to work with 80° and 80°, that is 160° instead of 180°, avoiding repetitive shots in the last rotation.

Figure 3.10: Automatic panoramic head GigaPan EPIC Pro

Figure 3.11: Parameters of panoramic taken with Canon EOS 600D and HDR acquisition

As in each survey, it is important to be clear in advance of the aim of the project in order to operate correctly for its realization. In the case studied, a balance was made between the quality and the resolution of the photo given that it will be shared on the web and for the sole purpose of visualization.
Generally, during the shooting phase we worked with Canon EOS 600D and with a focal length of 35mm ensuring an overlap of 30% shots. Moreover, having to work outside with different exposures, we have acquired in HDR; this involves triples the number of photos calculated from the FOV (Figure 3.11).[5]

3.3.3 Workflow with Nodal Ninja

The second tool used is the Nodal Ninja 4 from FANOTEC (Figure 3.12). Differently from the previous one this hardware is a manual panoramic head so, the calculation of the optimal overlap between the shots is not automatically evaluated by the instrument.
As in the case of GigaPan EPIC Pro, the fundamental stage is the placement of the instrument on the entrance pupil so as to avoid the parallax error.
Usually, two adjustments on instrument have to do for properly positioning it. The first step consists in setting the lower rail. The camera, mounted on the upper rail, has to rotate so that it is perpendicular to the ground and with the lens directed downwards.
Next, slide the camera so that the camera's viewfinder points toward the lower rotator knob. The lower position not change for each camera and it is independent from the lens of focal length used.

Figure 3.12: Panoramic head NN4 and parameters of panoramic photo with Nikon D60

In the second step, we have to set the upper rail. In this case we rotate the upper rail with camera so that it is parallel with the ground. At this point, slide the camera until the correct no parallax point of the lens is centred with the upper rotator. Differently from the previous case, if you only modify the lens or the focal length you have to reset the instrument. [6]
Once again, the aim of this project was the realization of a virtual tour for sharing on web, so it was not so important the very high resolution of the shots. Therefore, in this case we worked with Nikon D60 and its fisheyes with a focal lens of 8mm, taking shots every 45° horizontally and vertically. Working in this way the quality of the panoramic picture is not maximum but sufficient for our purpose, and above all it allows operating in much faster times, generating panoramas that are easily navigable and shared on the web.

3.3.4 Realization of shots

The final quality of the panoramic images depends on several factors, among these also the resolution and sharpness of the individual shot. Surely, this aspect depends from the type of camera that we use during the acquisition phase: sensor type, focal lengths and other characteristics of the selected hardware.
However, there are some parameters to consider for generating adequate panoramas. In fact, given that the photos are stitched between them, it is necessary to have some devices during the survey phase and also remember that if good photos will be generated, then minors will be the problems that will arise when we will operate with the software.

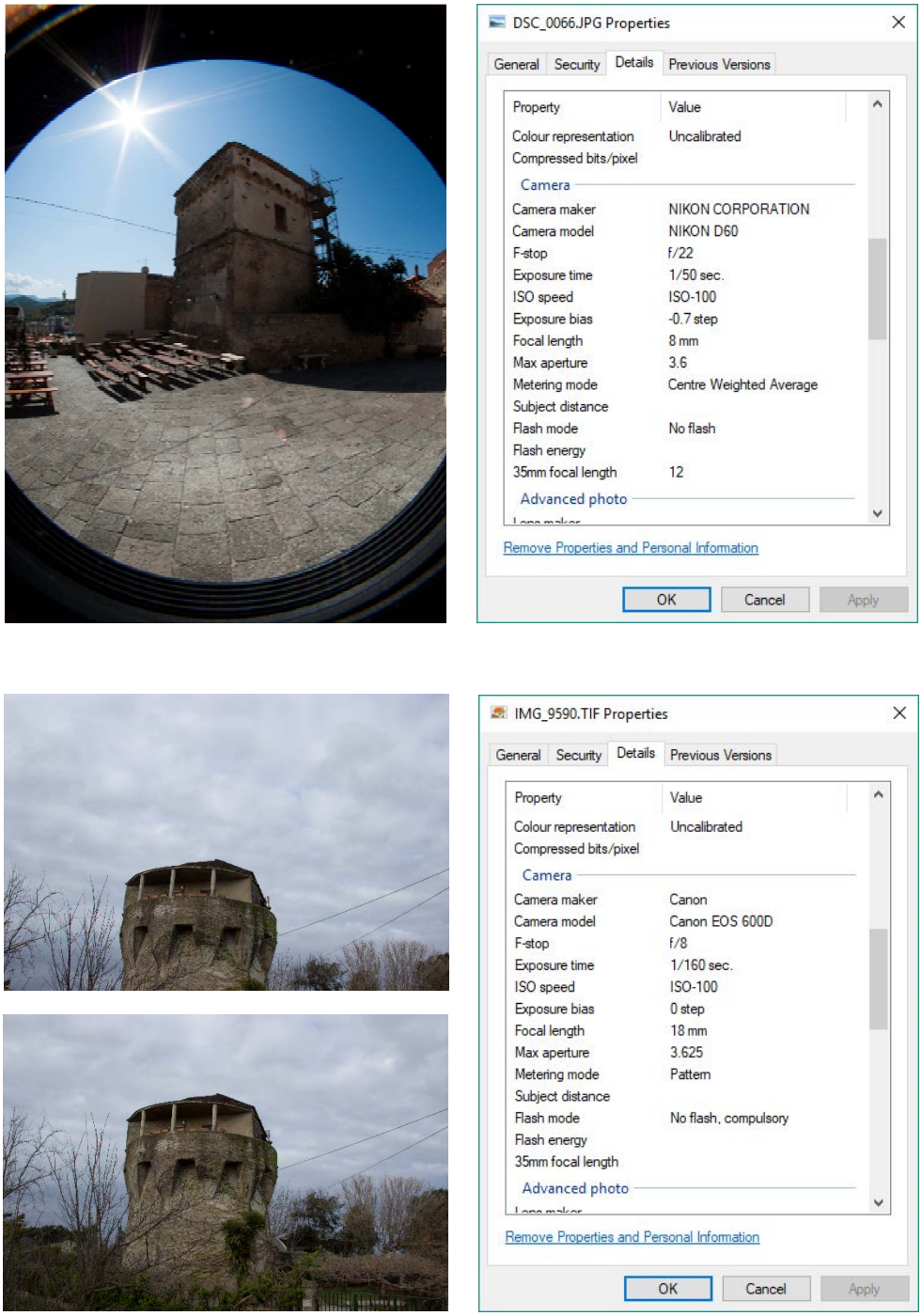

Figure 3.13: Exif data of the photos with Nikon D60 and Canon EOS 600D

One of the basically aspect is the *exposure*, often not so easy to evaluate for the non-homogeneity of lighting above all in outside area. This problem can be solved in two ways, or working in HDR mode during the shoots or in post-processing phase with photo-editing software.
Another aspect to consider is the *sharpness*, usually, at higher *apertures of the diaphragm* there is a better value of it, but consequently decreases the *depth of field*. Given the particular condition in which it was operated, so, it is better slightly reduce the aperture of the diaphragm and increase the field of view; in this case we worked with values close to f/8 with standard lens and f/22 with fisheye.
Normally, furthermore, it is preferable working with a *fixed focus* to avoid even minimal displacements of the nodal point. For this reason is better to set the manual mode; in fact sometimes, given the lack of contrast, the camera is not able to focus automatically.
The *shutter speed* depending on the aperture of the diaphragm and the amount of light needed, so we use different values in relation at the space to acquire, longer time are not problematic because generally the camera is mounted on a tripod.
Also the *sensitivity* of the sensor is important, high values of it involve an increase in noise; reason why it should be carefully weighed without ever exceeding the value of 200 ISO. Finally, it is important block the *white balance*, too in the same value throughout the acquisition phase to obtain a homogeneous image.
In any case it is a good idea to take pictures in RAW format in order to be able to intervene later on some photographic aspects and above all it is necessary that there is a good overlap between the images, so that the edge between the photos are invisible and to avoid “ghosting” or “blurring” effects (Figure 3.13).

3.3.5 Generation of panoramic images

Once the photos have been made it is possible to proceed with the stitching of them; the software used for this part of the project is Autopano Giga 4.2 version from Kolor company. Founded in 2004, it was one of the first to perceive the potential of SIFT technology for the identification of interest points in an image and to obtain its user license issued by the University of British Columbia in Vancouver. Autopano is an image-stitching application and, despite the advanced algorithms used for data processing, it has a very simple and user-friendly interface. The workflow to follow is quite simple and intuitive; of course if a good survey has been carried out less will be the manual interventions. Are shown below the main steps followed.

Select images and setting for the panorama image; we proceeded by importing the photos manually, so a first selection was necessary. In fact, as previously written, often we worked in HDR mode and hence, some photos are overexposed or underexposed. Moreover, in order to improve processing, the some parameters have been modified in Camera Raw, trying to level out the exposure between the shots. Once adjusted and selected, we proceed setting some options in order to obtain a good stitching of the images. In the *detection* tab you can choose and modify different features that affect the way in which the shots will be linked to each other.

Following various test, we decided to operate checked the option *force every images to be in one panorama*, so that the entire group image appear in the last picture (Figure 3.14). However sometimes it places the image(s) without any connection with the others; in this case, you can operate manually and place the photo(s) in the right position.

*Panoramas editor; t*o the panorama image thus generated can be made some changes; among which rotation, change the point of view or horizontal and vertical inclination, crop or increase the picture. Anyway, the most useful purposes for us were the option *Images Mode* that let see how the source images are situated in the panorama. This tool permits to revise positions, to check overlap, mistakes or remove images (Figure 3.15). In addition, with the option *Moving Images* it is possible manipulate manually not only the position of the entire panorama but also the single image that compose its (moving, rotating and zooming it).

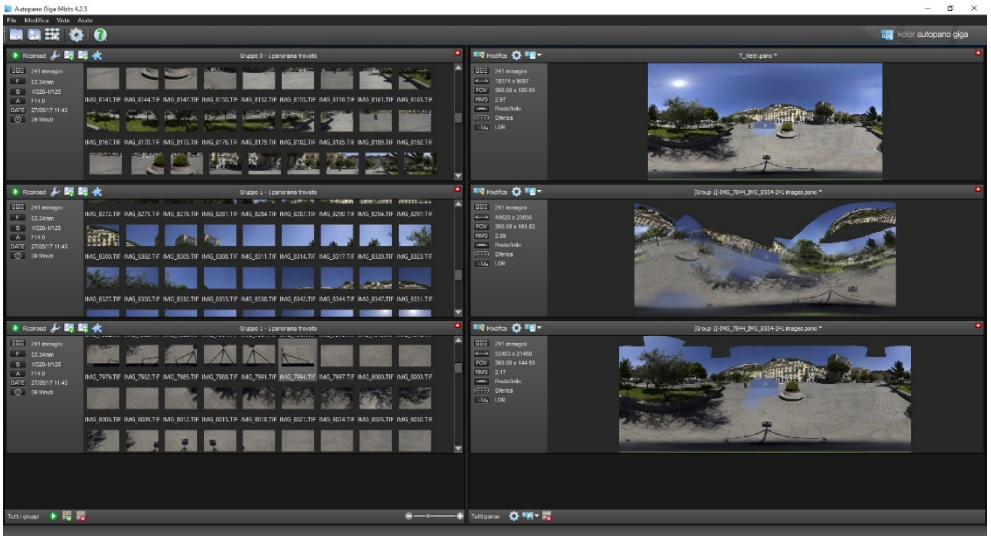

Figure 3.14: Various panoramic results obtained from stitching images

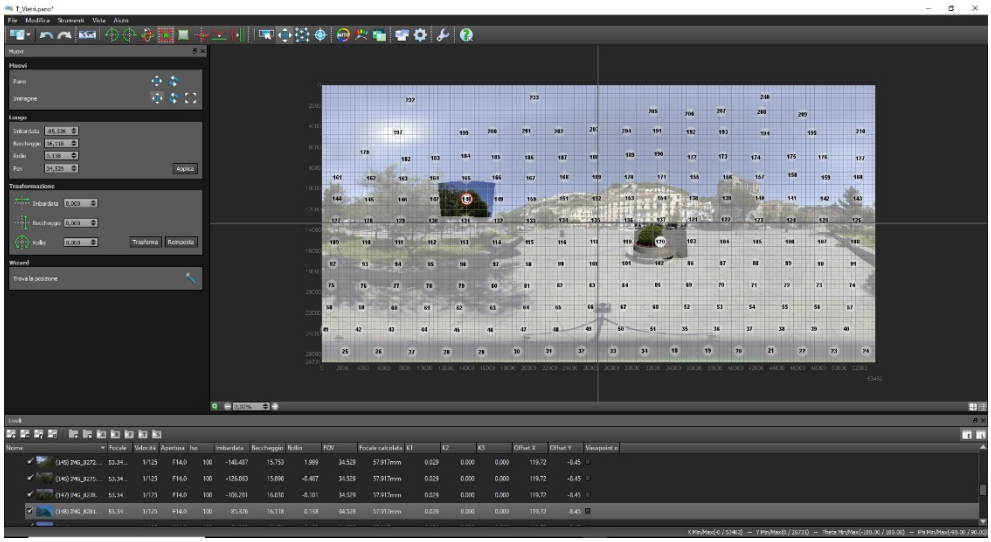

Figure 3.15: Image Mode windows to revise position of the photos

In other cases, it was convenient to intervene directly on the control points with the option *Control Point Editor*. It let you manually correct the link and this kind of points so that optimal images positioning is achieved. The quality of the link is evaluated through various colors representative of the RSM (Root Mean Square) value : RMS lower than 5 means good quality link (green), RMS between 5 and 10 average quality link (orange) and RMS more than 10 bad quality link (red); when

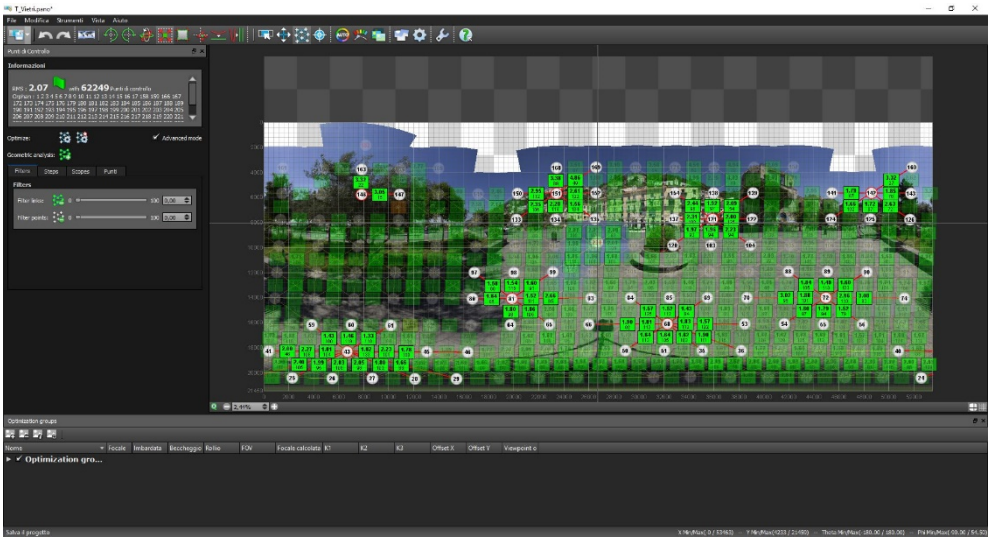

Figure 3.16: Evaluation of the RSM of the points links

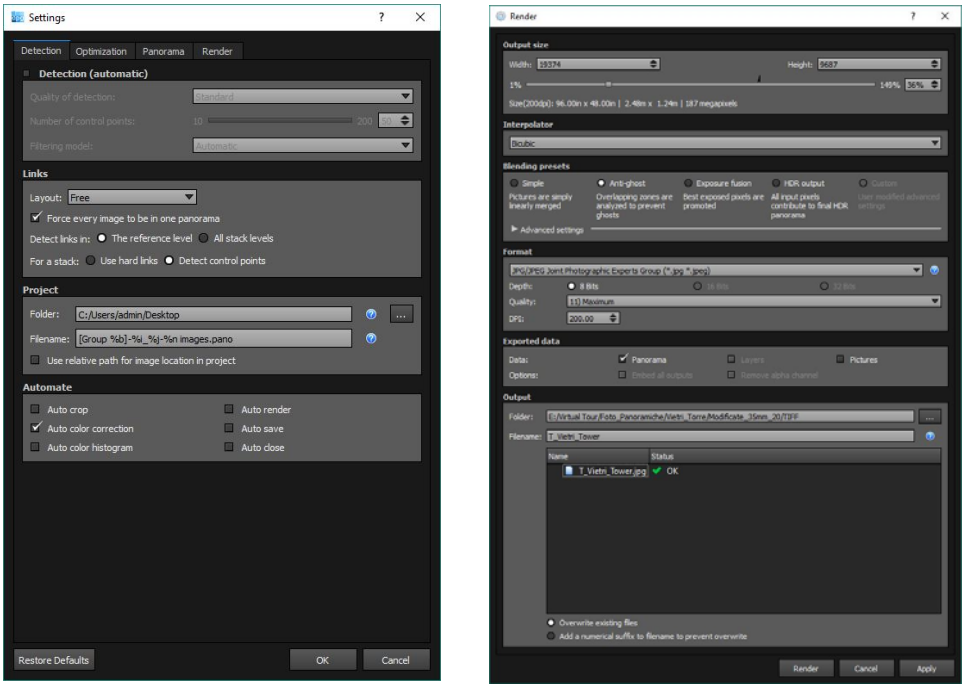

Figure 3.17: Setting of the Detection and Render windows

the color is blue the RMS value is not very important so it is necessary to modify the link (Figure 3.16). The next phase is an improvement of the exposure and the color of the panoramic in order to have a more homogeneous image. The option make this is Color Correction. It is possible to intervene on color in three different ways: LDR Correction (standard correction), No Correction and HDR Correction.
In our case the default or no correction were the most used ones, the purpose of the first adjustment is to align the small differences in brightness, contrast and color in the series of pictures that make up the panorama. The HDR Correction, while, use a different algorithm from the LDR mode and allows for the harmonization of panoramas when the differences in brightness are much larger. *Render*; it is the last step in creating panorama. As repeatedly highlighted having to share the project on the web it is convenient to create not very heavy pictures. For this reason it was decided to work with jpg formats and without exceeding the output size, generally it was 20000x10000 and 200dpi (Figure 3.17).
Another setting to tick is the blending preset *Anti-ghost* that not modify the image characteristics when mixing but automatically removing objects that have been moved. Working outside, this instrument was very helpful for the elimination of moving scenes.[7]

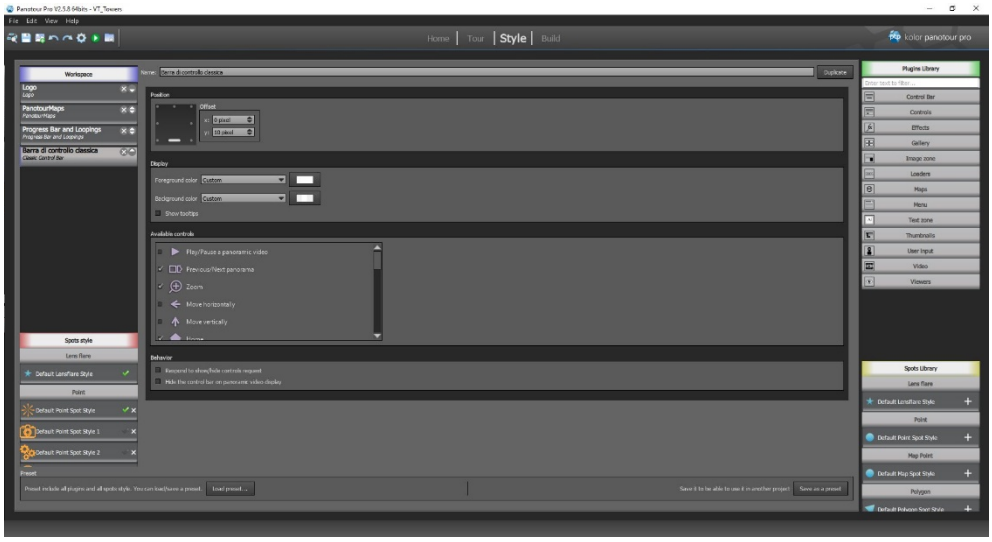

Figure 3.19: Style tab to personalize the interface of the virtual tour

3.3.6 Generation of virtual tour

The last stage of this unit was carried out through the use of the software Panotour, once again of the Kolor company. It gives the possibility to generate virtual tours by relating the various panoramas and, subsequently, to share it on the internet.
The interface provides several tabs to follow for the creation of the project: *Home, Tour, Style* and *Build*.
The first tab is the landing area where it is possible to open or create projects. Instead, in the second one you generate the structure of the tour; it is the area where it is possible to add panoramas and manage the relationships between them as well as chancing the default values parameters (Figure 3.18).
Once the pictures have been added we proceed editing the hotspots. These are the tools that regulate the interactions between the scenes, it is possible to bind a panoramas to one or more pictures. There are different kinds of hotspots and each one plays a specific role; some upload another panorama, others a photo gallery but also a 3D model or information sheets and map. It is a very dynamic and interactive tool.
The *Style* tab is useful for customize your project; it is divided in two areas: *Plugin* and *Spots library*. Depending on the different needs, which the first one you can personalize the interface of your virtual tour. It is possible to add different function

Figure 3.20: Examples of additional panels included in the virtual tour (http://virtualtourtorricostiere.altervista.org/)

and also customize the parameters of your plugins and assign actions on it. In our case, some of those used are visible in the figure 3.19, personalizing them according to our needs.

The *Spot library*, while, ménage the features of the hotspots; allows the possibility of loading different actions and organizing them by categories.

The procedure for both libraries is the same, the element that you want to incorporate it is selected, and it is added to the workspace. Once added each parameter can be modify from the same tab.

Finally, in the *Build* files are exported and it is possible to choose options for the creation of virtual tour. Once the process is completed, it is ready to be loaded on Internet and to navigate it (Figure 3.19).

As understandable this application allows the generation of different virtual tours according to our needs and preferences. It is an innovative database with which it is possible to navigate from one building to another or through visual connections or

through geo-referencing on the map; furthermore, the tour can be correlate with additional information such as historical or technical panels (Figure 3.20).

What we have done in our project (visible at the following link http://virtualtourtorricostiere.altervista.org/) is just an example of a possible intervention; the idea is not to focus only on the individual building but to concentrate on what was the strategy of the project. The aim of this virtual tour, therefore, is that of encouraging a greater digitization of cultural heritage. In this way it will be imaginable to have a unified source of information and also easy access not only for technical personnel but also for less specialized users in order to encourage the diffusion, the knowledge and the safeguard of our heritage.[8]

[1] Giribet J., (2011). La fotografia de molt alta resolució aplicada a la pintura mural, In *Revista cultural de l'Urgell*, 2011; p. 199-207.

[2] Jacobs C., (2004). *Interactive Panoramas: Techniques for Digital Panoramic Photography*. Berlin (Germany), Springer, 2004; p. 5,6,7

[3]Lowe D. G., (2004). Distinctive Image Features from Scale-Invariant Keypoints. In: *Iternational Journal of Computer Vision*. Vol. 60, Issue 2. Netherlands, Kluwer Academic Publishers, 2004.

[4] Douglas A. K., (2008). *The Proper Pivot Point for Panoramic Photography, s.l., s.n.,* 2008.

[5]GigaPan EPIC Pro User Guide (http://www.gigapan.com/cms/manual/pdf/epicpro-manual.pdf).

[6]Fanotec Spherical Panoramic Tripod Head Nodal Ninja 4. Manual (http://www.nodalninja.com/Manuals/NN4_USER_MANUAL.pdf).

[7]Autopano Giga Documentation (http://www.kolor.com/wiki-en/action/view/Autopano_Giga_Documentation).

[8]Panotour Documentation (http://www.kolor.com/wiki-en/action/view/Panotour_Documentation).

4. Basics of photography for photogrammetry survey

4.1 Brief overview of photography

The invention of photography dates back to 1826 with the first shot and the generation of a photo that today would seem almost handmade (Figure 4.1). The author of this shot was Nicéphore Niépce (1765-1833) and he made this with a pose of eight hours on a heliograph plate prepared by him.
The photography arose from the man's desire to reproduce what was actually seen in reality. The first needs were manifested around the XVI-XVII century, during this period, the conditions of travel were not the best, so the erudites and the curious, who wanted to know new parts of the world, had no alternative solution if not to use travel books with above reported incisions and representations of the cities[1].

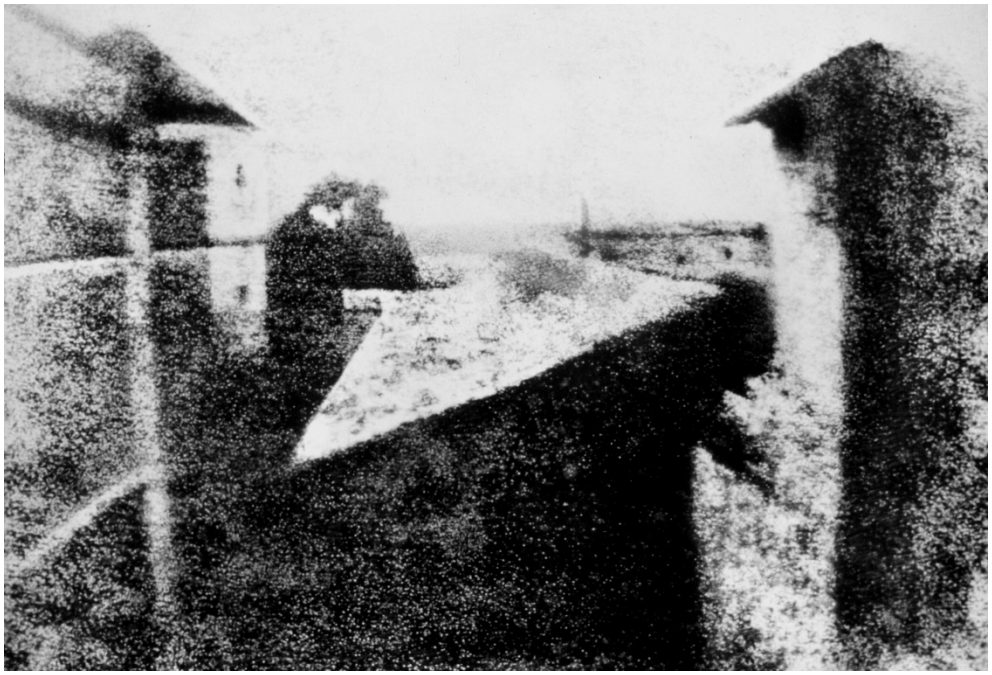

Figure 4.1: Joseph Nicéphore Niépce, View from the Window at Le Gras, 1826

Several, in fact, are the example of architectural representation of the painters and architects of the past; the graphic representation, in fact, was the main training tool of architects[2] but also the only way to stop the time and to impress a memory (Figure 4.2). A first goal was reached with the invention of the *Camera Obscura* (darkroom); a completely dark box where light penetrated only by means of a small hole near one of the walls. Therefore, in this way it was possible to reproduce a smaller and inverted image of the framed object, on the opposite side of the opening. From the renaissance onwards, this procedure was widely used, especially by the great Italian and foreign landscape painters (Figure 4.3).
However, the images that were projected could not be imprinted and fixed in time; these were representations only generated from the light, in fact, if the passage of the light rays was blocked, the image in the box disappeared. As previously anticipated, the first durable image and, so, unalterable from light, was made by the French J.N. Niépce achieved the expected result placing on the back of the black box a sheet covered with light-sensitive material, this process was called by himself heliography.

Figure 4.2: Leo von Klenze, Place before the Cathedral of Amalfi. (Cardone V., 2014)

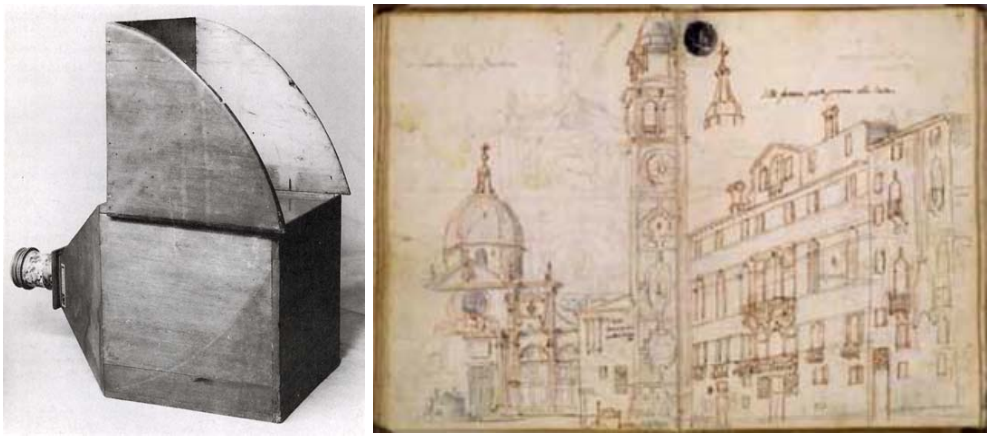

Figure 4.3: Canaletto's camera obscure (Museo Correr, Venice) and his sketch of the Santa Maria Formosa in Venice. (http://www.cultorweb.com/ottica2/Canaletto.html)

The term photography derives from the Greek φῶς (phôs) = light and γραφή (graphè) = writing, i.e. the writing make with light; it was only proposed in 1839 by the English astronomer John Frederick William Herschel (1792-1871) and immediately the name became universal. Subsequently, the process was further improved by Louis Daguerre (1787-1851) with the procedure called *daguerreotype*.
These were small photos printed on a metal plate sensitized with silver nitrate in which the passage of the light leaving the sign; with this process it was obtained photos in a very short time (a few minutes) and with very precise and defined results as seen in the image in figure 4.4.
After that, photography began to spread throughout the world both for landscape shots and for the realization of portraits. The possibility of obtaining copies of these images, one of the main limits of the daguerreotype, was superseded by the Englishman William Henry Fox Talbot (1800-1877) with the development of a technique that allowed an unlimited number of copies starting from a negative and also ensuring a greater detail of the shots. The method, called *calotype*, developed in 1840 and provided for the use not of slabs but of a paper negative; this is how current analogic photography is born.
In the rest of the years, there are different variations and developments that have been obtained, such as in 1861 with the colour projection by James Clerk Maxwell (1831-1879) obtained with the acquisition of three photographs of the same subject on three different plates through the red, green and blue filters.
The different slides, obtained from the three plates, were then projected by superimposition through three projectors, thus obtaining a colour image.

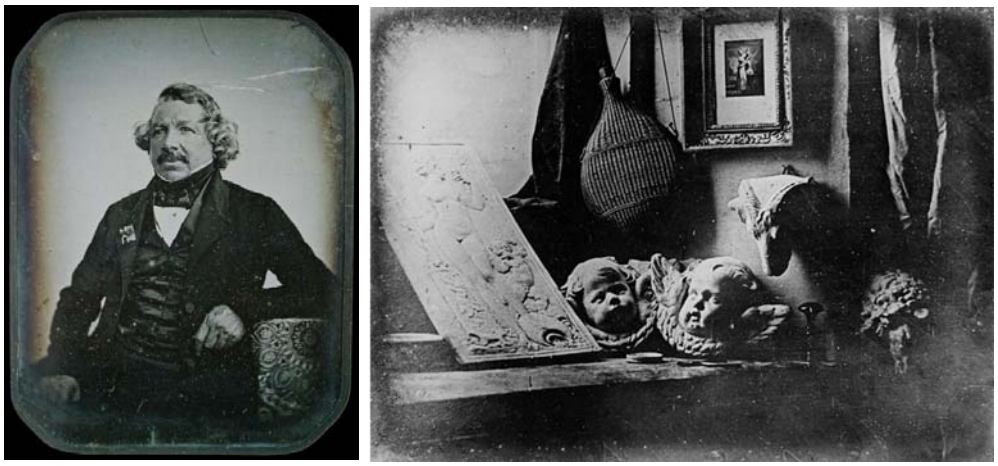

Figure 4.4: Louis Daguerre (1844) and his atelier (1837), daguerreotype

It is clarify that this chapter is not intended to reproduce the history of photography but simply introduce and intrigue the reader to a better understanding the photographic and photogrammetric technique in the field of Cultural Heruitege

4.1.1 Rapid evolution path of the instrument

The great and rapid development of photography, of course, was combined by the incessant evolution of instrumentation indispensable for acquisition that is the camera. The first photographers of the 800, in addition to the camera and the tripod, needed a real mobile laboratory (a tent or a dark carriage) necessary for the development of the photo. Around 1884, the American George Eastman (1854-1932) produced the first rolls film that in 1888 allowed him to market a camera with small dimensions and able to guarantee 100 snapshots. Once completed, the instrument had to be sent back to the manufacturer that developed the photos and recharged it with a film of 100 other shots; it was called KODAK camera and was produced by the famous Kodak Company (Figure 4.5a).
A further step took place in 1890 when a sort of external casing was used to protect the film from light and in order to replace it independently. In the 1904 there was a first patent of colour photography by the Loumière brothers, the *autochrome*, and in 1913 Oscar Barnack (1879-1936) designed a camera, with the Leica Company, light, pocket-sized and compatible with the film 35mm (Figure 4.5b). In 1914 was the year when Kodak designed the *Kodachrome*, a new photographer film commercialized

Figure 4.5: a. *Kodak camera advertising;* b. *Leica pocket-size camera;* c. *Polaroid camera*

since 1936 and out of production around 2010 when analogue photography was overwhelmed by digital photography. The year 1936 is also famous for another event, the development of reflex technology where it was possible observe the scene to be acquired through the viewfinder. The presence of a small mirror placed inside the instrument, allows straighten the image and, so, to analyse and refine the scene before acquiring it. Since then the system has evolved a lot but the basic functions have remained unchanged. Among the major advances in time we must also remember the first *instant cameras*, made in 1947 by Edwin Herbert (1909-1991) with the Polaroid system, which allowed to develop the film inside the camera (Figure 4.5c). In 1981 the founder of Sony introduced the *Mavica* (magnetic video camera), the first SLR that recorded colour images on a floppy disk and that could subsequently be printed or displayed on screen; therefore a first step towards the disappearance of the film.
In the following years there have been several developments in the field of photography; above all digital sensors where nowadays has completely replaced the use of the film.

4.2 Main types of digital cameras

There are different kind of cameras and each of which responds to different needs; below is a short list of the main types.
*Compact***:** this category includes all the pocket size cameras that are equipped with a photo sensor smaller than those used in SLR cameras. They can have zoom with external or internal excursion; in the first case they have a mobile zoom that extends outside the camera body, while in the second case the zoom, also called *periscopic*, occurs by means of mirrors placed inside of the machine body and, generally, do not exceed 5x zoom. The latter solution, despite permits the creation of more compact cameras, have more problems of brightness than the equivalent with external zoom.

However, in both cases these are photographic devices used by the "mass" and suitable for making souvenir photos without high quality levels. In recent years, nevertheless, have been produced high level models often used by many professionals as a second camera, obviously they are not comparable to a mirrorless or a SLR, since they have a sensor generally smaller and lower quality lenses.
*Bridge***:** allow the full control of the commands, but as in the case of compact, they have small sensors to the detriment of the final quality of the image. They come in sizes similar to SLR cameras and with lenses that are not interchangeable but with a high focal excursion.
*Reflex mirrorless***:** these are compact body cameras but with the sensor of a half-frame camera. They are interchangeable-lens like a reflex, but they have not optical viewfinder and consequently the scene is framed on the display (in some models there is the digital viewfinder). This type of camera is having a good success; above all because it is smaller than a reflex and also for the good performance that can obtain; however, despite the great developments that are taking place in the field of photography, the final quality at the moment is not comparable to that of reflex.
Monocular Reflex (SLR): interchangeable-lens cameras and with the mirror necessary to frame the scene in the viewfinder. They allow changing any parameter and are characterized by sensors of greater dimensions than the previous ones, to the detriment of the weight and the physical size of the instrument.
In the full frame SLR the sensor size is 24x36mm, as the size of a frame of the previous photographic films. There are also some entry level SLRs where the sensor is smaller, about 16x24mm.
Medium format monocular reflex: they are similar to the previous ones, only the size of the sensor is different with dimensions until 6x6cm able to guarantee images of remarkable quality. They are the machines used by studio and landscape photography professionals because they have a great dynamic range, a very low noise even at high ISO and a high number of megapixels.

4.3 Main elements of a camera

The *box* which consists of the outer envelope and contains most of all the other elements of the instrument; the fundamental characteristic is that it is perfectly light-tight and completely black inside.
The *lens* that allows the passage of light inside the camera body and whose role is to adjust the focus, the energy at the input (amount of light) and the geometry of the

shot. The simplest case consists in a single lens near the tiny hole (called *pinhole*) which through the passage of light rays generates an overturned image inside a dark room. However, in this case, the acquired object is subject to optical distortions; the problem can be solve with more lenses.
Among the main characteristics that define a lens, we certainly have the *focal length* that, as shown in figure 4.6[3], represents the distance between the centre of the lens and the plane where the image is formed, *focal plane* (or *camera senor)*. As mentioned above, lenses often have more lenses, so the distance is not measured from one lens in particular, but by the optical centre of the lens. The focal, in turn, is fundamental for the determination of the *angle of field* and, consequently, of the image size on the focal plane. As comprehensible in the image in figure 4.7 with the same distance between the subject and the lens, a long focal length produces a larger image than a short focal length. Consequently, if you want to keep the size of the projected image fixed, as the focal length changes, the distance of the subject detected by the lens have to also be changed; in particular move away in case of long focal length and move close with short focal length.
Another characteristic to consider is the *angle of view*, measured in degrees and depended on the lens and the frame size on which the image will be projected. The latter, generally, has a rectangular format and, so, two angles (vertical and horizontal) should be considered. However, in order to avoid misunderstandings, as a rule we refer to the angle relative to the diagonal of the rectangle.

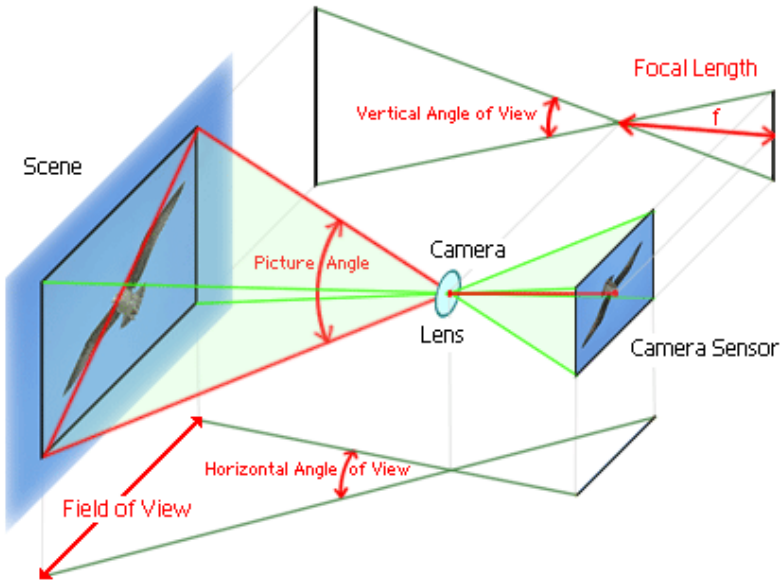

Figure 4.6: Representation of focal length and angle of view

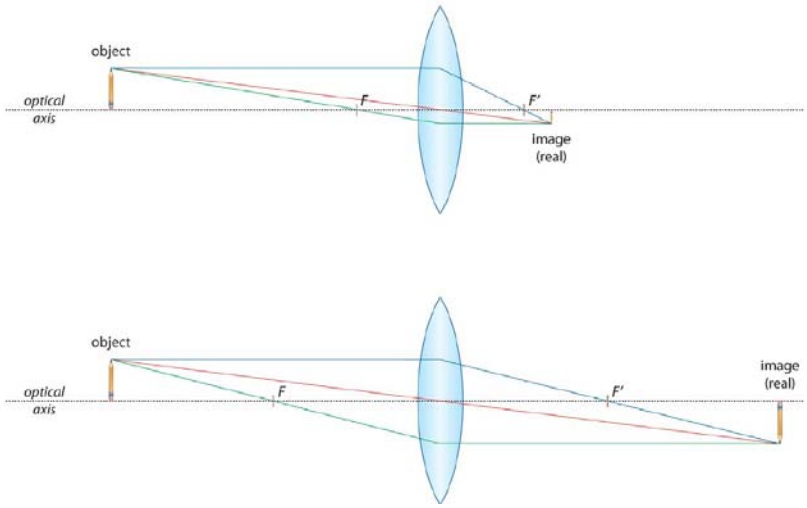

Figure 4.7: The effect of increased focal length on subject. (Verhoeven G., 2016)

On the market there are different types of lenses, the following are the most common: *standard* (or normal), with a focal length about 50mm and a field angle of about 45°-55°; *wide-angle lenses*, with shorter focal length than normal and, consequently, with a large angle of view that varies between 60° and 80° but that can extend up to 180° in *ultra-wide angles* (these lens modify the perspective and so the perception of depth); *telephoto lenses* with a deep focal length and with angle of view ranging from 20° to 5° or even, in extreme cases also with lower values (Table 4.1).
The *mirror*, the element that allows to show in the viewfinder the scene visible from the lens. Generally, it is inclined at 45° so as to direct the light towards the pentaprism; at the moment of shooting, this mirror rises, making it possible to pass the light towards the sensor.
The *pentaprism* is the system to observe real and non-inverted image of the scene inside the viewfinder. For economic reasons, many cameras use a system of five mirrors, known as a less expensive and lighter *pentamirror*, but at the same time, returning a less luminous frame of the scene, makes manual focusing more difficult; it has no influence on the final quality of the images.

Lens focal lengths	Lens type	Photography type
Less than 20mm	Extreme wide angle	Architecture
21mm – 35mm	Wide angle	Landscape
35mm – 70mm	Normal	Documentary
80mm – 135 mm	Medium Telephoto	Portraiture
135mm – 300mm	Telephoto	Sport and Wildlife
Greater than 300mm	Super Telephoto	Wildlife

Table 4.1: Main type of lens (the values are for 35 mm equivalent cameras)

The *viewfinder* is the device where the scene is displayed and often the indicators for focus and exposure too. It is right to underline that a total coverage is possible only with professional cameras, while, in the cheaper ones, only 90-95% is visible and, therefore, an inequality between the scene observed and the one that will actually be acquired can be generated.
Unlike digital compact cameras on digital SLR cameras, it is not possible to view the scene on the LCD monitor. This happens because the mirror cover the sensor; however, the progress made in the last years in the photographic field has made this possible with the so-called *live view* (function that allows you to see the scene in real time on the camera's LCD screen).
The *diaphragm* generally is located in the lens and determines the amount of light that will impress the film or the sensor. This element can be fixed or not; in the first case it is characterized by a single hole of predetermined diameter, while in the second one it is possible to adjust the size of the opening. Most of the devices on the market today are equipped with an *iris diaphragm* (which works similarly to that of the human eye); it consists of a fixed metal ring on which blades are hook, the number can vary from six to fifteen. Its trend is connected to the brightness in the scene; in particular, in the presence of poor light it will be advisable to increase the opening of the hole, otherwise decrease it.
The value of the aperture of the diaphragm is the *f-number (*or *focal ratio)*, the ratio of the focal length of the lens to the diameter of *entrance pupil* (paragraph 3.3.1).
As can be seen in the image of figure 4.8 a diaphragm f/2,8 provides an aperture larger than f/8 and the diaphragm close as you move towards higher numbers, up to f/22 that has the opening as small as possible. As explained previously, the diaphragm is formed by a series of blades that open or close depending on the value that we set. Although the shape of the split is a polygon, it is convenient to approximate it to a circle in order to standardize and simplify the calculations; the results are sufficiently similar. As is well known, the area of a circle is πr^2 and, from the equations of optics, we know that:

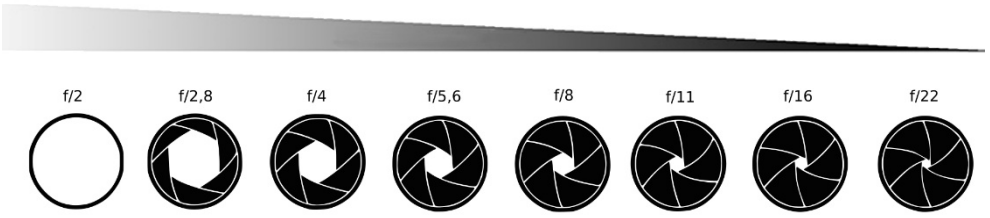

Figure 4.8: Diaphragm apertures and variation of light

$$N = \frac{f}{d}$$

where is it:
N = opening value;
f = focal length;
d = diameter of the entrance pupil.
From this formula, therefore, it is simple to calculate the diameter $d = f/N$ and consequently also its radius $r = f/2N$ which can be substituted in the equation of the circle area $\pi(\frac{f}{2N})^2$.
For example, the calculation on a 50mm lens and with a diaphragm at f/4, f/5,6 and f/8 respectively, the result will be:
- $Area\left(\frac{f}{4}\right) = \pi[\frac{50}{2*4}]^2 = 123mm^2$
- $Area\left(\frac{f}{5,6}\right) = \pi[\frac{50}{2*5,6}]^2 = 63mm^2$
- $Area\left(\frac{f}{8}\right) = \pi[\frac{50}{2*8}]^2 = 30mm^2$

Analysing the results obtained, it is possible to notice how the quantity of light go through the first value is twice that of the second; so for each stop the area of the diaphragm (and therefore the quantity of light that passes through it) is halved.
The *shutter* is the mechanical or electronic device, which control how long the sensor remains exposed to light once has passed through the diaphragm; they can be of *central* type and a *curtain*. The first, similar to the diaphragm, is made up of a series of movable blades, placed between the lenses of the lens, which open only at the time of shoot for the pre-set time. In the curtain shutter, instead, we have two metal surfaces placed near the sensor; when the photo is taken, they run at a certain speed

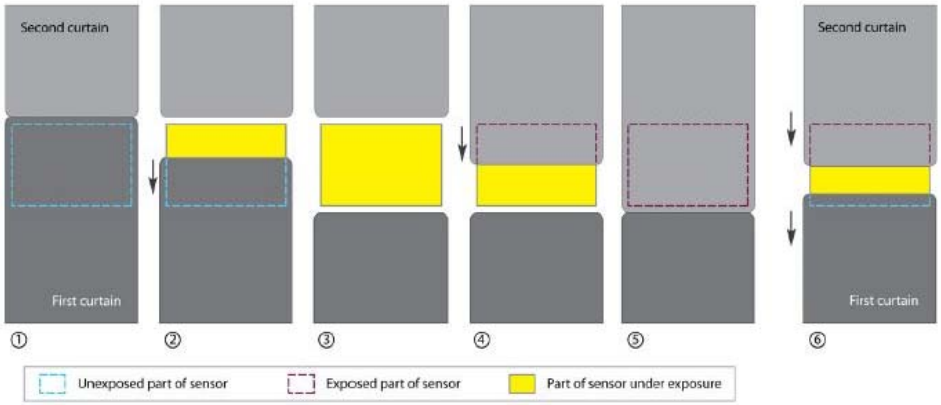

Figure 4.9: The appearance of the curtain shutter at various speeds. 1-5 are the steps of a slow shutter speed, while 6 is a fast shutter speed. (Verhoeven Geert, 2016)

exposing it to light. The time that device is open and, therefore, the amount of light that impress the sensor is used for valuate the *shutter speed* or *exposure time.* It can be expressed in seconds or fractions of a second: 1/32000s, 1/16000s, 1/8000s, 1/4000s, 1/2000s, 1/1000s, 1/500s, 1/250s, 1/125s, 1/60s, 1/30s, 1/15s, 1/8s, 1/4s, 1/2s, 1s and also higher values per second.
It can be noted that when the shutter speed varies the speed of movement of the curtains is not very different. What change is the area directly exposed to sunlight, so if less time is required, smaller the area will be exposed, as shown in figure 4.9 (the movement of the curtains was taken up again in 2008 by the photographer Marianne Oelund who made a slow motion visible at the following address http://regex.info/ blog / 2008-09-04 / 925).
Another type of shutter, which has been spreading in recent years and used mainly in mobile phones and low-cost machines, is an electronic type. In this case the operation depends on the interruption or not of the current flow in order to allow the *photosites* to transmit the charge; the main advantages are above all for the high energy saving and its reduced dimensions.
Based on what has been said, it is possible to understand how both the shutter and the diaphragm contribute to regulating the passage of light towards the sensor; it is

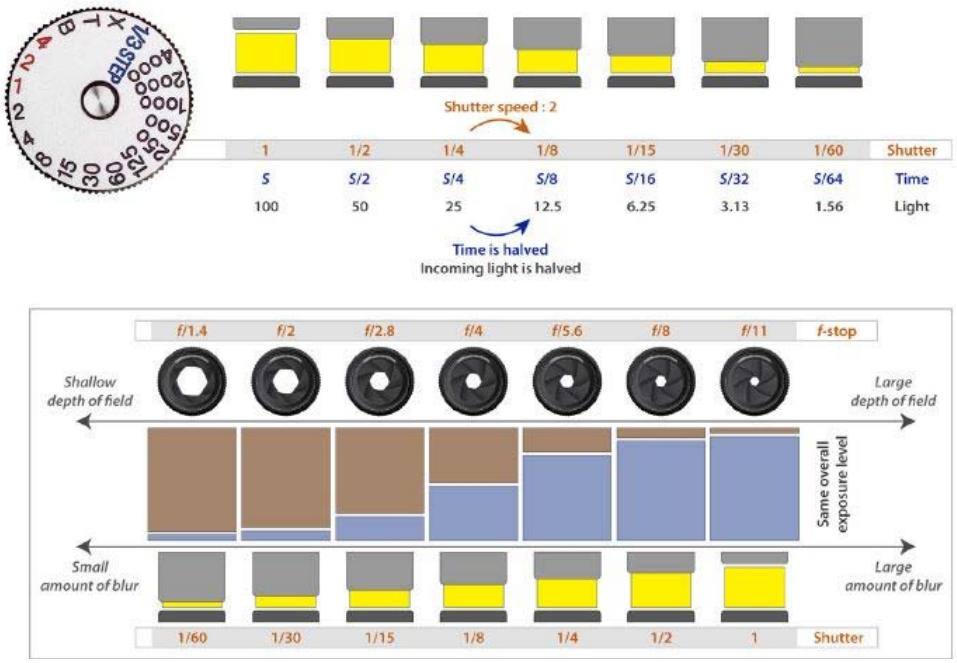

Figure 4.10: Explanation of shutter speed and its reciprocal relationship with aperture. (Verhoeven Geert, 2016)

therefore necessary to highlight the close relationship that exists between them. To make it easier to understand, we can imagine the diaphragm as a window that can be more or less open, while the shutter as a curtain that regulates the passage only for a certain time. The relationship that binds these devices is called *reciprocity*: the opening of the diagram and the exposure time are inversely proportional to each other; that is, if we double one we must halve the second so that the quantity of light necessary is unchanged (Figure 4.10).
The *sensor*, consists of a particular silicon device able to detect and record the electromagnetic energy coming from a scene and convert it into useful information for subsequent analysis. Therefore, it translates the incident power into a signal more easily manageable as the electric voltage; it corresponds to the ancient film used in previous cameras.
The *photodiodes* are the smallest photosensitive particle of the sensor, they convert light into an electrical signal, the pixel (Picture Elements). The size of this photographic element, therefore, depends on the number of micro-detectors that compose it and that have various dimension in relation to the type of sensor that we consider; from 4µm to 80µm for CCDs up to 1,4µm for new CMOS sensors. The differences between CCD and CMOS, subsequently more analysed, depend on the manufacturing process and the layout of the circuits, but in both cases, they are platelets that collect and convey the light.
Once the shutter is pressed, the exposure of the sensor for the pre-set shutter speed begins, from this moment every particle composing it is discovered in order to collect and store the photons of the light. Once the shutter speed has elapsed, the data transfer stops and the number of photons fallen in each photodiode is evaluated. The absorbed quantity is commensurate with intensity levels to which different depths of bit correspond and therefore of final precision of the photo (in figure 4.11 the example for an 8-bit image is proposed). The optical sensor, therefore, is a sort of photon counter; it conveys and transforms the light that hits it into electrons in relation to the quantity of the photons that have been collected by the micro-detectors.

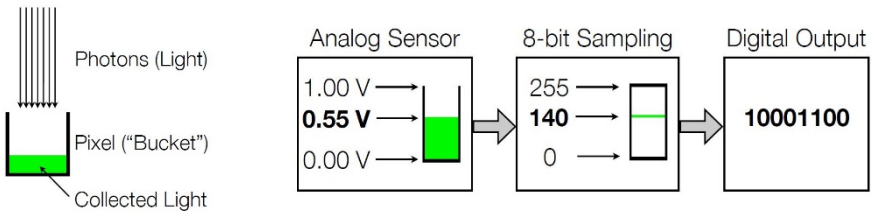

Figure 4.11: Scheme of how a sensor collects and convey the light. (Digital Photography course, ALISON)

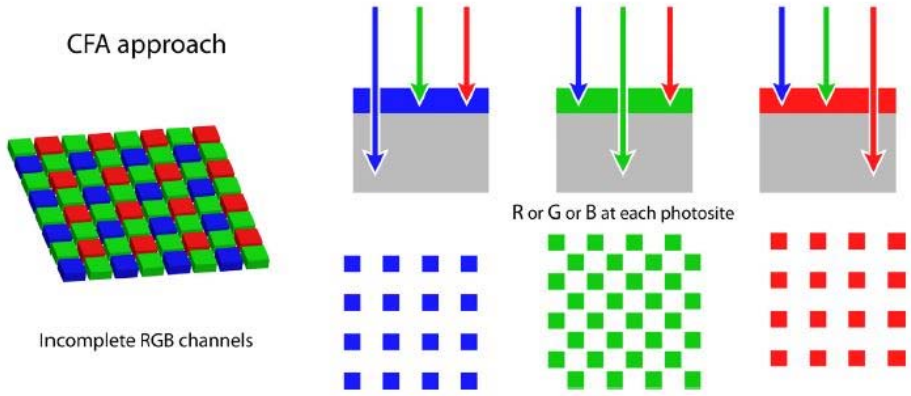

Figure 4.12: Photosite-specific spectral information acquired by the Bayer filter. (Verhoeven Geert, 2016)

Quantum efficiency (QE) is a design feature of the sensor and describes its response to different wavelengths of light. Generally, the same amount of photons absorbed is converted into equal quantities of electrons, regardless of what are the options set in the camera during the shot. A fixed maximum number of electrons that can accumulate inside, indicated by the acronym FWC (Full Well Capacity), characterizes each microelement of the sensor. When the number of electrons exceeds the capacity of absorption, a part of these will flow into adjacent pixels. In this regard, it is easily deduced that at least the amount of light that impress the sensor will be less the electrons produced and, consequently, more defects on the picture will be possible.
Moreover, the sensors do not transmit any information on the colour, they only reacting to the photons that hit it and converting them into electrical charges; in fact, to obtain the colorimetric information, it is necessary to place an identical matrix

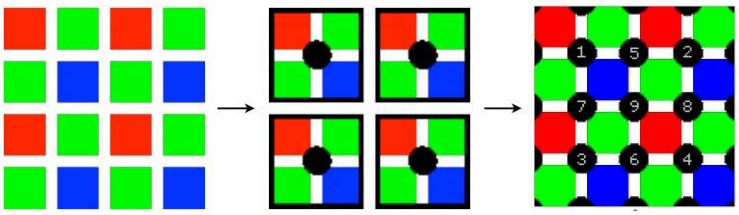

Figure 4.13: Bayer demosaicing process of translating the primary colours into a final image which contains full colour information at each pixel. (https://www.cambridgeincolour.com/tutorials/camera-sensors.htm)

filter with red, green and blue pattern before the sensor. Among the most common types of filters on the market, we find the Bayer filter and Foveon X3 sensor.
The first one is colour filter array (CFA) for arranging RGB and consists of a pixel pattern (Figure 4.12), each of which acquires a single colour, generally has a predominance of green because the human eye is more sensitive to this colour and, consequently, perceives more details and shades. It is composed of 50% green, 25% red and 25% blue pixels. Since each pixel is filtered to record only one of the three colours, the data obtained does not correspond perfectly to reality; for a truthful image, the photographic processor have to apply an algorithm called *demosaicing* (also *de-mosaicing*, *demosaicking* or *debayering*). The technique is an interpolation that allows the detection of the chromatic values in a point, starting from the adjacent pixels. For each group of 2x2 pixels (2 green, 1 blue and 1 red) the chromatic values information is mixed and, than, the resulting colour is interpreted for that precise quadrant. Starting from the three primary colours, therefore, it is possible to generate the final image with the respective colours.
In figure 4.13, for example, the first pixel is obtained starting from the red at the top left and, moving in a clockwise direction, from the green to its side and then, from the blue and the green placed below the first two. The next pixel on the same row, instead, is obtained starting from the green immediately following the first red and so on. With the exception of the pixels on the edge, therefore, all the others are used to obtain colorimetric information for 4 pixels. Photographic processors often reconstructing also missing chromatic information use several algorithms. The demosaicing, however, can give some affected, the most common is known as Moiré which occurs mainly when trying to reconstruct the lattices. To remedy this problem,

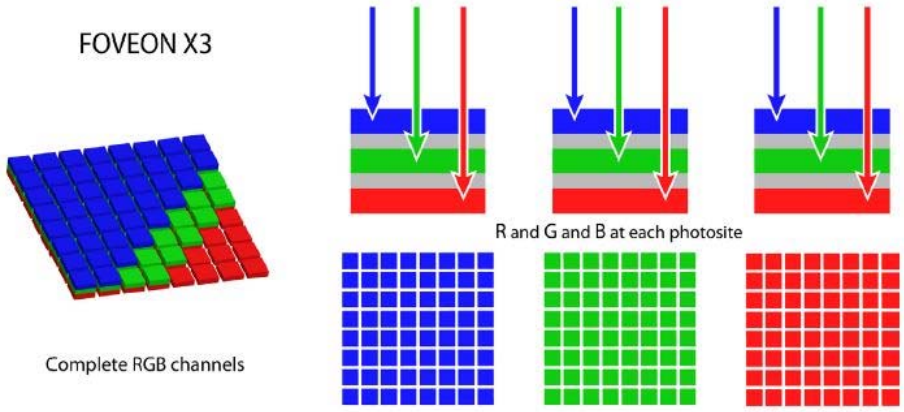

Figure 4.14: Photosite-specific spectral information acquired by Foveon sensor. (Verhoeven Geert, 2016)

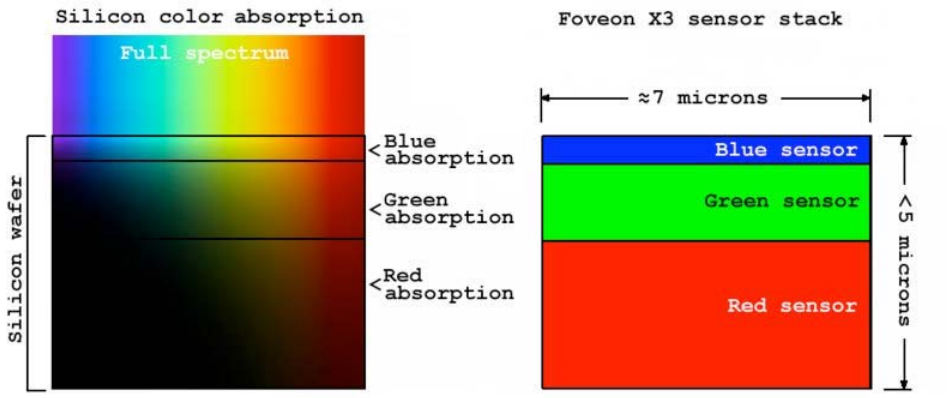

Figure 4.15: Color absorption in silicon and the Foveon X3 sensor. See text for explanation

classifiable as *spatial aliasing*, it is advisable to use physical filters consisting of a lens placed in front of the sensor.

The second type of sensor, instead, consists of three overlapping channels (from top to bottom blue, green and red as shown in figure 4.14) so that the single pixel of the pattern can return the signals of the three chromatic components of light (RGB). The chromatic information is obtained by analysing the incident radiation on the photodiode and its level of penetration; the deeper it is, the longer its wavelength is. From the image in figure 4.15 we can understand how the band of blue corresponds to shorter wavelengths and therefore with a reduced penetration capacity, followed by the green one and, finally, the red one.

Once again, so, the final chromatic value is obtained by the interpolation of three information, but in this case coming from the different vertically silicon layers. Moreover, unlike the Bayer filter, this information is not used to determine indications of adjacent pixels but only for itself; the demosaicization algorithm is not necessary.

As previously mentioned, there are two types of sensors on the market, the CCD (Charge Coupled-Devices) and the more modern CMOS (Complementary Metal-Oxide-Semiconductor). In the first, the electrical charge stored by the individual photodiodes is transferred, along the micro-detector lines, to the edges of the sensor where it is amplified and, finally, transformed into a digital signal from a ADC (Analogic to Digital Converter) converter. Mainly the reading process distinguishes the types of CCD sensors from the previous and, therefore, the way in which the charge transport stored in the sensor element is organized.

In the case of CMOS (Figure 4.16), the charge of the impress light is transformed by an integrated amplifier and directly attached to the single pixel, a transfer area is not

required. In this type of sensor, therefore, each pixel has its own voltage charge conversion, and often includes amplifiers, noise correctors and digitizing circuits.
The CCD sensors technology require more complex industrial processes than CMOS, however they are more sensitive to low lights and generate less noise. On the other hand, the greater simplicity of the CMOS design allows the creation of reduced sizes, and so greater versatility. In the last years, however, advances in technology have improved both technologies; the great difference that until now existed is coming less and less.
Another way to differentiate the sensors is also their resolution, i.e. the number of pixels that compose it. The abbreviation MP is the millions of pixels used in photo generation and is obtained by multiplying the number of units along the base and along the height of the sensor. Another feature to consider, besides the number, is the size of the single pixel of the sensor. The smaller pixels guarantee excellent resolution but suffer from noise, lower tonal range and low sensitivity. Being small, in fact, they intercept less photons and, therefore, can contain less electrons; these effects are evident above all in the compact ones whose pixels do not reach 4μm. Large pixels, on the other hand, have a good signal-to-noise ratio, good sensitivity and wider tonal range. However, they can suffer from aliasing phenomena, that is, in the case of photography, when there are not enough pixels to capture all the details of a scene.
The sensors dimensional information is indicated with fractions, such as 1/1.8” or 2/3”, even if they do not correspond to the actual length of the sensor’s diagonal. It derives from the techniques used in the 50s for the production of *cathode ray tube*

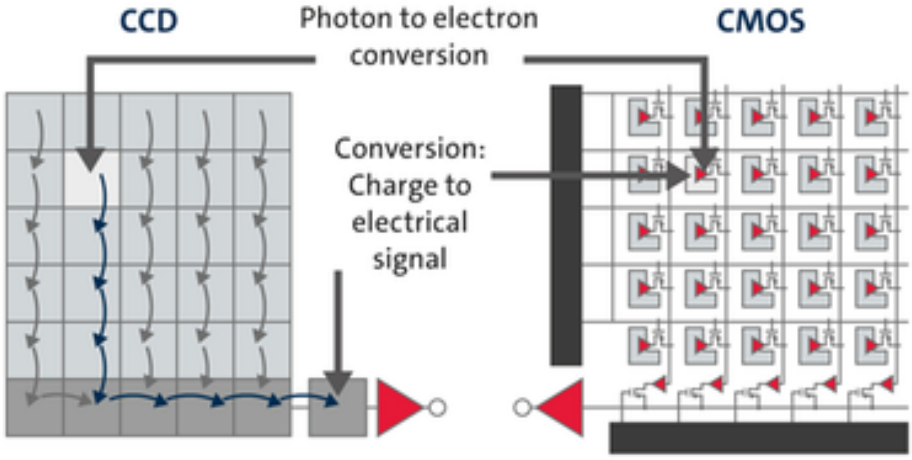

Figure 4.16: Different principles of CCD and CMOS. (http://fpvlair.com/wp-content/uploads/2015/08/ccdcmos.png)

Figure 4.17: Formats of some digital sensor and their related proprieties. (Verhoeven Geert, 2016)

televisions. Inches units were used and these fractions corresponded to the diameter of the outer circle in which the rectangle was inscribed. Soon, however, it was discovered that the real usable area of this plane was about two-thirds of those designated; imprecision transmitted even today to photographic sensors. In fact, to measure the real size of a sensor, it is necessary to consider about 2/3 of that indicated by the manufacturer (very similar to what happened for the tubes). For example, if we consider a 1/6" diagonal sensor, we had a real dimension of about 2,69mm.
The value in mm of the diagonal is obtained considering the inch size:
1/6" = 0,16"
where 1"= 25,4 mm is obtained
0,17*25,4 = 4,06 mm

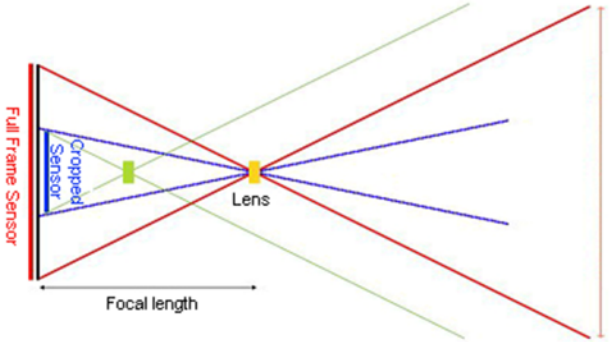

Figure 4.18: Full frame sensor vs smaller sensor and the impact on field of view

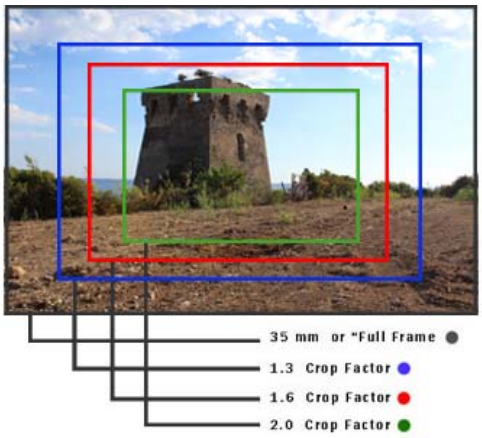

Figure 4.19: Difference between Full Frame and Crop sensor

that is the dimension in mm of the diagonal, but considering that only 2/3 correspond to the really used diagonal of the sensor, it will be about
d = (4,06*0.66)/1 = 2,69 mm (as shown in the figure 4.17).
One of the characteristics that strongly related with the sensor size is the geometric resolution of the frame, with the same focal length. If we analyze the figure 4.18 we can see how, keeping the focal length constant, the field of view varies as the sensor size changes; increases to increase in size. Essentially, it is possible to identify two types of sensors in relation to the dimension: *full frame*, 24x36mm equivalent to the classic 35mm film format and *smaller sensor*, such as the CMOS of the Canon APS-H of 19x29mm (equal to 63% of the full frame). The latter are characterized by a multiplication factor with respect to the full frame known as the *crop factor*, so, at the time of the shot, the same scene can be captured differently depending on the sensor on the instrument.
Figure 4.19, for example, shows a capture made by three different types of sensors; in the case of scale factors of 1.3, 1.6 and 2.0 there is the sensation that the focal length is extended by a certain value; in reality the only variation regards the angle of field, while the focal length remains unchanged.
It should also be noted that on each lens will always be given the focal length relative to a full frame and that therefore this value must be multiplied by the crop factor in the case of a smaller size sensor. It is important to know this aspect during the acquisition; in case of wide-angle, for example, if we wanted to get the result of a full frame with a 24mm lens on a sensor with multiplication factor 1.6, we should use a 15mm lens.
Finally, we have to remember that, at the time of the shot, the signal acquired by the sensor is a Raw file that means “not processed”, “unrefined” or “raw”. This epithet

indicates that the captured image is recorded in its original form, i.e. it only undergoes conversion from analog to digital.
The *flash* is a device that emit blazes of light during a snapshot for illuminate the scene. It is generally incorporated in the camera but, in some reflex cameras, there is the possibility of adding a much more powerful and functional external device, housing it in the special slide.
Another component of the camera is the *optical filter* that is interposed between the light information coming from the outside and the photosensitive layer. They are different in relation to the type of signal that allows to pass, such as hindering the passage of precise wavelengths or simply to attenuate their intensity, below are some of the most widespread.
UV filters are used to protect the lens from dirt, water drops, scratches and accidental impacts. The main purpose is to filter ultraviolet rays that, even if not visible to the human eye, are perceptible by film and photographic sensors and are present above all at high altitudes. It is possible to obtain slightly more clear skies and sharper images, in addition to reduce blue dominant possibilities.
Neutral Density filters reduce the amount of light pass through the lens and are useful for long exposures in brightly lit environments; they do not introduce any chromatic variation but simply attenuate the incoming light in a neutral way.
The *polarizing filters* reduce the effects of reflections coming from particular surfaces, such as glass or water, in this way, it is possible to restore the real transparency of the surface and so what is beyond is visible. It also allows you to obtain more saturated and contrasted skies, minimizing the reflections caused by the water vapor present in the air (Figure 4.20).

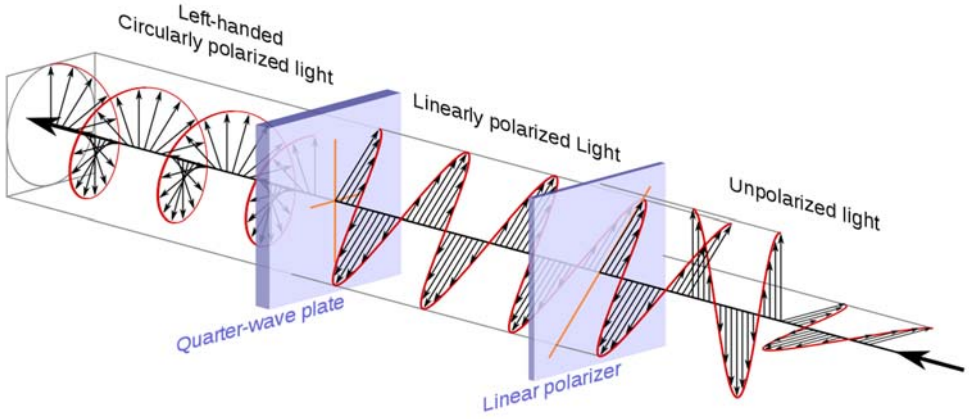

Figure 4.20: Polarizing filter that passes light of a specific polarization and blocks waves of other polarizations; the common types of polarizers are linear polarizers and circular polarizers. (http://enacademic.com/dic.nsf/enwiki/11546411)

4.3.1 Tips for an optimal shooting

In order that a framed scene can become a photo it is necessary that the light rays follow a precise path: they pass through the lens (with the diaphragm completely open) and reach the mirror which, inclined at 45°, reflects them towards the pentaprism which, in turn, send them to the viewfinder. When we press the shutter-release button, the diaphragm closes up to the value set by us, the mirror rises, the shutter opens, for the pre-set time, and the light rays are deposited on the sensor. The image will be imprinted on the latter, which will then be stored as digital data in the memory card.
Knowing the parts of the camera, so, it is just the starting point for obtaining a good picture. Below we will analyze the main elements to be evaluated for optimal shot.
The *focus* in order to obtain a clear image; consists in adjust the distance between the lens and the focal plane. It can be done in automatic or manual mode, in the first case, *autofocus,* it will be the electric motor inside the machine or the lens, to make all operations. In the second case, instead, the focus will be achieved by rotating the appropriate ring on the lens until the optimum sharpness is reached. Generally it is better to increase the focal distance if the subject is close, i.e. move the lens away from the film; and, vice versa, decrease the distance if the subject is far away.
The *depth of field* that identifies the area within which the subjects can be captured will appear sharp in the image. It should be noted that the lens can not focus objects placed at different depths at the same time, so the focus can only take place with respect to a plane and anything that is in front of or behind it will gradually be out of focus; however, within certain limits the eye is able to accept the image as clear.
As explained previously, the aperture of the diaphragm controls the amount of light passing through the lens; but not only. In fact, different depths of the field correspond

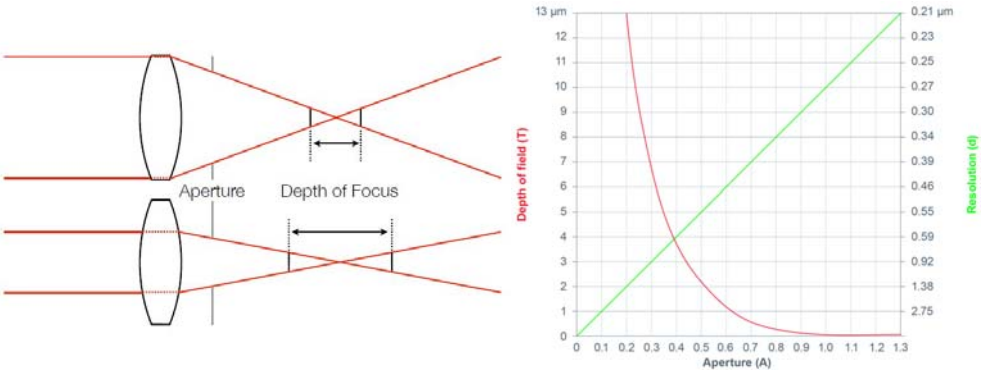

Figure 4.21: Diagram and scheme how the depth of field varies with the change of the aperture. (Digital Photography course, ALISON)

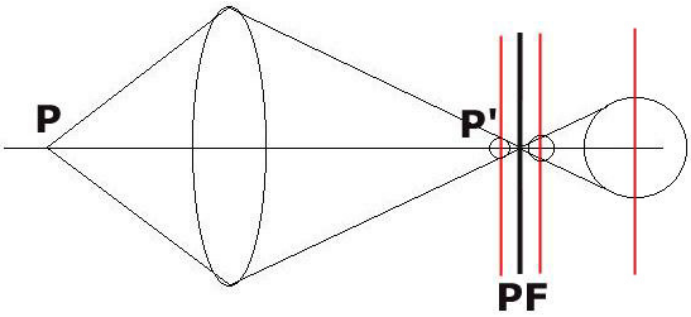

Figure 4.22: P' and P" to identify the depth of field in which the image appears sharp

to the variation of the aperture; reduced in the case of open and extended diaphragms with closed diaphragms. Also the sharpness is related with this variation; it tends to gradually decrease both forward and backward with respect to the framed subject (Figure 4.21). Another aspect to consider is the focal length of the lens; shorter focal lengths, in fact, have more extensive depth of field.
The formulas for determining the anterior (P) and posterior (P') limits in which the image appears sharp (Figure 4.22) are the following:

$$P = \frac{H \cdot D}{(H + D)}$$

$$P' = \frac{H \cdot D}{(H - D)}$$

where:
H = hyperfocal distance
D = shooting distance
The *hyperfocal distance* represents the distance on which to focus so that all objects at distances from half of it out to infinity will be acceptably sharp. In the case of a Canon EOS 300D with focal length 18mm and f/11 we obtain a value of 1,6m which implies that the whole scene in focus will be from about 0,8m to infinity.
These values result from the following calculation:

$$H = \frac{f^2}{Nc} + f$$

where:
H = hyperfocal distance
f = focal length

N = aperture of the diaphragm
c = limit of the circle of confusion
However, there are several applications that make the practice much more immediate and easier to download even on smartphones.
The *circle of confusion (CoC)* is the blur effect generated by the projection of a point on the plane sensor in the absence of a correct focus, it shows more with the points of maximum brightness. In figure 4.22 we can see the example of the focusing of an image point placed near the focal axis; when the lens focus is correct it will be clearly represented on the sensor. Moving forward or backward from this point (or by changing the focal length), the CoC will tend to increase or decrease, respectively. The concept of circles of confusion is related to the visual acuity of the human eye, in fact, it will come to a point where the eye will no longer be able to distinguish the circles and, therefore, the best focus of the point will be apparently reached up.
Following several studies done on a number of testers it was found that by observing a print of 20x25cm (8x10") from a distance of about 32cm (equal to the diagonal of the print) all the small circles with a diameter equal to or less than 0,25mm they will appear to us like points.
The CoC is particularly important for determining the depth of field, considered as the portion of space (delimited by the front and rear planes) in which all the points have a diameter smaller than the circle of confusion related to the shooting format that we are using. Seeing again the images in figure 4.22, in fact, as closing the diaphragm, the angle of the light cone becomes more acute and consequently the

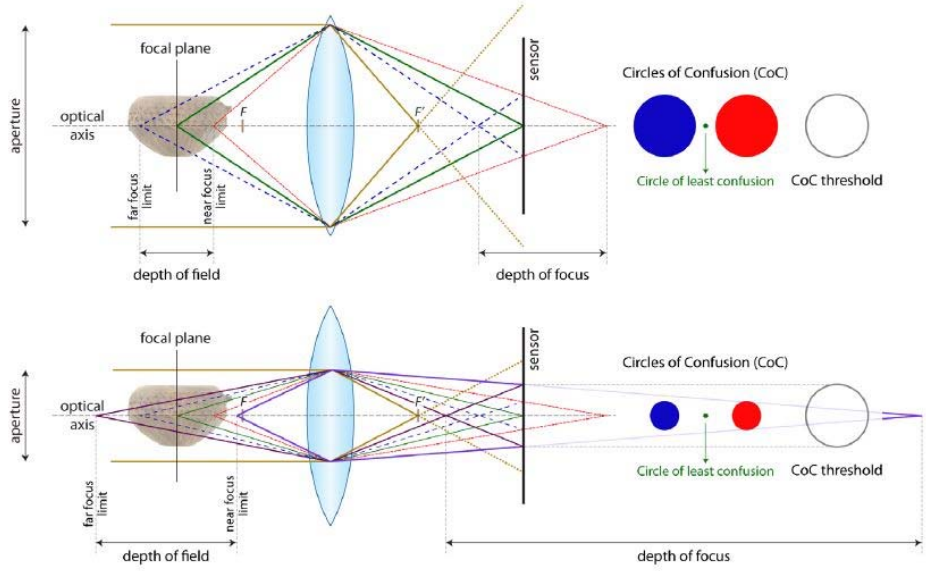

Figure 4.23: The influence of depth of focus for the CoC. (Verhoeven Geert, 2016)

limit defined as the diameter of the circle of confusion is reached at greater distances, increasing the area of focus.

ISO Sensitivity indicates the sensitivity to light that the camera sensor can take. At the time of the film, to each of it corresponded a value and, therefore, as the needs changed it was necessary to replace the roll. In the case of digital photography, instead, this problem does not exist because, when the lighting conditions change, it is sufficient to modify the settings in the camera. For these values a conventional sequence has been established and, as for the films, the highest image quality is opting for lower ISO values which, however, require a greater quantity of light in the environment. High numbers of sensitivity imply a greater ability to capture images in poorly lit sites but, at the same time, increase the risk of noise in images.

Exposure is the process in which the light, reflected by a subject, passes through the lens until it hits the sensor for a specific time, where the image is formed.

There are three factors that mainly affect it: diaphragm aperture, exposure time and ISO. For an optimal result, in fact, it is necessary to check the right quantity of light that have to pass through the lens by setting an appropriate diaphragm aperture. Then, the shutter opens for the time necessary for the light to impress the sensor in order to record the scene. The three elements, as can be understood, are closely related to each other; each modification of one corresponds to a change in the other two. In order to understand this concept, in a simple and intuitive way, we imagine having to water a garden. We have two tubes, connected to a tap and having different diameter (ISO). In the case of plants that require a lot of water, it is convenient to use a wide tube (ISO high), otherwise, a tube with a reduced section (ISO low). Once established the diameter to use, the time to fill it (exposure time) will depend on how long the tap will be open (diaphragm aperture); if you open a little the flow will be small and precise and the filling will be slow; on the contrary, by opening a lot, the container will quickly fill.

It is easy to deduce that it is possible change one or the other parameters to obtain the same result; if, for example, at the same ISO, we set an aperture of f/11 with an exposure time of 1/50s, will enter a quantity of light identical to that one would have with an aperture of f/8 and a time of 1/100s. However, this will be valid only with

Figure 4.24: The interplay between aperture, shutter speed and ISO value. ((Verhoeven Geert, 2016)

regard to the amount of light that will enter the device, but not with regard to the depth of field. In fact, despite the amount of light entering remains unchanged, using a certain aperture diaphragm and exposure time rather than another is not completely indifferent; in particular, as the aperture of the diaphragm decreases (and consequently increases the shutter speed), the depth of field increases, as already seen above.
When operating in manual mode it is possible to see the values set by us inside the optical viewfinder. In particular we should see the pre-set configuration and a scale in which the camera interprets the available light: if placed to the left, there is not enough light, otherwise is too much.
Practically, to calculate the different set values and consider the relationship between one and the other it is used the exposure *light meter*. This instrument measuring light: fixed the ISO value, in fact, provides an exposure value function of time and aperture. It allows, therefore, to establish the correct parameters to be set in order to avoid images *overexposed* or *underexposed* (concepts deepened later). The *light meter* can be both internal and external. The first ones are inside the camera, and measure the intensity of the light reflected by the subject framed in a certain direction and that passes through the lens; TTL (Through The Lens). The latter, on the other hand, make it possible to measure not only the reflected light, but also the incident light; in particular the measurement of the reflected light occurs by pointing the instrument in the direction of the subject to be detected, while the incident one is acquired by placing itself next to the subject and pointing it towards the light source.
Generally, digital SLR cameras are characterized by a TTL light meter. In this case the measurement can be: *manual*, setting both the value of the diaphragm and the times; *automatic partial aperture priority*, so we set the value of the diaphragm and leaving to the automatic procedure the correct evaluation of the shutter speed; *automatic partial shutter priority,* differently from the previous case by setting the value of the shutter speed and leaving to the automatic procedure the correct evaluation of the aperture and finally *fully automatic* in which the camera will decide which values of aperture and shutter speed to use depending on the lighting conditions.
The aforementioned instrument is a light intensity indicator but, nevertheless, it works perfectly only in certain situations and in some cases it can also give wrong results. This occurs because the light meter inside the SLR is calibrated to reproduce an average grey at 18%, i.e. able to reflect this percentage of light. In this regard, every time a shot is made, the camera considers the tone of the subject as if it was of medium tone, consequently if the scene presents a brightness comparable to the average grey one will obtain correct values, otherwise a lighter or darker scene, we will have unreliable values. When, for example, a white subject is acquired, the light

meter interprets it as if there was an excessive reflection and, therefore, tends to compensate it considering that it requires less exposure; with the purpose of returning a grey instead of white. In the case of a black subject, on the other hand, it tries to compensate for it by lightening it and returning a grey.
In these situations it is advisable to compensate the exposure with the appropriate command (Figure 4.25) which allows to increase or decrease the measured exposure: in the dark scene it is necessary to compensate by applying negative values, that is underexposing it because the exposure meter lightens the blacks; if it is clear we must compensate with positive values, therefore overexposing it because the exposure meter darkens the whites.
As previously mentioned there are *light meters* for the measurement of reflected light or incident light and those external are certainly the most accurate because they evaluate the light that falls on the scene that is not influenced by the color of the different surfaces that reflect light.
The same result, however, can be achieved by using a TTL internal light meter with reflected light; once the scene is framed, it will be necessary to position, in front of the camera, an 18% grey card in order to receive uniform light and to evaluate the correct exposure value (substitution method).
Another option to set is the *metering mode* of light, it can be: *average*, we calculate the average brightness framed in the viewfinder (recommended only in low contrast situations); *multi-zone*, the brightness measurement takes place in various areas of the scene (the number of areas varies from the manufacturer); the results of the acquired data are combined to find the settings for the best exposure (it is convenient when you want to work quickly without worrying too much about exposure or when there is a sudden change in light); *partial (selective)*, useful when the background is much brighter than the subject because the calculation takes place on about 20% of the area in the center of the viewfinder, while the remaining part of the image is not considered; *center-weighted average*, the measurement is done in the center, over an area roughly equal to 1/3 of the entire scene, and based on it is calculated the average to be applied to the whole framed scene and, finally, the type *spot*, in which the calculation takes place on about 3% of the area of the framed, this is mainly

Figure 4.25: The bars under the meter indicate the amount of under or overexposure

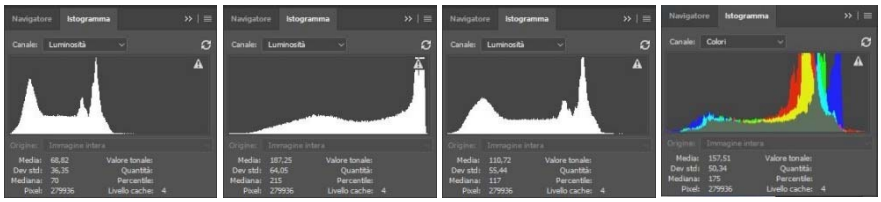

Figure 4.26: Underexposed, overexposed and good exposed histogram of brightness and RGB histogram in Adobe Photoshop

recommended when it is necessary to measure a precise point of the subject or of the scene.

The *histogram* is the graph that allows you to have immediate feedback on the exposure level of the photo and viewable directly on the camera's LCD screen. To understand this diagram, however, we must briefly introduce the concept of dynamic range; that is, the ratio between the strongest and the weakest level of brightness that the sensor can record, thus determining the maximum difference in brightness between lights and shadows. This graph, therefore, allows to establish if the stored image falls within a range of brightness that the sensor can capture; the graph shows the different brightness values that each pixel absorbs.

Consider an 8-bit image as an example, it will be possible to identify 256 brightness values; from black (corresponding to the value 0) to absolute white (value 255). Along the abscissa of the graph the pixels will be identified and along the ordinate the brightness values (0-255), in this way we will have a graph made up of 256 columns, as shown in the graph in figure 4.26; what mainly interests, are not the absolute values of the pixels but the overall trend.

A good balanced image will be presented with a histogram that extends across the entire width and with the typical bell shape; this indicates that the dynamic range of the recorded subject covers all levels of brightness at which the sensor is sensitive. In the case, however, there are peaks near the areas outside the graph the so-called *clipping* is obtained, that is the loss of data of an image following the exceeding the sensor dynamic range. In the case where the peak is in the right side, the image is said to be *overexposed* and part of the image is burnt, that is, the information of the part in light are lost. If the peak is to the left, instead, the image is *underexposed* and a part of the shaded areas are lost. Finally you could verify the case in which the histogram shows with peaks both on the right and on the left of the graph, this implies loss of information both of the parts in shadow and in light.

Moreover, reading the histogram can also be useful to evaluate the contrast in a photo. If it shows a narrow trend it implies a limited range of tones and therefore little contrast, vice versa if wide is an indication of an extensive range of tones and,

therefore, high contrast; obviously the correctness or not of a histogram can hardly be established a priori because it is strongly related to the image that one wants to obtain. In addition to the histogram of the brightness, it is possible to display the RGB histograms where the 3 values Red - Green - Blue are shown for each pixel; at the same time you can see the values of the individual brightness channels R, G and B. Lastly, many cameras allow to use the Blinking Highlight Indicator set, where the overexposed areas of the image is blinking.

[1] Sánchez Rivera J.I., (2004). La emocionante evolución de la fotografía. In: La audiencia imaginaria 3. Valladolid (Spain) Universidad de Valladolid, 2004; pp. 169-182.
[2] For further information see the book Cardone V., (2014). *Viaggiatori d'architettura in Italia.Da Brunelleschi a Charles Garnier.* Salerno (Italy), Università di Salerno, 2014.
[3] For every image that has been subjected to subsequent original reworking by the author has not been reported, for an easier reading, the original source; in any case it will be easy to re-appear to the origin and the author declares himself as of now available to fulfil the relative credits

5. Close-range photogrammetry techniques

5.1 Frame the photogrammetric paradigm

The method of photogrammetry is one of the possible survey techniques, it allows interpreting and extracting metric information of an object acquired from a series of photos; working in this way, the photographs or images represent an archive of information that can be accessed again at any time without having to go back every moment on the site. The name came from Greek, it is composed in *φως* (phos) which means light, *γράμμα* (gramma) that indicates letter or something draw and μετρήσει (metrísei), the noun of measure.
One of the main purpose of this method is the three dimensional reconstruction of an object in digital form in order to be able to identify from it not only form but also brightness or colour distribution. For this reason, close range photogrammetry has a strong interdisciplinary character and so it has a vast application; an extensive use of this technique is also taking place in the field of engineering detection, which is why good measurement accuracy is required. Generally, it may be said that close range photogrammetry applies to objects ranging from 1m to 200m in size, with accuracies under 0,1mm at the smallest end (manufactory industry) and 1cm accuracy at the largest end (architecture and construction industry).[1]
Differently from the laser scanner technique, photogrammetry used ambient light (*passive vision*) to survey the morphological and colorimetric characteristics of an object. Consequently, photogrammetry is a technique based on the light waves which operates based on triangulation.
In the process of digital photogrammetric system it is possible to distinguish some principal stage: *recording, pre-processing, orientation, measurement and analysis* (Figure 5.1, connections in red represent the sequence that can be automated).
As for any surveying project it is important a good planning of the work, before to proceed with a *recording* phase, in fact, is fundamental evaluated the scene and choose if use or not artificial target. In the case of these are necessary it will be important to select and stich them to the object with a right distribution in order to improve automation and increase the accuracy of target measurement in the image. Nonetheless, as we know, photogrammetric method reproduces images or models

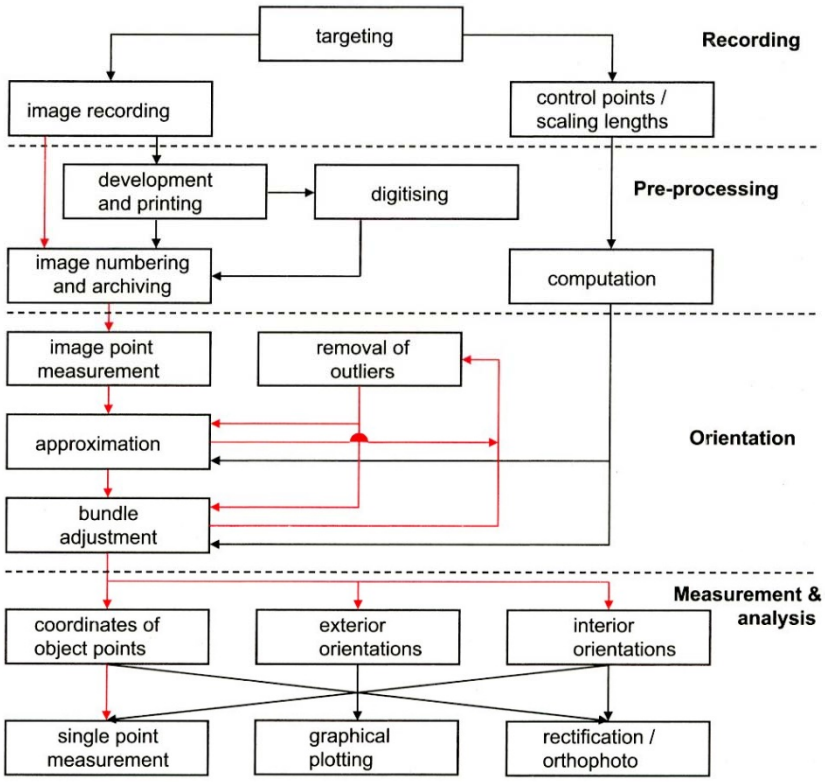

Figure 5.1: Recording and analysis procedures. (Luhmann T. et al, 2006)

not in scale, for this reason it will be also important the determination of control points or the identification of scaling lengths. After this, it will be possible to take pictures by turn around the object and guaranteeing a good overlap between the shots.

The next step is the *pre-processing* phase with the calculation of reference point coordinates and/or the distances previously surveyed and the download of pictures on computer for their subsequent storage.

Successively, there is the phases of *orientation*, interior and exterior that ensure respectively the correct position of the camera station with respect to the frame and the object referent system.

Finally, there is the *measurement* and *analysis* phase with the creation of three dimensional model necessary for Graphical plotting and generation of rectification and orthophoto.[2]

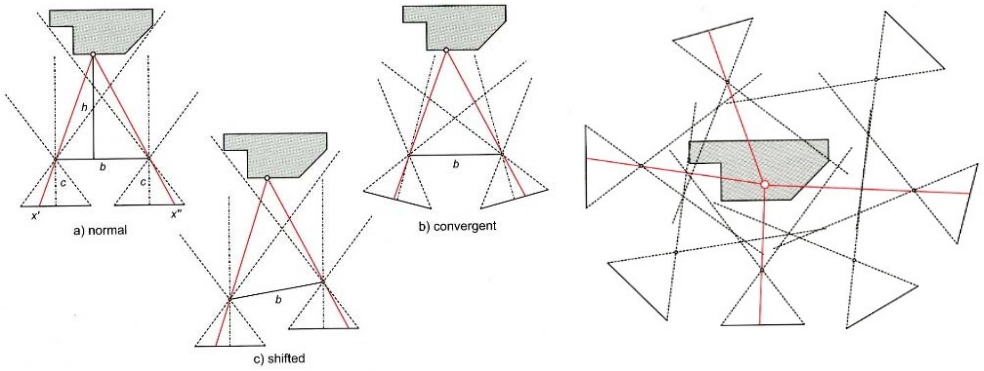

*Figure 5.2: Stereo image configuration (*a. *normal;* b. *convergent and* c. *shifted) and multi-image configuration. (Luhmann T. et al, 2006)*

5.2 Imaging configurations

In the field of photogrammetry, *imaging configurations* is referred to as the arrangement of camera stations and viewing directions for object measurement.[3] It is possible to distinguish three different kinds: *single*, *stereo* and *multi-image* acquisition.

The first one is a process typical for the generation of rectification and orthophotos starting from a single shot, in this case the prospective configuration of the photographic image will be projected to the Monge plane (II image); the three-dimensional reconstruction of an object is possible only if there are available additional geometric information.

The *stereo* imagery implies that the same object is photographed by two different points of view, in order to obtain the three-dimensional vision (Figure 5.2).

In this case, can only process images comfortably within a limited angle of convergence, as the human visual system. As shown in the image there are three different case: *normal,* that required a parallel viewing direction*; convergent,* where the parallelism is not necessary and *shifted,* where we have to provide a different scale for both images and with an enough overlap.

Finally, there is the *multi-image* configuration with the possibility of a large number of images taken from different points of view around the object and chosen to enable sufficient intersecting angles of bundles of ray in object space (*bundle adjustment*). It is the most common case in the field of close-range photogrammetry.

5.3 Coordinate System

To understand the photogrammetry process is better to introduce the main coordinate systems used. In fact, the basic principle of this technique is the relation between the object space (three-dimensional) with the image space (two-dimensional), thus generating a two-way correspondence between the points of the continuous image space to the corresponding points in the object space. Hence, the first to know is the *image coordinate system* that defines a two-dimensional image-based reference system, x'y' and its physical relationship with the instrument is obtained through the reference points[4] that are projected on the acquired image. When the image coordinate system is extended by the z' axis normal (coincident with optical axis) to the image plane (the sensor) it is possible to recognise the relationship between the plane image and the camera. With the reference at the figure 5.3 the perspective centre O' defines the origin of 3D *camera coordinate system*, while the image position B_1 and B_2 correspond respectively to a location in the physically acquired image (negative) and the real image position (positive). In this figure we can also observe that the vector **x'** is the projection ray, with respect to the image coordinate system, from the image point to the object point P; the principal distance must be defined in the following way:

$$\mathbf{x}' = \begin{bmatrix} x' \\ y' \\ z' \end{bmatrix} = \begin{bmatrix} x' \\ y' \\ -c \end{bmatrix}$$

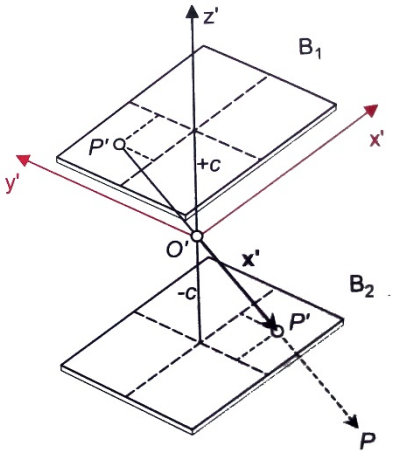

Figure 5.3 Image and camera coordinate system. (Luhmann T. et al, 2006)

where the position in the image coordinate system of the perspective centre is given by the parameters of *interior orientation*.
To understand the transformation from the space at the camera we have to introduce other three different kinds of coordinate system. The first one is the *comparator coordinate system* x*y* that is the coordinate system identified by an image measuring device in order to give length measurements in machine coordinates; the transformation establishes a relationship between the measuring system (x*y*) and the fiducial coordinate system (x'y').
As we know, although several pictures show the same area, they had taken in different places and so have not the same camera positions. In order to describe the relative position and orientation of two or more images (image coordinate systems) is used the *model coordinate system*; usually the origin is the prospective centre of one of the image. Finally, there is the *object coordinate system* or *world coordinate system* XYZ used for every spatial coordinate system as geodetic.

5.4 Orientation of a camera

One of the main step in the process of close-range photogrammetry surely it is the orientation of the camera, both *interior* and *exterior*, in order to obtain measuring information from the object analysed.
The *interior* one describes the internal geometric model of camera and its parameters (principal point, principal distance and lens distortion parameters) are calculated with *calibration* process, while the *exterior orientation* defines the spatial position and orientation of the camera in a global coordinate system. It is described by the coordinates of the perspective center in a global system and three suitably defined angles expressing the rotation of the image coordinate system with respect to the global system. Then they will be analyzed in more detailed way.

5.4.1 Interior orientation

As previously introduced the purpose of this kind of orientation defines the internal parameters of the camera, it can be associated to a special system with a planar image area (sensor) and the lens with its prospective centre. In the model shown in the figure 5.4 we can see how the position, distance of the prospective centre (*O'*) and

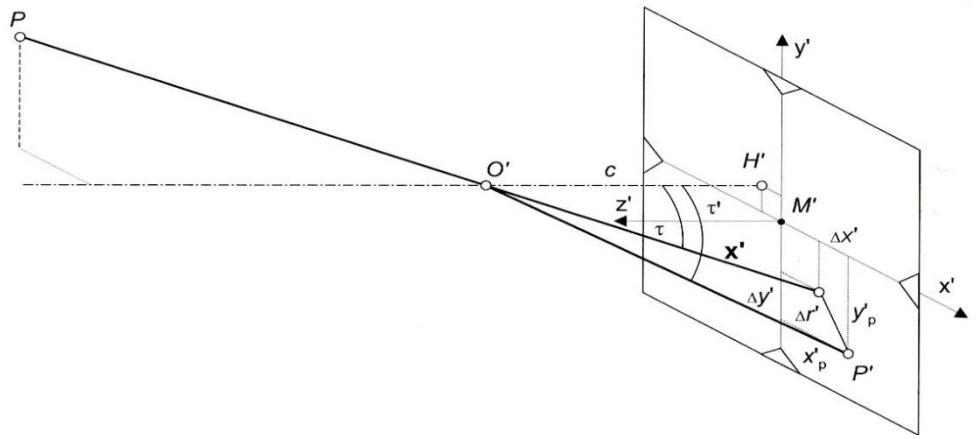

Figure 5.4: Model to interior orientation. (Luhmann T. et al, 2006)

deviations from the central perspective model are described respect the image coordinate system which has the origin (*M*') is in the image plane. The parameters that will have to be calculated in this phases are, as previously anticipated: *principal point H'* that is the nadir of the prospective centre with image coordinates (x'_0, y'_0) and normally *H'≈M'*; *principal distance c,* that is the normal distance to the prospective centre from the image plane and approximately it coincided with the focal lens when focused at infinity *c'*≈ f' and finally parameters of functions describing *imaging errors,* above all the radial-symmetric distortion Δ*r*.
When these parameters have been determined, the vector **x'** can be defined as:

$$\mathbf{x}' = \begin{bmatrix} x' \\ y' \\ z' \end{bmatrix} = \begin{bmatrix} x'_p & -x'_0 & -\Delta x' \\ y'_p & -y'_0 & -\Delta y' \\ 0 & -c & 0 \end{bmatrix}$$

where
x'_p, y'_p coordinates of image point P'
x'_0, y'_0 coordinates of principal point H'
$\Delta x'$, $\Delta y'$ axis-related correction values for imaging errors[5].

The determination of the parameters of interior orientation is called calibration and they are calculated indirectly from photogrammetric image coordinate observations. However, this ideal model does not faithfully correspond to reality, so it is necessary, if we want to obtain the highest possible precision, we will include additional parameters in the function that modify the position of perspective centre and image

distortion effects; usually *bundle adjustment* is used to estimate the calibration parameters. The name referred to the bundles of light rays leaving each 3D feature and converging on each camera centre, which are adjusted optimally respect to both feature and camera position. In the same way all the structure and camera parameters are adjusted together. Hence, it is a procedure to estimate some geometrical parameter: the combined 3D features coordinates, camera poses and calibrations.[6]

5.4.2 Correction functions

Analytically deviations from the ideal central prospective model could be expressed in the form of correction functions $\Delta x'$, $\Delta y'$to the measured image coordinates.
Hence, the image coordinates related to the principal point are

$$x^o = x'_p - x'_0$$
$$y^o = y'_p - y'_0$$

and the image radius, distance from the principal point is

$$r' = \sqrt{x^{o2} + y^{o2}}$$

however, they are only approximations that have to be corrected, interactively, in order to obtain the final image coordinates

$$x' = x^0 - \Delta x'$$
$$y' = y^0 - \Delta y'$$

5.4.3 Imaging errors

During the acquisition phase, the lens structure of the cameras causes some errors that affect both the quality and the geometry of the images, therefore, the metric information obtained from it.
Some physical effects generate the principal deviation. One of the major imaging error is *radial distortion* (symmetric and asymmetric) and it is attributable to variations in refraction of each individual component inside the lens. The first one depends not only from the lens but also by chosen focusing distance or by the object

distance (with constant focus). The curve of this kind of distortion is usually modelled with a polynomial series[7] (Seildel series) and the values from K_1 to K_n are the distortion parameters:

$$\Delta r'_{rad} = K_1 r'^3 + K_2 r'^5 + K_3 r'^7 + \ldots$$

consequently the image coordinate will be

$$\Delta x'_{rad} = x' \frac{\Delta r'_{rad}}{r'}$$
$$\Delta y'_{rad} = y' \frac{\Delta r'_{rad}}{r'}$$

This distortion may change with image scale or principal distance as shown in the figure 5.5. There are different corrections functions and one alternatively to the previous one is the following type:

$$\Delta r'_{rad} = A_1 r'(r'^2 - r_0^2) + A_2 r'(r'^4 - r_0^4) + A_3 r'(r'^6 - r_0^6)$$

$$\Delta r'_{rad} = A_1 r'^3 + A_2 r'^5 + A_3 r'^7 - r'(A_1 r_0^2 + A_2 r_0^4 + A_3 r_0^6)$$

In this case, the r_0 depends on the parameters $A_1 A_2 A_3$ and should be chosen such the minimal and maximal distortion values are more or less equal with respect to the

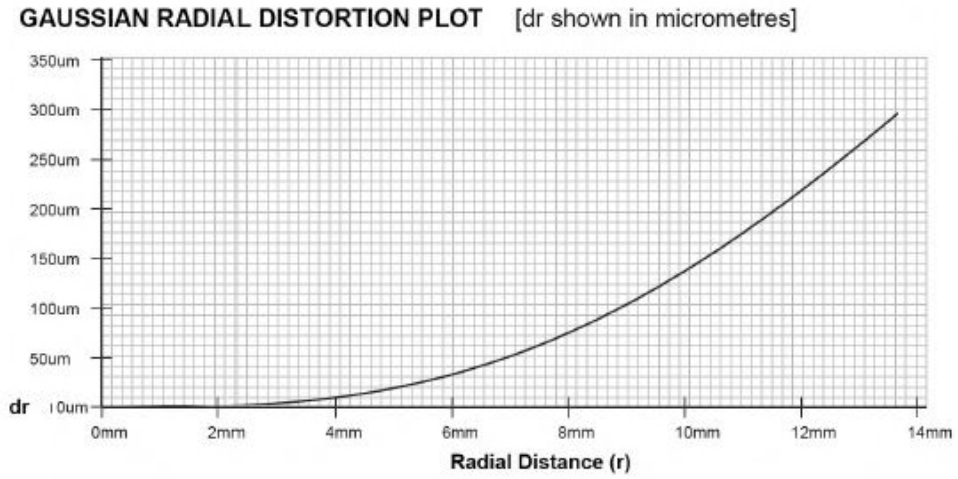

Figure 5.5: Radial and decentring distortion plots of the AF Nikkor 24 mm f/28. The radial distortion d_r are given as a function of radial distance r. (Verhoeven G., 2016)

complete image format, usually is set to approximately 2/3 of maximum image radius. The effect of this distortion is a displacement of the projection of a point respect to the position that this image would have assumed if the lens had been perfectly corrected (Figure 5.6). It can have both positive and negative values. The first one it is also called *barrel distortion* because radial line from the principal point bow outward, while the second one is termed *pincushion* distortion and, the picture appears with its sides bow inward.
In addition to *radial-symmetrical* there is the *radial-asymmetric distortion*, called *tangential* or *decentring distortion.* It is a consequence of imperfections in the manufacture and misalignment of individual lens elements within the objective; the effect is shown in the figure 5.6.
The function used to delate the error are:

$$\Delta x'_{tan} = B_1(r'^2 - 2x'^2) + 2B_2 x'y'$$

$$\Delta y'_{tan} = B_1(r'^2 - 2y'^2) + 2B_1 x'y'$$

Generally this kind of distortion is determined if low cost lens are used and its magnitude is smaller than the previous one.
Another error image are *affinity* and *shear*, it is used to describe deviation of the image coordinate system with respect to orthogonality and uniform scale of the coordinates as shown in the figure 5.6. In the case of digital camera these error appear if the light sensitive elements in the sensor have a rectangular shape rather than square. The function to reduce these are:

$$\Delta x'_{aff} = C_1 x' + C_2 y'$$

$$\Delta y'_{aff} = 0$$

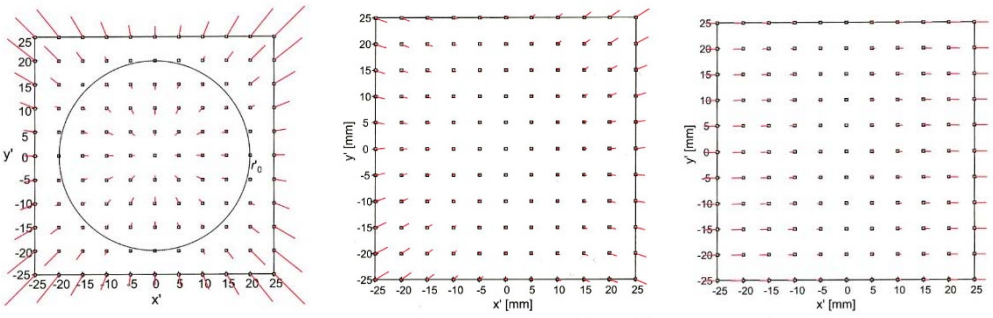

Figure 5.6: Effect of radial-symmetric distortion, radial-asymmetric and tangential distortion and affinity and shear. (Luhmann T. et al, 2006)

Hence, known all the individual imaging errors is possible write that:

$$\Delta x' = \Delta x'_{rad} + \Delta x'_{tan} + \Delta x'_{aff}$$

$$\Delta y' = \Delta y'_{rad} + \Delta y'_{tan} + \Delta y'_{aff}$$

Nevertheless, additional parameter sets are included in the mathematical modelling process; they do not depend to the mechanisms of the camera but are considered to reduce systemic effects identifiable in the image residuals. In the case of digital imaging systems, Bayer (1992) has developed the following approach to considerate the parameter sets:

$$\Delta x'_{Beyer} = \Delta x'_0 - \frac{x'}{c}\Delta c + K_1 x' r'^2 + K_2 x' r'^4 + K_3 x' r'^6 + P_1(r'^2 - 2x'^2) + 2P_2 x' y' - C_1 x' + C_2 y'$$

$$\Delta y'_{Beyer} = \Delta y'_0 - \frac{y'}{c}\Delta c + K_1 y' r'^2 + K_2 y' r'^4 + K_3 y' r'^6 + P_2(r'^2 - 2y'^2) + 2P_1 x' y' - C_2 x'$$

where
K= radial-symmetric distortion
P= radial-asymmetric distortion
C= affinity and shear
$\Delta x'_0$, $\Delta y'_0$, Δc= small corrections to the spatial position of the prospective centre.

5.4.4 Exterior orientation

This step is necessary in order to evaluate the six parameters which describe the spatial position and orientation of the camera coordinate system with respect to the global object coordinate system[8](Figure 5.7).
The problem of establishing the relationship between the camera and object system can conveniently be solved by the collinearity mode; it expresses the condition that the perspective centre O', the image point P' and object point P must lie on a straight line.

The vector $\mathbf{X_0}$, from the origin to the perspective centre O', defines the spatial position of the image coordinate system.

$$\mathbf{X_0} = \begin{bmatrix} X_0 \\ Y_0 \\ Z_0 \end{bmatrix}$$

The angular orientation, while, is defined by the orthogonal rotation matrix **R** that is the result of three independent rotations ω, φ, κ about the coordinates axes X,Y,Z.

$$\mathbf{R} = \mathbf{R}_\omega \mathbf{R}_\varphi \mathbf{R}_\kappa$$

$$\mathbf{R} = \begin{bmatrix} r_{11} & r_{12} & r_{13} \\ r_{21} & r_{22} & r_{23} \\ r_{31} & r_{32} & r_{33} \end{bmatrix}$$

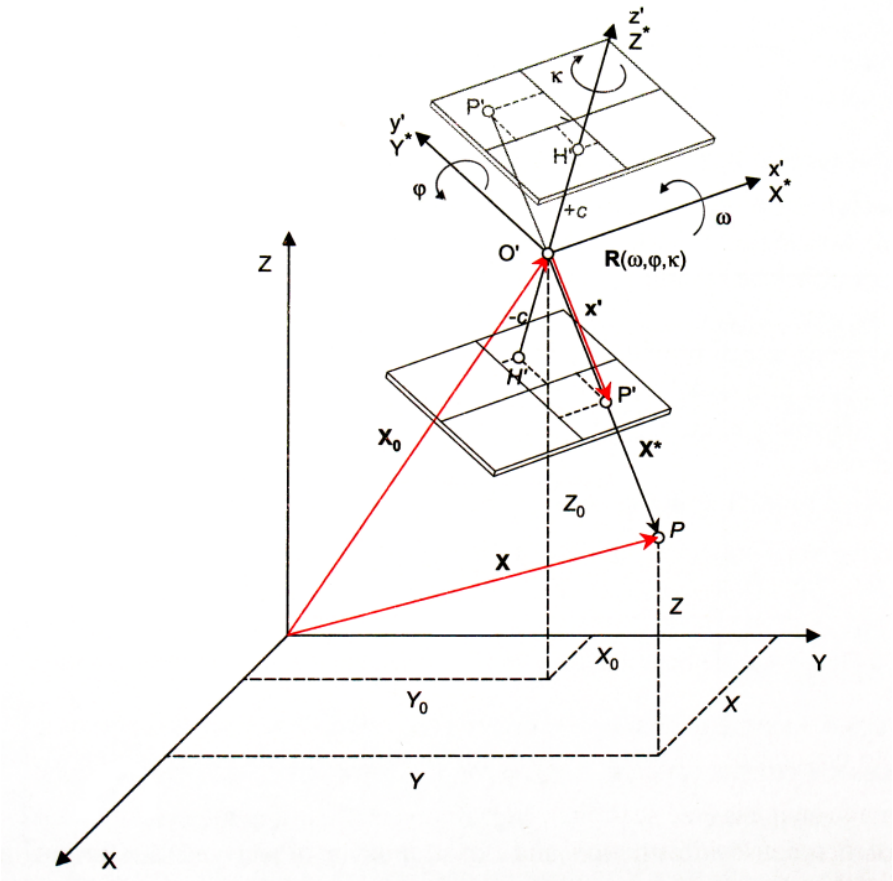

Figure 5.7: Exterior orientation and projective imaging. (Luhmann T. et al, 2006)

where the elements of the rotation matrix r_{ij} can be defined either as trigonometric functions of the three rotation angles. Known the parameters of exterior orientation, the vector $\mathbf{x}'$ can be transformed in an absolutely oriented spatial ray, from O' to the object point P.

5.4.5 Collinearity equations

The coordinates of an object point P can be calculated from the location of the position vector to prospective center $\mathbf{X_0}$ and the vector from the perspective center to the object point $\mathbf{X}^*$ visible in the figure 5.7

$$\mathbf{X} = \mathbf{X_0} + \mathbf{X}^*$$

The coordinates system used to place $X^*$is that of the object. For this reason, the vector $\mathbf{x}'$could be transformed into the object space through a rotation matrix **R** and a scaling factor *m*, in order to achieve the same direction of the vector $\mathbf{X}^*$

$$\mathbf{X}^* = m\mathbf{R}\mathbf{x}'$$

with
m= scale factor and it is an unknown values which change for each object point. However, if we want to have the projection into the coordinates of the object point we have:

$$\mathbf{X} = \mathbf{X_0} + m\mathbf{R}\mathbf{x}'$$

$$\begin{bmatrix} X \\ Y \\ Z \end{bmatrix} = \begin{bmatrix} X_0 \\ Y_0 \\ Z_0 \end{bmatrix} + m \begin{bmatrix} r_{11} & r_{12} & r_{13} \\ r_{21} & r_{22} & r_{23} \\ r_{31} & r_{32} & r_{33} \end{bmatrix} \begin{bmatrix} x' \\ y' \\ z' \end{bmatrix}$$

It is important to underline that a necessary condition in order to obtain absolute position in the space of the point P is that this spatial direction intersects another geometrically known element, for example another ray from a second image or a surface in the space.
By inverting the previous equation, adding the position of the principal point $H'(y'_0, x'_0)$ and considering the correction terms $\Delta\mathbf{x}'$ (before explained), the image coordinates will be:

$$\mathbf{x}' - \mathbf{x}'_{\mathbf{0}} - \Delta\mathbf{x}' = \frac{1}{m}\,\mathbf{R}^{-1}(\mathbf{X} - \mathbf{X}_{\mathbf{0}})$$

$$\begin{bmatrix} x'_p & -x'_0 & -\Delta x' \\ y'_p & -y'_0 & -\Delta y' \\ 0 & z' & 0 \end{bmatrix} = \frac{1}{m}\begin{bmatrix} r_{11} & r_{12} & r_{13} \\ r_{21} & r_{22} & r_{23} \\ r_{31} & r_{32} & r_{33} \end{bmatrix}\begin{bmatrix} X - X_0 \\ Y - Y_0 \\ Z - Z_0 \end{bmatrix}$$

The inverse rotation matrix is equal to its transport, for this reason it is possible to divide the first and the second equations by the third equations, in this way the scale factor *m* is not present in the equations and the collinearity equations will be:

$$x' = x'_0 + z'\frac{r_{11}(X - X_0) + r_{21}(Y - Y_0) + r_{31}(Z - Z_0)}{r_{13}(X - X_0) + r_{23}(Y - Y_0) + r_{33}(Z - Z_0)} + \Delta x'$$

$$y' = y'_0 + z'\frac{r_{12}(X - X_0) + r_{22}(Y - Y_0) + r_{32}(Z - Z_0)}{r_{13}(X - X_0) + r_{23}(Y - Y_0) + r_{33}(Z - Z_0)} + \Delta y'$$

where:
x', y' = image coordinates of the point P;
X, Y, Z = object coordinates of a point P;
z'= principal distance (it coincides with the value -c in the figure 5.7);
x'_0, y'_0 = image coordinates of the principal point H';
$\Delta x', \Delta y'$= lens distortions;
X_0, Y_0, Z_0 = coordinates of the projection center O';
r_{11}, r_{12} ...= elements of the rotation matrix.

Hence, this equation represents the transformation of object coordinates into the image coordinates; it will possible only to know the functions of the interior $(x'_0, y'_0, z', \Delta x', \Delta y')$ and exterior $(X_0, Y_0, Z_0, \boldsymbol{R})$ orientation parameters of each photo. The collinearity equations, thus, are very fundamental equations of analytical photogrammetry and shows as each point is projected in a single image point. In addition, they are suitable both for the generation of orthophotos and for the direct use as observation in an over-determined least squares adjustment.
The latter are the techniques essential to determine a number of unknown parameters from a number of observed (measured) values which are related each other. Being more observations than required for the unknowns to determine, there is not only one solution. For this reason, the unknown parameters are estimated according to functional and stochastic models.[9]

5.5 Case Studied

5.5.1 From monoscopic photogrammetry to BIM

The coastal defence system of the province of Salerno is well suited as a case studied to experiment the innovative digital techniques for the representation and preservation of cultural heritage. The interpretation of the building, its forms and its nature have been developed through the integration of monoscopic photogrammetry with BIM, this in order to reach the realization of an infographic image summary with the high knowledge content, and for the enhancement and conservation of these architectures.
The following work was realized with the support of the colleague Eng. Davide Barbato and the interest was focused on the Torre Fenosa, building in the 1569 and located on high rocky spur in the municipality of Camerota (Figure 5.8). Its characteristic suggests that this tower belonged to the type of tower defence. It is a pyramidal trunk construction and has very thick walls in limestone. Nowadays it is in abandonment condition, but in spite of that, internally it preserves its original division into two large overlapping spaces. The ground floor, with a square base, is covered by a barrel vault, with orientation of sea-mountain, and was formerly used

Figure 5.8: View of Torre Fenosa, Camerota

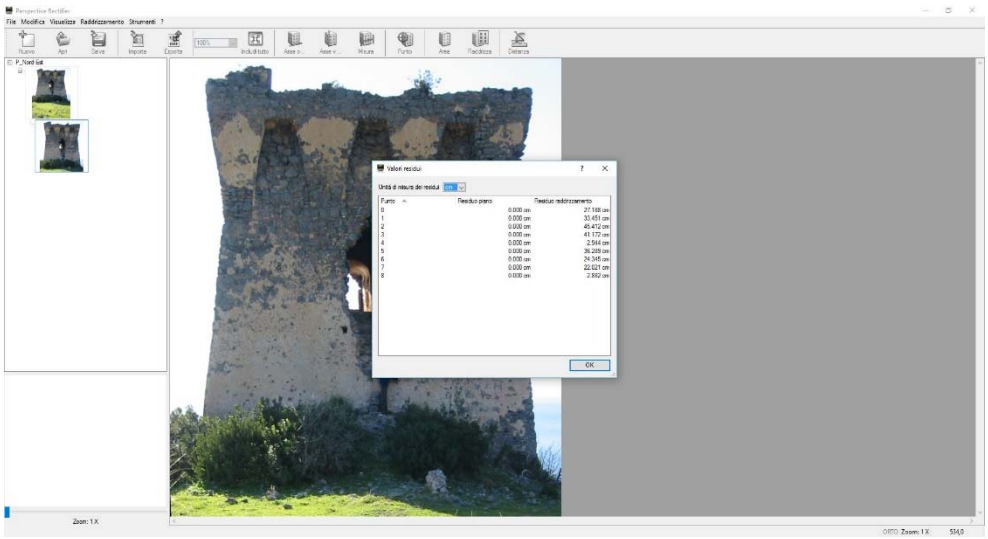

Figure 5.9: Software interface Prospective Rectifier after Rectification process

as a cistern for collecting rainwater, channelled through a hole in the wall and that it extends along the entire height of the built.
The upper level, also in this case, is covered by a barrel vault, but with orientation perpendicular to the lower floor (then with a coast-coast alignment); also it presents a series of arched recesses of various sizes and an opening on the sea to enable a wide view and able to supervise any enemy attack. The last level, the terrace, is accessible by a staircase built into the wall itself, and presents a parapet, which is the crowning of the tower; these volumes, slightly jutting, are interrupted by embrasure that were used for the placement of weapons.
As written in the paragraph 2.3, also this tower was included in the decree of King Vittorio Emanuele II on December 30, 1866; so that it ceased to perform the function as a fortress and, so, could be subject to the sale.
Torre Fenosa then, is a building guardian of past and represents the history of our territory, for this reason the use of the Design represented the starting point for the analysis and interpretation of the artefact; indispensable condition for the realization of adequate technical and infographic drawings to high information and knowledge content. In this case, the technique used was the photogrammetric survey, which allow the acquisition of the data necessary for the post-process; that is the rectification of three images for the return of photoplane of the main prospects of the tower. The software implemented was Perspective Rectifier (Figure 5.9), produced and distributed by RectifierSoft.com it is possible to work in two different mode: *Geometric Rectification*, identifying the vanishing lines and specifying two measures

Point	x	y	z
0	0,00	0,00	0,00
1	-9,66	0,00	0,00
2	-0,33	-3,68	0,00
3	-9,52	-3,68	0,00
4	-6,97	-5,39	0,00
5	-4,07	-3,68	0,00
6	-4,07	-11,48	0,00
7	-7,17	0,00	0,00
8	-6,52	-4,22	0,00

Point	x	y	z
0	0,00	0,00	0,00
1	-9,64	0,00	0,00
2	-0,41	-3,68	0,00
3	-9,44	-3,68	0,00
4	-4,75	-2,89	0,00
5	-4,78	-9,16	0,00
6	-5,42	0,00	0,00
7	-10,60	-11,20	0,00
8	0,31	-11,20	0,00

Point	x	y	z
0	0,00	0,00	0,00
1	9,74	0,00	0,00
2	0,33	-3,68	0,00
3	9,45	-3,68	0,00
4	5,74	-3,68	0,00
5	5,39	0,00	0,00
6	5,74	-12,58	0,00
7	2,69	0,00	0,00
8	0,00	0,67	0,00

Figure 5.10: Rectified images of the South-East, North-East and North-West elevation

or *Points Rectification*, which provides the identification of points with known coordinates (x, y, z); in both case the application rectifying and scales the photograph of the building to be surveyed (Figure 5.10). However, there was some problems during the survey of the South-West facade, in fact it was impossible to do a direct survey of the same because it is located near a precipice; for that reason, it was decided to proceed doing a hypothetical reconstruction based on the metrics information extracted from the drawings already completed.

Once the images were rectified and scaled, they were inserted into the CAD application where they were used as a basis for the extraction of the necessary measures at the three-dimensional model generation.
Beyond the interpretation of the external structures, the study and the survey of the existing building heritage require a greater interpretative and communicative effort other than theoretical: if the classical projects permit an interpretation of the structures and the textures of the tower studied, they are lacking from the perspective of the preservation of the geometrical other than alphanumeric information.
This was possible thanks the Building Informational Modelling (BIM), an optimal instrument both for architectural modelling that the store of information data; an essential prerequisite able to promote management and enhancement policies of the cultural building heritage. In fact, aim of this model is, in addition to define the structures in the three dimensions, realizes a communication model, a communicative standard, which can be read and reinterpreted by all the experts.
Certainly, the reconstruction of the three-dimensional model is more difficulty than a simple representation of 2D lines, even more when you examine the existing building heritage made of unconventional forms that you can hardly parameterize. These difficulties depend also from the Level of Detail and Development (LOD) we want to reach: higher is the level required, greater will be the level of difficulty to overcome.
The latter, LOD specifications, let you specify and articulate with a high level of clarity of the content the reliability of the BIM model, during the different stages of the implementation of the design process, or the reliability of the graphical and informative content put in place for that specific model. It is, once again, a communication language through which users can define the requirements for their own studies or projects. This division into levels of detail allows to define as the models are reliable and which usability and limitations they present.
For the first model no descriptive information is associated with it that is nothing but an “empty box”. A container thus devoid of any content, it is itself that represents the whole; its achievement is of simple execution being the result of elementary operations between surfaces and volumes. The accuracy of the model is such that it provides a rough idea of the work studied and nothing else.
The second model, more detailed, represents a conceptual evolution of the previous one: the box initially empty and with generic forms is gradually modelling and conforming itself to the actual state of the Tower (Figure 5.11). Is highlighted, more accurately, the structure of the Tower attacked by time and historical events that characterized it, it is crumbled in several places and in ruins. It perfectly showed the space covered on the ground floor by the barrel vault and the hole placed on the North-East side of the same made for conveying of rainwater.

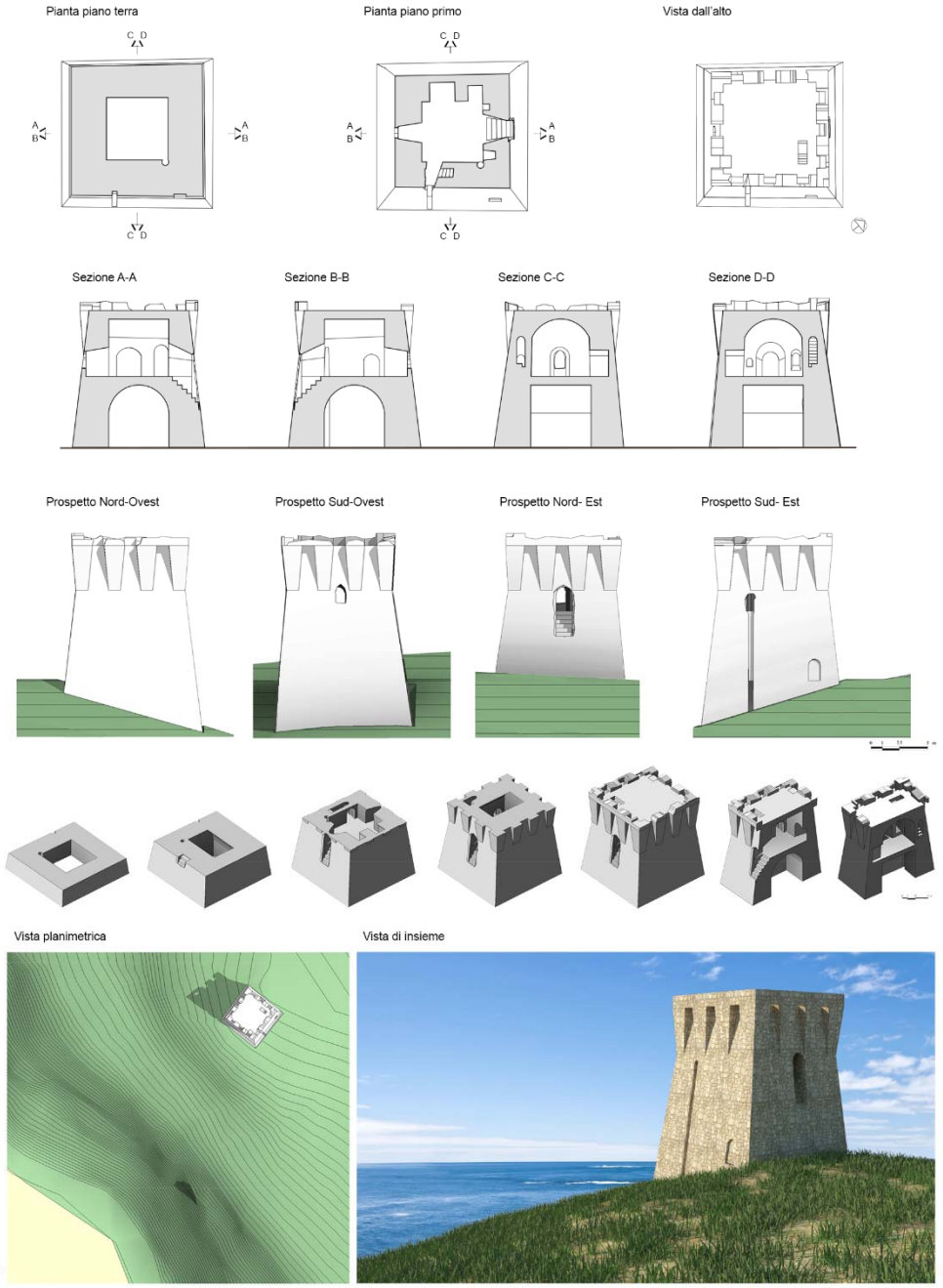

Figure 5.11: Infographic reproduction of Torre Fenosa

Upstairs, in the transverse direction compared with the one below, there is the other barrel vault and the stairwell – carved into the wall – that allow the access to the terrace and its breathtaking view.
As well as geometrical, however, for the enhancement of the structure, the level of the supposed detail requires the enrichment of the "box" with additional data, increasing the database also with non-graphical information: construction period, type, classification, land registry data, location, properties and materials are part of the information implemented in this phase.
The tower has been directly inserted into its geographical context of belonging, as well as to obtain additional information regarding the orientation, to the sunlight during the different periods of the year and the effects they have on the territorial context.
This work underlines the importance of new technology to analyze and enhancing the historical and artistic heritage of our cities. The use of photogrammetry was the starting point for the generation of the BIM; an instrument of protection and conservation of the existing architectures: the system makes possible not to lose, but rather to save and record the information precisely ensuring a real continuity among the planning stages and during the entire life cycle of the building.
The final result we achieved is nothing but the digital and infographic concretization of the structure studied, provided with a high cognitive content, which is a necessary means for the enhancement and preservation of these buildings.[10]

5.5.2 From multi-image photogrammetry to BIM

The aim of this case of study is a multidisciplinary approach to the protection and management of the building heritage, adding to the historical documentary investigations, a careful phase of photogrammetric survey and a conscious geometric and informational modeling of the pre-existence.
Once again, the work was realized with support of the colleague Eng. Davide Barbato and, in this case, was focused on the Torre di Vietri sul Mare; a building of the 16th century and belonging to the more elaborate coastal defence project adopted by the ancient Principality of Citra in the viceroy era (see paragraph 1.11).
Through previous studies, as well as direct archival and iconographic surveys, it was possible to identify the volumetric evolution of this tower.
The digital and three-dimensional representation would then extend the reading of the information acquired to a wider public, facilitating the diffusion and understanding of the transformations that took place over time.

Figure 5.12: Unknown author, Marina di Vietri, XVI century; Coll. Villa Guariglia, Via Nuova Raito. Raito di Vietri sul Mare (SA)

To achieve the purpose of this work, four main phases were essential: the study and review of literature that characterizes the tower, architectural survey, modeling in function of historical evolution, add information to the model.
Hence, the first step was an historical investigation of the tower. It is one of the largest viceroy towers realized with five embrasures and the main function was the barrage to carry out a task of signal the arrival of the enemies and to prevent from landing. It was built near the sea, but following the flood of October 1954 and the violent storm of 1987, is today integrated into the urban context of the city. The tower, furthermore, over time has undergone a series of transformations until the present shape.
Originally, around 1565, for its defensive function the tower was made of large size and with a square of dimension sufficient for the installation of the cannons. The inviolability of the tower was guaranteed by the absence of openings for the first six meters and with an entrance that took place at the second level in the direction of the city. According to a watercolor of the nineteenth century, visible in the publication

of L. Santoro, access was guaranteed by a fixed staircase, located near the tower and connected by a drawbridge.
Even if larger than Torre Fenosa, it also has a pyramid shape and develops internally on two large rooms with a square based and covered with a barrel vaults placed orthogonally one from the other. The ground floor was the sole function of a cistern for collecting rainwater. The upper level, initially accessed only by the above mentioned external staircase, while was used to lodge the tower. The upper terrace, whereas, was accessible by an inner staircase built in the thickness of the wall which often also served as a storage of food and ammunition. On the top of this square, there were bartizans that is the room with barrel vault, once the site for the territory guard (Figure 5.12).
Between the end of the eighteenth and the beginning of the nineteenth century, the tower was transferred to the Battalion of the Invalidi to repulse, along with other towers on the coast, the phenomenon of contraband. Probably this is the time when some changes to the tower are made with the addition of more volumes on the squares: “Tower of Vietri, half a mile from the prec. (T. d’Albori) with a piece of

Figure 5.13: Clarkson Stanfield (1793–1867), A View of Vietri in the Gulf of Salerno, 1840; Coll. Royal Collection Trust/© Her Majesty Queen Elizabeth II 2017

Figure 5.14: Richard Dölker (1896-1955), Torre di Vietri sul Mare; Coll. Raccolta Arti Applicate di Villa De Ruggiero, via Nazionale 102. Nocera Superiore (SA). Torre della Marina di Vietri, 2017

bronze and a small Mojana pie, is gutted by Invalidi Soldiers, consider repairs for 86 ducats. The expenses are attributed to the University of Cava, which holds five Towers and the five added"[11]. These extensions are visible from some of the draws by Clarkson Frederick Stanfield (1793-1867) during his stay in the Amalfi Coast in November 1838. The painting *A View of Vietri in the Gulf of Salerno*, now keep at the Royal Collection in London (Figure 5.13) clearly shows the changes made by the

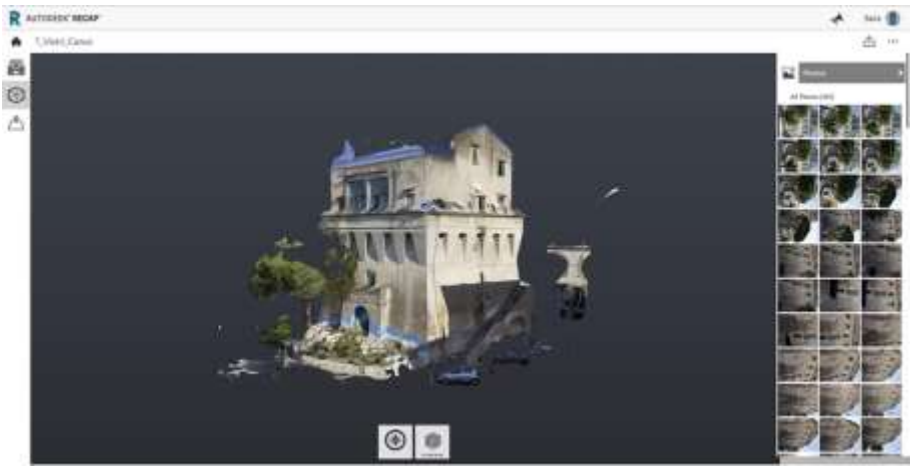

Figure 5.15: 3D model generated with ReCap Photo software

tower. Subsequently, in 1860, it was used as a customs and was not introduced in the list of the abandoned towers in the decree of Vittorio Emanuele II.
From what is visible in the pencil drawing by Richard Dölker (Figure 5.14), it is probably at the end of the nineteenth and early twentieth centuries that the tower undergoes further variations: adding an entryway to the base and eliminating the drawbridge for to facilitate the entrance to the upper floors through an external stairway near the wall of the construction. In the following years, the tower became the seat of the Fiscal Police with the addition, on the monitoring terrace, of other volumes suitable to use the artifact for the new function and a balcony that is supported by a large arc connected at the wall (Figure 5.14).
After the first historical-architectural research followed a photogrammetric survey realized with the instrument Canon EOS600D Digital Reflex. The data gained during this survey was then developed with free software ReCap Photo (Figure 5.15), a cloud service from the Autodesk manufacturing company, which bases its work on automating the reverse modeling process (the survey and photogrammetric data-processing phase is analyzed specifically in the paragraph 6.2.2).
The digital model so obtained was the starting point for the implementation in BIM environment. Through a backward path, we tried to reconstruct the initial morphology of the artefact and all the superfetations that happened over time. Although there was availability of historical material, there is an objective difficulty

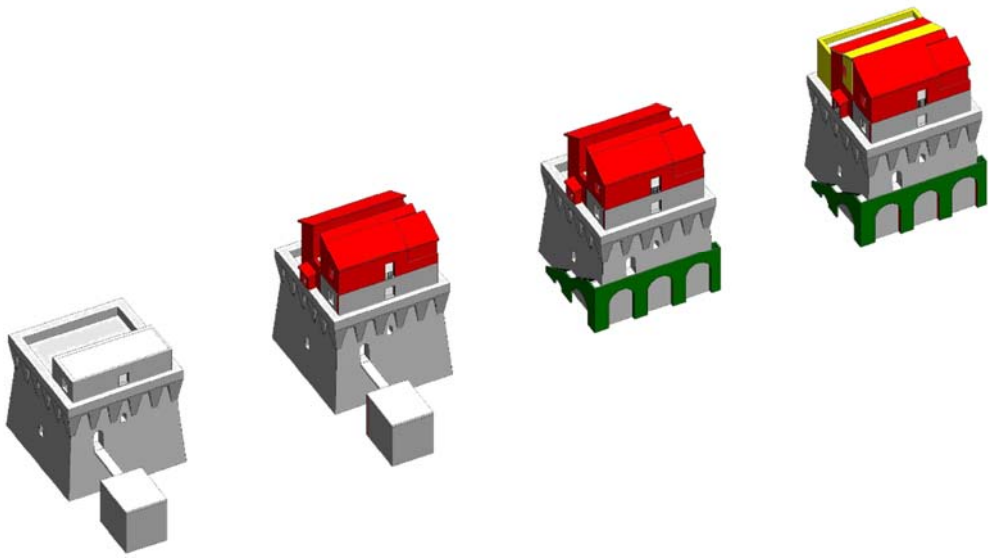

Figure 5.16: Evolution of the geometry of the Tower from 1540 to today

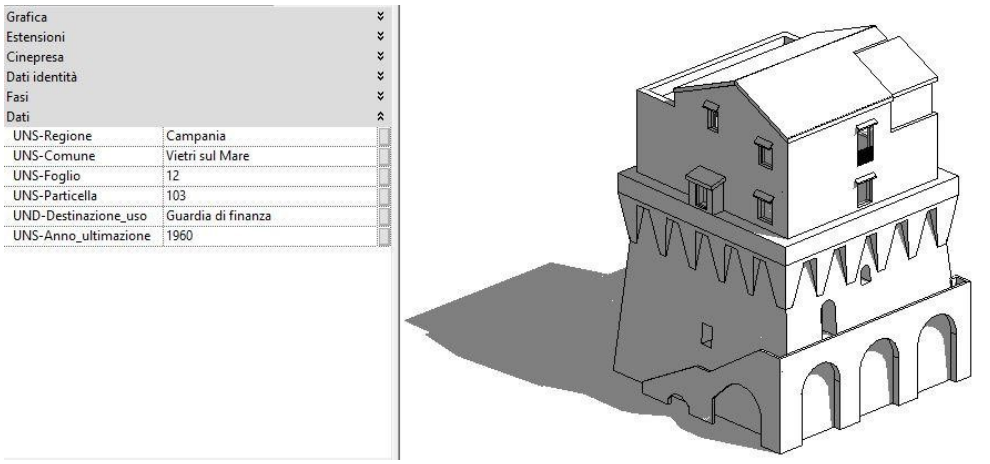

Figure 5.17: BIM Model of the Tower representing its present state

in developing the third dimension in a precise and meticulous manner due to the absence of metric data. In this case, vintage images and points in the space were the only elements available to investigate that unique building heritage.
In the following dissertation, we focused on the partition of the models into graphic and information parts. The graphic part is nothing but the volume of the Tower and its transposition from the level of representation to the three-dimensional space. This stage is a direct consequence of the surveys and the typology of the data (in our possession). On the other hand, the information aspects of the model – and their maintenance – actually make BIM the volumes previously implemented.

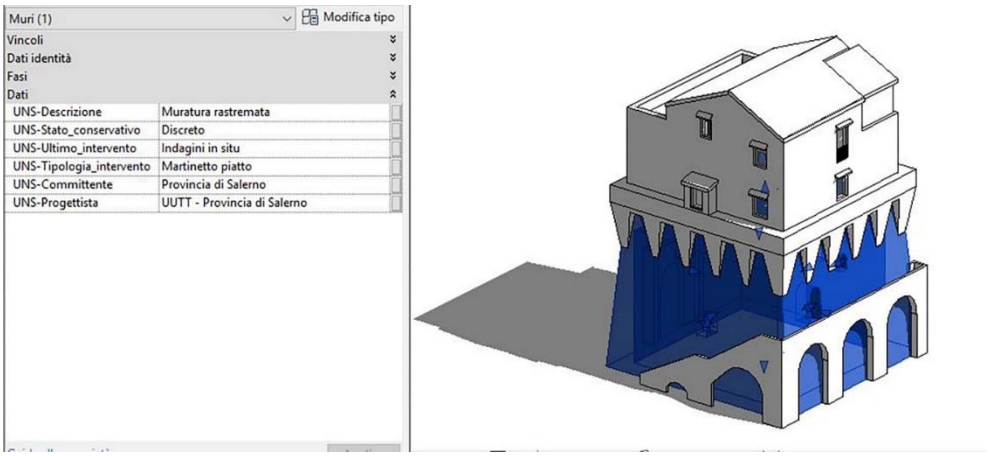

Figure 5.18: Part of the semantic modelling implemented

In the present case, we attempt to reproduce in the digital environment the geometry of the Tower during the ages, respecting – albeit conditioned by the lack of certain metric data – the quantitative and qualitative characteristics. In some cases, such structures have been simplified in objects that are still coherent.
Starting from what may be the original hypothesis given in Figure 5.16, three more evolutions of the model have been implemented. The first depicts the Tower at the beginning of 1800, when three bodies were added to the parade ground. These volumes were represented in red and portrayed the first addition to the starting model. Subsequently the addition of an entry at the bottom and the elimination of the battiponte have further modified the tower, which assumed customs function. Finally, the realization of three more volumes and the covering of the parade ground, give us the tower as we see it today. Even if, currently, there is a lack of a programmatic definition of the maintenance operations to be performed over time, the volumetric superfetations has been identified both graphically and semantically, the maintenance interventions realized over time, and a brief description of each part of the structure (Figure 5.18). [12]

[1] Luhmann T., Robson S., Kyle S., Harley I., (2006). *Close Range Photogrammetry. Principles, Methods and Applications*. Caithness (Scotland), Whittles Publishing, 2006; p. 4.
[2] Luhmann T., Robson S., Kyle S., Harley I., op. cit.; p. 11.
[3] Luhmann T., Robson S., Kyle S., Harley I., op. cit.; p. 98.
[4] Either fiducial marks or rèseau in the case of digital camera.
[5] Luhmann T., Robson S., Kyle S., Harley I., op. cit.; p. 115.
[6] Triggs B., McLauchlan P. F., Hartley R. I., Fitzgibbon A. W., (1999). Bundle Adjustment – A Modern Synthesis. In: B. Triggs, A. Zisserman, R. Szeliski (Eds) *Vision Algorithms: Theory and Practice.* Corfu (Greece), Springer, 2000.
[7] It is only one of different possible correction functions.
[8] Luhmann T., Robson S., Kyle S., Harley I., op. cit.; p. 202.
[9] Luhmann T., Robson S., Kyle S., Harley I., op. cit.; pp. 202-204.
[10] Barbato D., Morena S., (2016). Infographic techniques for the representation of marginal buildings of Salerno coast. In: *Bertocci S. (Eds) The reasons of drawing. Thought, Shape and Model in the Complexity Management. XIII Congresso UID, Firenze (Italia)*. Rome (Italy), Gangemi Editore, 2016.
[11] Santoro L., (2012). *Le torri costiere della Provincia di Salerno: paesaggio, storia e conservazione*. Salerno (Italy), Paparo edizioni, 2012; p. 270.
[12] Barbato D., Morena S., (2017). BIM and low-cost survey techniques for the preservation of building heritage, In: *Convegno Internazionale e Interdisciplinare IMG2017*. Bressanone (Italy), MDPI AG, 2017.

6. Photogrammetric survey

6.1 Instruments for the architecture survey

The attention devoted in the last years to the protection and conservation of architecture has contributed to increase the interest in the new technologies and the innovative methodologies of architectonic survey. In particular, this unit is focused on the possibility of making acquisitions and useful data through the implementation of low-cost terrestrial photogrammetry.
The record of the ancient tower has performed with a commercial digital compact camera Fujifilm XF1 and Canon EOS 600D Digital Reflex. The first one possesses a sensor EXR CMOS (8,8x6,6 m) which offer a maximum resolution of 12 Megapixel. The second one, while has a sensor CMOS APS-C 18 Megapixel and it was used with a lens Canon EF-S 18-200mm.
They are two different kinds of camera (compact vs reflex) and, of course, with a lot of dissimilarity at which also corresponds to a price difference; in the figure 6.1 there is a scheme with the main features. In any case, both are not excessively expensive tools when compared to laser scanner technology; the latter, in fact, consists of a very expensive instrument that, however, guarantees the taking of a large amount of

Name	Fujifilm XF1
Sensor	EXR CMOS 8,8Xx6,6 mm
Pixel	12 megapixel
Pixel size	4,84 μm²
Lens	Manual optical zoom Fujinon 4x
Focal length	6,4-25,6 mm
ISO	100-12800
File	JPEG, RAW, JPEG+RAW

Name	Canon EOS 600D
Sensor	CMOS da 22,3x14,9 mm
Pixel	18 megapixel
Pixel size	18.4 μm²
Lens	EF/EF-S
Focal length	18-200 mm
ISO	100-12800
File	JPEG, RAW, JPEG+RAW

Figure 6.1: Camera technical specification of the Fujifilm XF1and Canon EOS600D

data in a very short time and therefore the possibility of surveying monumental complexes of remarkable extension in short times.
The aim of this study, however, is to verify the possibility to use "cheap" tools for the knowledge of the cultural heritage, useful for both metric and historical-artistic research, thus providing sufficient elements not only for its conservation but also for its valorisation and dissemination.

6.1.1 Planning for an optimal survey

Before proceeding to survey any type of architecture or object, it is fundamental a proper planning and organization of the work. In the field of photogrammetry in order to obtain metrically correct results it is necessary to know how to interpret each phase of survey, like foresee the problems and know the equipment used.
The valuation of *GSD* (Ground Sample Distance) is sure one of the first data to set for an organization of a photogrammetric survey. As we know, it is the distance between consecutive pixels measured on the ground; in other words, it is the "amount" of soil contained in a pixel. About that is easy to understand how there is an inversely proportional relation between *GSD* and image sharpness, that is, the larger is the pixel, the lower is the level of detail of the picture. The definition of this parameter, so, is all a question of similar geometry: two triangles are similar if they have equal angles and sides in proportion and therefore the ratio between two homologous sides is constant.
The calculation of the GSD is, moreover, strongly influenced by the scale that we need from the survey; that is different if we require an architecture or archaeological instead of territorial survey. Generally, in the field of architecture technical drawings with 1:50, 1:100 or more scale are generated, so would be appropriate to reduce the distance from the building and use an adequate lens. Before proceeding to the concrete survey, so we proceeded to evaluate what would be the optimal values to be set.
The know parameters are:

- real focal length of the camera [mm], f_r;
- sensor width [mm], s_w;
- sensor height[mm], s_h;
- digital image width [pixel],i_w;
- digital image height [pixel], i_h;
- length of the building to be surveyed [m], B_l;
- height of the building to be surveyed [m], B_h;

- height of shoot plane [m], q;
- distance from building [m], d;
- operator speed [m/s], v;
- time lapse [s], t;
- Ground Sample Distance [cm/pixel], GSD;
- pixel size, p_s;
- longitudinal dimension of the captured image [mm], L;
- elevation dimension of the captured image [mm], H.

As visible in the image the relation that exists between the scale of the photos and that of the reality is (Figure 6.3):

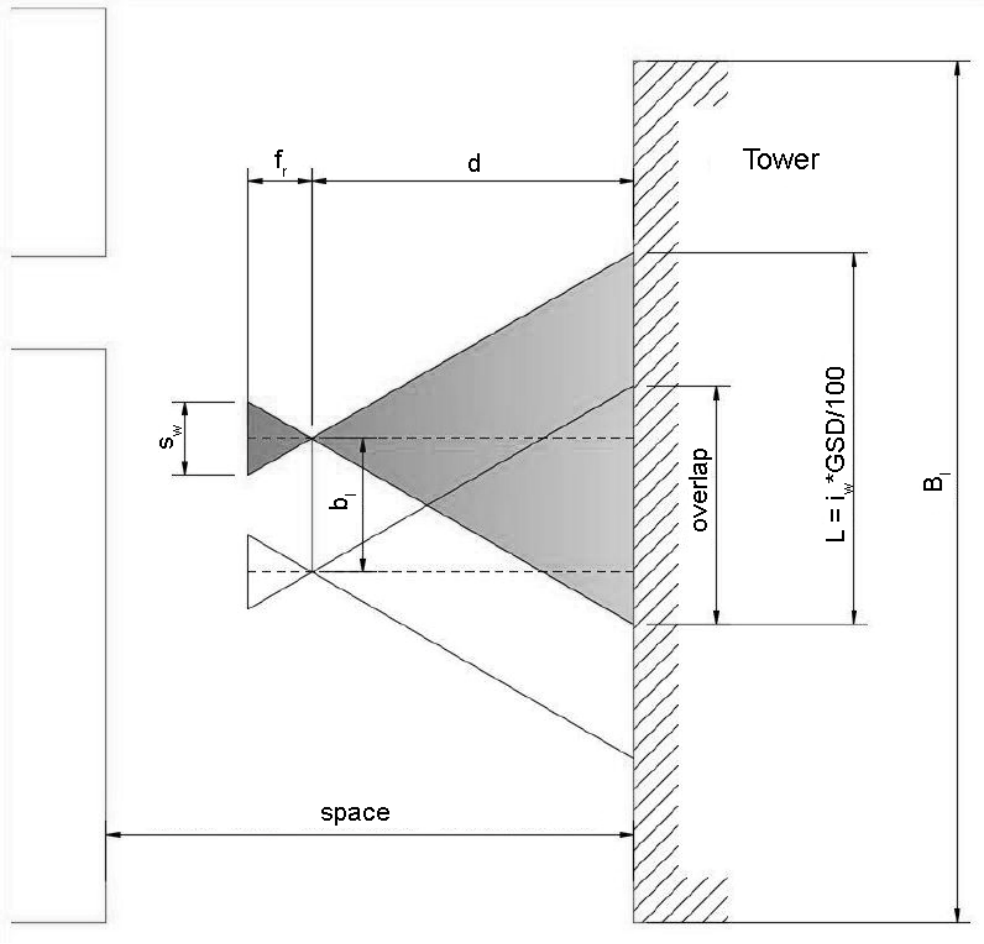

Figure 6.2: Representative model of a photographic acquisition

$$s_w : L = f_r : d$$

and we know also that *pixel size* is

$$p_s = \frac{s_w}{i_w}$$

Where the sensor size is a technical data of the camera, while number of pixels in picture (data contained in the EXIF) change and it depends by the setting selected in the camera during the shoot; therefore given a various focal length, with the same sensor used, different GSDs can be obtained.
If we know this, it will be easy to rewrite the relation

$$p_s : GSD = f_r : d$$

and so

$$GSD = \frac{s_w \cdot d}{i_w \cdot f_r}$$

Usually, the graphic accuracy request is 0,02cm multiplied by the denominator of the drawing scale. So, in the case of a scale 1:50 the *admissible error* is

$$0.02 \cdot 50 = 1cm$$

To obtain technical drawings of this scale, so we will have to proceed with an appropriate value of *Ground Sample Distance* during the survey; that is less than 1cm/pixel. Therefore, the first step will be to establish the aim and the desired GSD then, in relation also at the dimension of the building, we will have to fix the focal length that we will use. Only in this way, it is possible to proceed to evaluate the other parameters.
Returning to the geometric similarity previously established we could affirm that

$$\frac{d_s}{L} = \frac{f_r}{s_w}$$

with

$$L = i_w \cdot \frac{GSD}{100}$$

and so we can obtain

$$d_s = \frac{f_r \cdot L}{s_w}$$

and analogously the height will be

$$H = i_h \cdot \frac{GSD}{100}$$

Of course, we always have to evaluate that d_s must be less than the available space in front of the building.
Once these values are known, it is possible to proceed to calculate the other values in order to have an optimal survey.
The baseline in order to have enough overlaps η will be

$$b_l = t \cdot v$$

with

$$\eta = 1 - \frac{b_l}{L} > 75\%$$

From which we can evaluate the number of shots to be realized to cover the entire surface of the building:

$$N_{ph} = 1 + \frac{L}{b_l}$$

that will be approximated to the upper whole number Nph^*
Anyhow, the real condition is often different from the theoretical ones. For this reason, it is not easy to respect what has been calculated up to now.
The optimal values that should have been used during the field work with the two different cameras are shown in the Table 6.1 and 6.2.
As anticipated, the object of investigation is the Torre di Vietri, or Torre della Marina or Vito Bianchi, and it is one of the largest viceroy towers built along the Amalfi Coast in 1564. It has five embrasures and a 17x17m plant that slowly decrease upwards for a height of 25m.
During the survey stage, some problems have been encountered. First of all the space around the tower is various and so different are the distance (d) considered, above

all in the north facade where there was not sufficient space for parallel shot. Furthermore, the presence of surrounding buildings generate shadows on it and the existence of vegetation adjacent to the main facade has made the survey of it difficult. Another problem is the height of the building because the telescopic stick was not used, we have operated with at a fixed height, increasing only the inclination value, so this makes difficult to acquire the highest part of the tower and consequently the loss of some information.

Know parameters	
camera	Fijifilm XF1
focal length fr [mm]	6
sensor width sw [mm]	8,80
sensor height sh [mm]	6,60
digital image width iw [pixel]	3000
digital image height ih [pixel]	4000
length of the building to be surveyed Bl [m]	17,00
height of the building to be surveyed Bh [m]	25,00
shoot plane compared with the ground connection of the building q [m]	0,00
distance from building d [m]	20,00
operator speed (on foot) v [m/s]	0,28
time lapse t [s]	5
longitudinal baseline bl [m]	1,40
Ground Sample Distance GSD [cm/pixel]	0,50
Optimal values	
longitudinal dimension of the captured image L [mm]	15
elevation dimension of the captured image H [mm]	20
shot distance ds [m]	10,23
longitudinal overlap η [%]	91
angle view of the vertical direction [deg]	89
Real values	
longitudinal dimension of the captured image L [mm]	15
elevation dimension of the captured image H [mm]	20
shot distance ds [m]	7,00
longitudinal baseline bl [m]	1,40
longitudinal overlap η [%]	91
angle view of the vertical direction [deg]	110
GSD [(Sw*Dp)/(Fr*Iw)]*100 (cm/pixel)	0,34

Table 6.1: The optimal values and those used during the field work with Fujifilm camera

Know parameters	
camera	Canon EOS 600D
focal length fr [mm]	18
sensor width sw [mm]	22,30
sensor height sh [mm]	14,90
digital image width iw [pixel]	5148
digital image height ih [pixel]	3456
length of the building to be surveyed Bl [m]	17,00
height of the building to be surveyed Bh [m]	25,00
shoot plane compared with the ground connection of the building q [m]	0,00
distance from building d [m]	20,00
operator speed (on foot) v [m/s]	0,28
time lapse t [s]	5
longitudinal baseline bl [m]	1,40
Ground Sample Distance GSD [cm/pixel]	0,50
Optimal values	
Larghezza della zona catturata nell'immagine L= Iw*(GSD/100) (m)	25,74
Altezza della zona catturata nell'immagine H= Ih*(GSD/100) (m)	17,28
Distanza di presa Dp=(Fr*L)/Sw (m)	20,78
Overlap longitudinale h = 1-(Bl/L) < 75% (%)	95
Angolo di apertura del cono di presa verticale w=2*arctg[(H/2)/Dp]	45
Real values	
longitudinal dimension of the captured image L [mm]	25,74
elevation dimension of the captured image H [mm]	17,28
shot distance ds [m]	7,00
longitudinal baseline bl [m]	1,40
longitudinal overlap η [%]	95
angle view of the vertical direction [deg]	102
GSD [(Sw*Dp)/(Fr*Iw)]*100 (cm/pixel)	0,17

Table 6.2: The optimal values and those used during the field work with Canon camera

The field work ended with a series of photos of 69 with the compact camera Fujifilm XF1 and 247 with Canon EOS 600D Digital Reflex, guaranteeing a greater overlap of picture than those required and obtaining respectively a GSD of 0,34cm/pixel and 0,17cm/pixel.
As visible, the substantial difference between the sensor sizes of the two cameras involves also the various values of GSD, with obvious consequences on the results, but in any case less than 1cm/pixel.

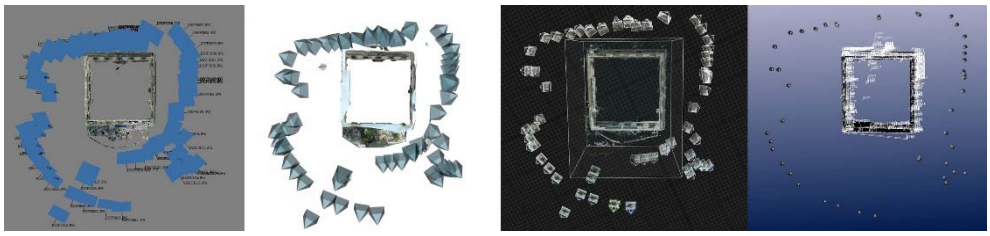

Figure 6.3: Camera station in PhotoScan, Recap photo, Reality Capture and Photo Modeller of the models obtained with photos taken with Fujifilm XF1 camera

6.2 Data processing

6.2.1 PhotoScan

PhotoScan is a software from the Russian Agiscan company and is based on the multi-viewing 3D reconstruction. This software works with the method Shape from Stereo (SfS) and, therefore, the 3D reconstruction is based on detection of homologous points (RGB pixels) in multiple image pair[1]. In fact, it allows to obtain a model starting from shots coming from different cameras, in different conditions and from any point of view; fundamental is that the object from photo-reconstruction has been captured by at least two photos. Below are the main phases that have been followed.

The first one was *Align Photos* to align the photos imported into the project, through the calculation of the exterior and interior orientation. The homologous points are identified to position the images in the space and find the calibration parameters of the camera; the result is a scattered cloud of points. We proceed with the purpose to obtain the best results, so the *Accuracy* option selected was *Highest* in both cases. For the option *Pair Preselection,* while*,* we have opted for *Disable* mode, in order not to consider any constraints in data processing.

Build Dense Point Cloud allows to generate a dense point cloud model after adjusting the bounding box. The reconstruction parameters selected were *Ultra High* for the compact camera and *High* for the reflex (because we had more photos to process and therefore we needed more time for data processing). The filter algorithms that we have chosen to sort out the points outliers that could be generated was the option *Moderate* in the set *Depth Filtering.* It is an option between the *Mild* and *Aggressive* approaches, because we had neither such a simple scene but also there were not even small details spatially distinguished in the scene to be reconstructed. Once the model

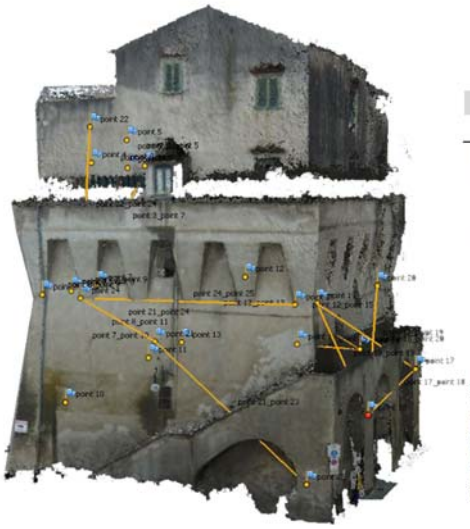

	Distances			
	Points	d (m)	x (m)	z (m)
1	1-2	1,81	1,81	0,03
2	2-3	2,77	0,20	2,76
3	3-5	2,71	2,25	1,51
4	5-6	1,67	0,01	1,67
5	6-4	4,09	0,09	0,15
6	4-3	6,33	6,33	0,01
7	3-7	8,83	5,16	7,16
8	7-9	2,84	2,84	0,04
9	9-8	2,84	2,84	0,03
10	8-7	5,68	5,68	0,01
11	7-10	6,98	2,52	6,51
12	1-11	15,30	0,94	15,27
13	11-8	14,20	13,16	5,36
14	14-12	8,68	8,68	0,06

	Distances			
	Points	d (m)	x (m)	z (m)
15	12-13	6,62	4,81	4,55
16	13-14	14,24	13,48	4,61
17	14-16	6,87	5,34	4,31
18	16-15	4,11	4,11	0,07
19	15-12	8,65	7,50	4,32
20	17-18	10,92	10,91	0,61
21	18-19	7,15	3,93	5,98
22	19-17	15,54	14,59	5,35
23	18-20	9,35	7,29	5,88
24	23-21	10,30	8,39	5,98
25	21-24	4,80	4,39	1,94
26	24-25	11,59	11,59	0,14
27	25-22	15,64	13,03	8,64
28	22-24	8,91	1,53	8,78

Figure 6.4: 28 measures acquired with TopCon GPT 3002 on the model

was created is useful delete excess points or parts of scenes not useful for our aim, this is possible in the software with *Selection* button which can be *Rectangle*, *Circle* or *Free-Form*. At the end, the models obtained have respectively 61602950 points for the model generated by the photos taken with the Fujifilm and 67336611 for those of the Canon.

As we know, a photogrammetric model is not in true shape and size, which is why it is necessary to insert some reference measurements to scale the building. The tool used for the survey was the total station TopCon GPT 3002 employed without prism; it is from TPS (Topcon Positioning Systems) company and allows to perform efficient no-prism measurements; guarantying, according the manual, an accuracy of 0,005m. During field work, thus, 24 points and about 28 measures were acquired on all 4 facades of the building, they were chosen arbitrarily but guaranteeing a fair spatial distribution.

To identify the points on the point cloud model it is required placing markers on it. We proceeded in manually mode, so the first step was the collimation of the control point on the model, then PhotoScan automatically projects the position of the *Marker* on the other photos and finally we improve the real position of it on each pictures. Placed the *Markers* in the scene the *Create Scale Bar* command can be used; in this way, the distances previously detected with the total station can be reported and the model will be scaled (Figure 6.4).

The next phase was *Building mesh* in both cases the option set were *Arbitrary* for *Surface type* parameter and *High* for the *Polygon Count* used *Dense Cloud* as *Source*

data. In the *Advanced* section, we operated without any type of interpolation (*Disable*) so that only areas corresponding to dense point can be reconstructed without, therefore, any falsification of the data. The final models had 12320589 faces for the compact camera and 13467263 faces for the reflex, the main parameters of the models are shown in the figure 6.4.
Once the polygonal model was generated, it is possible to proceed with *Building Texture* phase. In this case, we have selected the default mode *Generic* for the *Mapping mode* because in this way the application tries to create the most uniform texture possible and *Average* in *Blending mode* so that for the realization of the texture will be used the weighted average value of all the pixels from individual photos. In addition, in advanced option we also set *Enable color correction* because there is a lot brightness variation in the taken shots, although it takes up more time.
The last stage, before proceed to export orthophotos, was *Building Orthomosaic* useful for generation of orthophoto based on the reconstructed model. The comparison between the orthophotos will be done only on the South-Est elevation made with the compact camera, so, we proceed to generate this data only with the model obtained from Fujifilm XF1. Hence, it is necessary to choose the project plane to export, in which we will select the markers mode because, the 3D model

Model Fujifilm XF1	
Cameras stations	69
Ground resolution	4,97 mm/pix
Tie points	35326
Reprojection error	2,08 pix
Points	61602950
Faces	12320589

Model Canon EOS 600D	
Cameras stations	224
Ground resolution	2,59 mm/pix
Tie points	56363
Reprojection error	1,55 pix
Points	67336611
Faces	13467263

Figure 6.5: PhotoScan models with photos taken from Fujifilm XF1 and Canon EOS 600D

generated, is not perfectly aligned with the reference system and, therefore, proceed identifying the horizontal axis directions through the previously marked points 3 and 4. Once again, we set *Average* in the *Blending mode* parameter ticking *Enable color correction.* Another option selected is *Pixel size,* the default program value is referred to GSD in mm/pixel (it was 0,0050 for the compact camera and 0,0026 for the reflex) so is useless to decrease this value. From now on, the orthophoto can be exported in different format; having to import them in AutoCAD software, we selected the option JPEG (Figure 6.6).[2]

Figure 6.6: Ortophoto of the South-Est elevation of Torre di Vietri with PhotoScan

6.2.2 ReCap Photo

The data gained during this survey was also developed with free software ReCap Photo, a cloud service from the Autodesk manufacturing company, which bases its work on automating the reverse modeling process.
This process, again a *SfS* mode, is possible only if the point on the real model is identifiable at least in three shots, so through triangulation rules it will be possible the right position of the camera in the space. The distinctive trait of this software is that the intricate operations of collimation of homologous points are entrusted to the web through cloud computing.
To start to use this application is necessary an account to Autodesk 360 that gives access to several cloud services. Once we have logged it was possible to select *New Project* from the landing page. The next step was chosen some settings like *Project name*, *quality* for the model that we wished create and, finally the *export format* in both cases (Fujfilm XF1 and Canon EOS 600D) we operated with the *Ultra* values and exported in .obj format for a mesh model and .rcs for a point cloud appropriate to be opened in ReCap Pro.
The next step was uploaded photos and before to start the process it was possible to insert the survey points on least three pictures and set the distance values in order to scale the model. To done this stage we defined manually matching points; on the left window there was a photo to select a point as reference and on the right side, another photo that is different from the previous one but had some common points. Once the pair of points has been selected (at least in three images), the reference distance can be set.

Figure 6.7: Recap Photo models with photos taken from Fujifilm XF1 and Canon EOS 600D

At the end, after clicked the option *next* the data was sent; being an online software it automatically detected homologous points on the photos, returning their spatial position and eventually generating a textured 3D model. Having to deliver high quality results, the program taken some time to reconstruct the model; even if it was not necessary to wait because an email notification was sent at the end of the process that inform you that the project is ready for viewing.
The web viewer only permit to show the model in a preview; to view the high quality results is necessary to export the scene and then to open it in another software.
The graphic interface is very easy, a navigation panel is displayed in the bar down the 3D scene, it gives you also the option to change the display of the model as a textured model (default setting), mesh only or mesh and texture. Moreover, it is

Figure 6.8: Ortophoto of the South-Est elevation of Torre di Vietri with Recap Photo

possible to add some notes in the 2DMap scene, but not delete or modify the model. If the results are satisfactory the model can be downloaded according to the desired format, if not it is possible to reprocess the scene overwriting the existing or creating a new one.
Even though the model obtained had ultra-quality meshes and a good texture it had some errors, holes and detached parts. To fix those, it was necessary to use another software ReCap Pro; a desktop product that allows you to load, crop, measure and permit to share the data between people distant from each other thanks to Autodesk 360. The same procedure was used for both 'set' of photos obtained from the two cameras, obtaining, however, different results.
In the case of Fujifilm XF1 the mesh model has 2453394 faces and the cloud points 3866900 points, while with Canon EOS 600D we obtained models respectively with 6965336 polygon and 6970498 points (Figure 6.7). Cleaned the model, it was saved to be able to be opened with AutoCAD and so proceed with the extraction of the orthophoto necessary for the next comparison phase (once again this phase has been realized only for the model obtained from the compact camera and it is visible in the figure 6.8).[3]

6.2.3 Reality Capture

This is an application that allow to create three-dimensional texture models and orthophotos from three or more photos or from laser scanner acquisition in automatically way. In the case studied, the free trial version was used following the registration on the site, so some operations were not allowed.
The interface is divided in three tabs useful for the data process: *Workflow*, *Alignment* and *Reconstruction.* The first one gives a general information and options to follow for the creation of the models, in the second one greater alignment settings are presented like the possibility to insert constraints or analyze the process and finally the last tab that is useful for the creation of mesh model and its texturizing. Once again, as PhotoScan, it is based on *Shape from Stereo* mode, so the first step, on the workflow tab, it was added the pictures taken before during the field work and to proceed with the alignment phase. In the second tab it was possible to selected the settings suited to our focus, in particular in *Alignment Settings* we decided to work with *Max features per mpx* 8000 and *Preselector features* 2000 (1/4 of the max features as recommended by the manual) and without changing the other default values. In this stage, it also was possible to insert the camera pose prior setting (if known) like GPS coordinates to be used during the alignment, and define the

distortion model to be used in relation to our lens; we selected *Brown3* being the most popular, it works for optic with less 180° and it is used as the default.
At the end of the process, it was possible, in the same tab, to assess the alignment quality in the option *Alignment report* and therefore see the maximal error (1,99px), median error (0,67px) and mean error (0,76px) committed; although the ideal values for the last two should be less than 0,5px. Another interesting option is *Inspection Tool* that analyzes dependencies among cameras in a scene and gives the possibility to change the interactions between one tool and another during the alignment phase.
The next step determines the real metric information of the model, there are several mode to do this, but we proceed with *Distance Constraint* mode. To define the measure necessary to scale our model we proceeded to generate only two control points, point0 and point1 that were subsequently dragged and placed in the precise positions of the photos. The second step was selecting *Create distance*. This option automatically entails the opening of a panel in which it is possible to identify the distance between two control points, assign them a name and finally specify the precise numerical value; of course adding more distance constraints allows getting more accurate results.
A further step, before the 3D model is generated, it consists in the definition of the *Ground Plane* and the restriction of the *Reconstruction Region* (in manually or automatic mode) in order to speed up a model computation; it is possible in the last tab. At this point, we proceed with the generation of the mesh desired; in *Setting* it is possible to set certain options for an optimal generation of it like the minimum distance between two vertices of a triangle and choose the *Calculate Model* (Preview, Normal or High quality). Although higher quality modes involves more

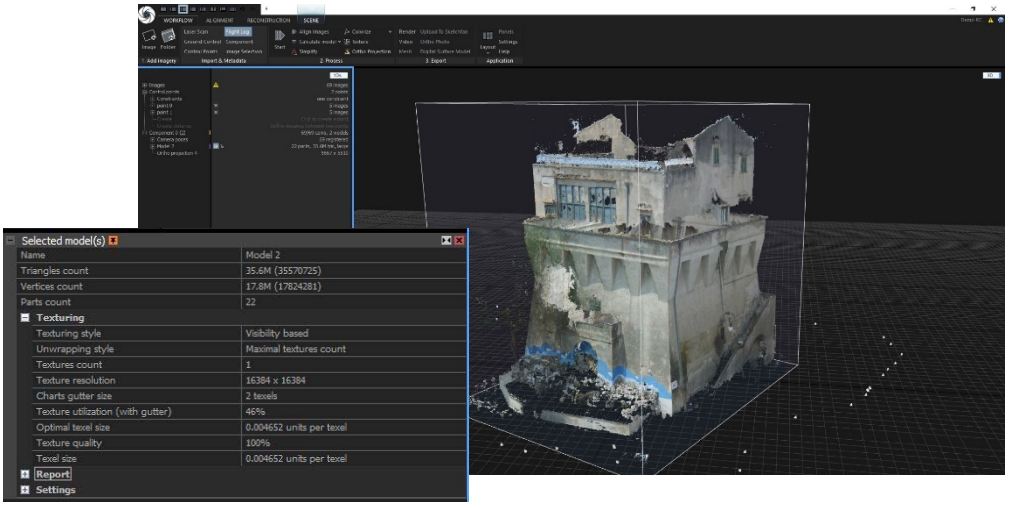

Figure 6.9: Reality Capture model from Fujifilm XF1 photos

computation effort and hence more time we selected this option in order to obtain a very dense triangular mesh that in the case studied was 355706725 faces.
Once 3D model was created we were able to proceed with adding color to it, these could be done either using *Colorize* or *Texture* function. The first one creates only color for model vertices, so it is better for denser object and it will be smaller in size than the textured model. The second one, instead, works with the unwrap mapping mode, this process involves the creation of a two-dimensional coordinate system, which are used by the 3D software to take certain portions of a texture and apply them on the surface of a polygon, this is then repeated for each polygon of a model 3D; we operated with the *Texture* function. After several trial combination between the option *Coloring method* and *Texturing/Coloring style,* we obtained the best result

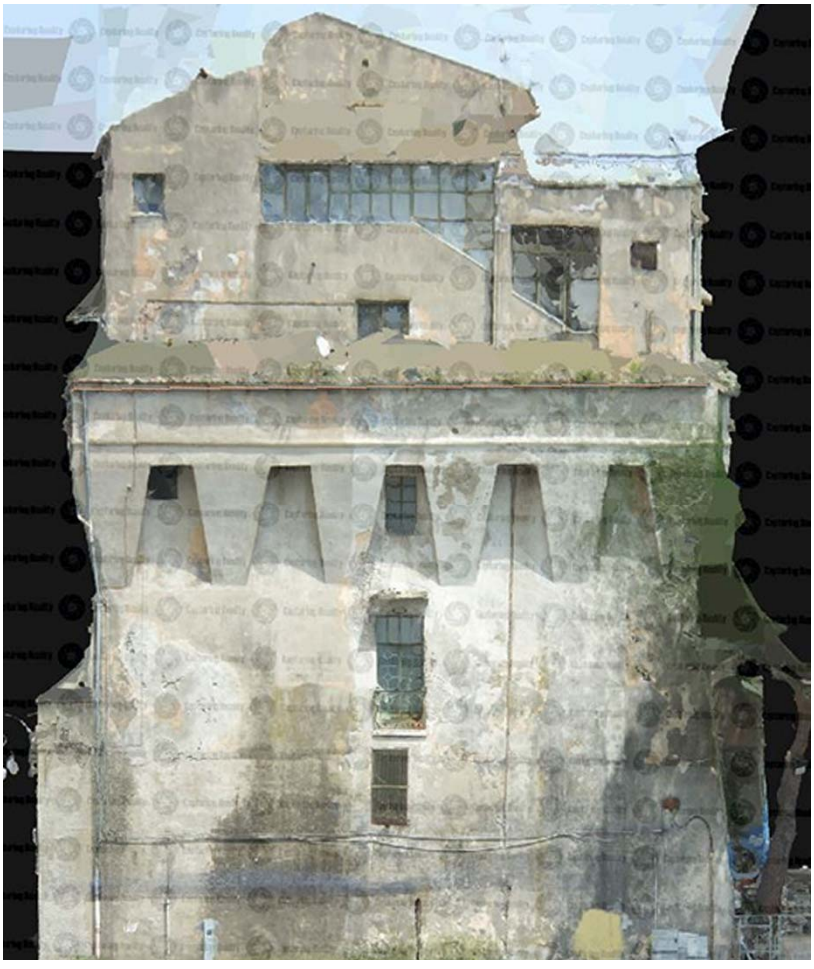

Figure 6.10: Ortophoto of the South-Est elevation of Torre di Vietri with Reality Capture

with the combination *Linear* that works in average values and *Photo consistency based* that is a slow process but has better and more complex results.
The last step was the creation of orthophoto with the option *Orthographic Projection*, again in the *Reconstruction* tab. When we clicked on *Ortho projection* button, it was necessary to select the region of interest and choose the projection side; automatically a new *Ortho Projection Panel* appeared in which it was possible to set the optimal values. The optimal resolution respect with to model proprieties was calculated with the button *Estimate optimal resolution;* in our case, the ortho pixel size was 0,002063 mm/pixel. Finally, the orthophoto was generated by clicking on the Render button (Figure 6.10).[4]

6.2.4 PhotoModeler

This software provides to create 3D model from photos shoots in order to extract metric information. Differently from the previous software, it, as base product that we used, works in with the method *Shape from Silhouette* (*SfSi*), based on the detection of the item shape from different viewpoints. This method, in fact, identifies the intersections between the visual pyramids formed by the silhouettes (generatrix) and the director ray from a well-known viewpoint (once again a visual pyramid)[5].
Photo Modeller in standard use allows to build models using points, line, edges, surface (like photo textured or shaded) and other entities; generating, at the end, not a cloud of point or a dense surface model (however possible with PhotoModeler scanner product) but a model consisting of the assembly of several surfaces of various sizes.
At the opening of the program, a window appears divided in four parts: *create new project*, *open a recent project*, *help and learn* and *access to web*. In our case, having to realize a new project, it is necessary to select the *Points-based project* option. From this moment, we had to select the images to be processed and imported them into the software
When the program loads the photos it is possible to operate with or without the calibration camera, not having previously provided for this, it was necessary to select the options: *An unknown camera* and *Approximation.*
The working space of the application allows closing or opening the necessary windows and organizing them in a personal way.
Operating without the presence of artificial targets, the first step we have done was identified in manually way the homologous points present on the photos. Hence, identified the first reference picture, with the command *Reference Mode* we

proceeded to select the points visible on at least three photos. The bottom bar of the window reported information about the point's data, like information of the coordinate xy, id, photos in which it was used and maximal residual error in the identification on the pictures.

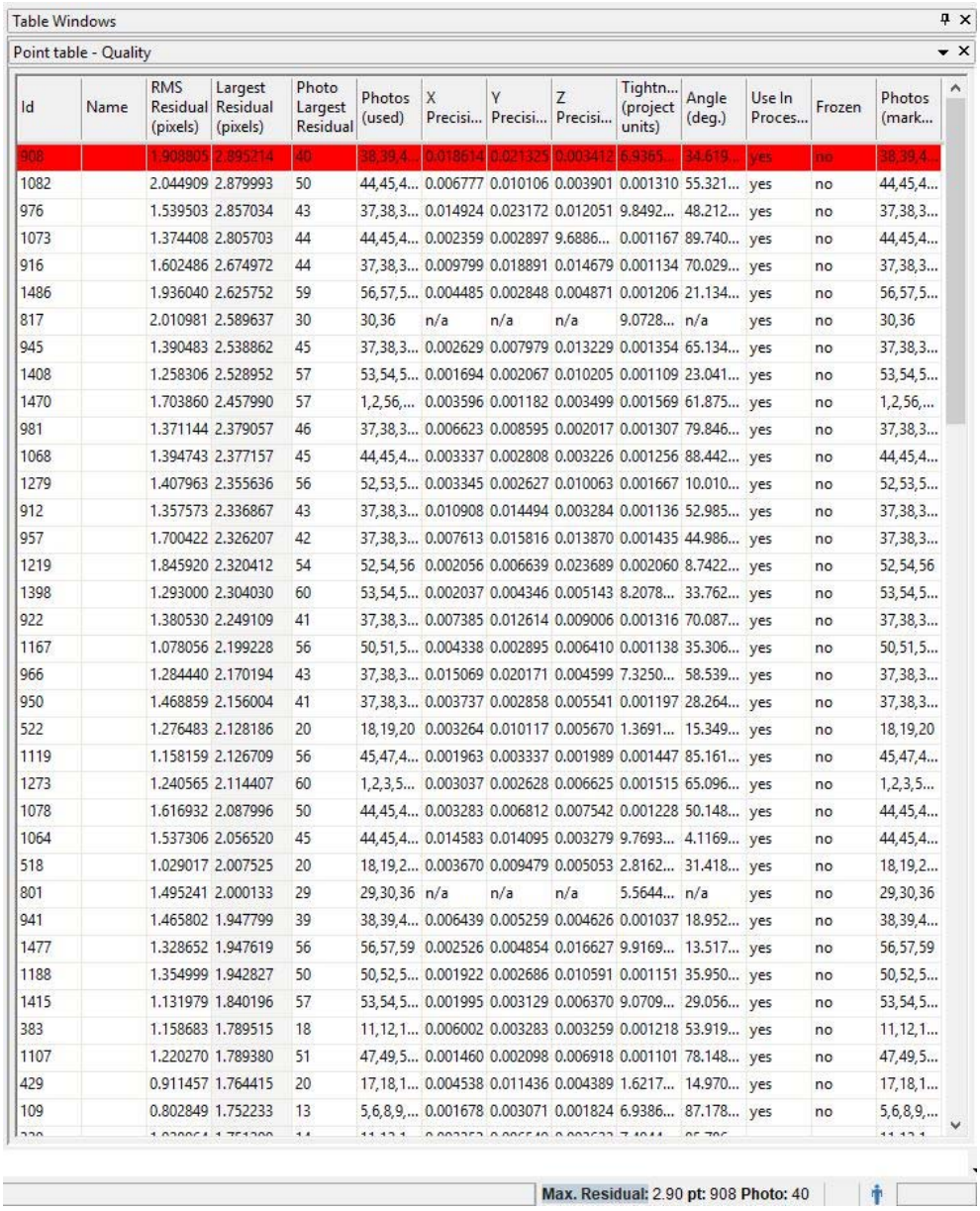

Id	Name	RMS Residual (pixels)	Largest Residual (pixels)	Photo Largest Residual	Photos (used)	X Precisi...	Y Precisi...	Z Precisi...	Tightn... (project units)	Angle (deg.)	Use In Proces...	Frozen	Photos (mark...
908		1.903805	2.895214	40	38,39,4...	0.018614	0.021325	0.003412	6.9365...	34.619...	yes	no	38,39,4
1082		2.044909	2.879993	50	44,45,4...	0.006777	0.010106	0.003901	0.001310	55.321...	yes	no	44,45,4...
976		1.539503	2.857034	43	37,38,3...	0.014924	0.023172	0.012051	9.8492...	48.212...	yes	no	37,38,3...
1073		1.374408	2.805703	44	44,45,4...	0.002359	0.002897	9.6886...	0.001167	89.740...	yes	no	44,45,4...
916		1.602486	2.674972	44	37,38,3...	0.009799	0.018891	0.014679	0.001134	70.029...	yes	no	37,38,3...
1486		1.936040	2.625752	59	56,57,5...	0.004485	0.002848	0.004871	0.001206	21.134...	yes	no	56,57,5...
817		2.010981	2.589637	30	30,36	n/a	n/a	n/a	9.0728...	n/a	yes	no	30,36
945		1.390483	2.538862	45	37,38,3...	0.002629	0.007979	0.013229	0.001354	65.134...	yes	no	37,38,3...
1408		1.258306	2.528952	57	53,54,5...	0.001694	0.002067	0.010205	0.001109	23.041...	yes	no	53,54,5...
1470		1.703860	2.457990	57	1,2,56,...	0.003596	0.001182	0.003499	0.001569	61.875...	yes	no	1,2,56,...
981		1.371144	2.379057	46	37,38,3...	0.006623	0.008595	0.002017	0.001307	79.846...	yes	no	37,38,3...
1068		1.394743	2.377157	45	44,45,4...	0.003337	0.002808	0.003226	0.001256	88.442...	yes	no	44,45,4...
1279		1.407963	2.355636	56	52,53,5...	0.003345	0.002627	0.010063	0.001667	10.010...	yes	no	52,53,5...
912		1.357573	2.336867	43	37,38,3...	0.010908	0.014494	0.003284	0.001136	52.985...	yes	no	37,38,3...
957		1.700422	2.326207	42	37,38,3...	0.007613	0.015816	0.013870	0.001435	44.986...	yes	no	37,38,3...
1219		1.845920	2.320412	54	52,54,56	0.002056	0.006639	0.023689	0.002060	8.7422...	yes	no	52,54,56
1398		1.293000	2.304030	60	53,54,5...	0.002037	0.004346	0.005143	8.2078...	33.762...	yes	no	53,54,5...
922		1.380530	2.249109	41	37,38,3...	0.007385	0.012614	0.009006	0.001316	70.087...	yes	no	37,38,3...
1167		1.078056	2.199228	56	50,51,5...	0.004338	0.002895	0.006410	0.001138	35.306...	yes	no	50,51,5...
966		1.284440	2.170194	43	37,38,3...	0.015069	0.020171	0.004599	7.3250...	58.539...	yes	no	37,38,3...
950		1.468859	2.156004	41	37,38,3...	0.003737	0.002858	0.005541	0.001197	28.264...	yes	no	37,38,3...
522		1.276483	2.128186	20	18,19,20	0.003264	0.010117	0.005670	1.3691...	15.349...	yes	no	18,19,20
1119		1.158159	2.126709	56	45,47,4...	0.001963	0.003337	0.001989	0.001447	85.161...	yes	no	45,47,4...
1273		1.240565	2.114407	60	1,2,3,5...	0.003037	0.002628	0.006625	0.001515	65.096...	yes	no	1,2,3,5...
1078		1.616932	2.087996	50	44,45,4...	0.003283	0.006812	0.007542	0.001228	50.148...	yes	no	44,45,4...
1064		1.537306	2.056520	45	44,45,4...	0.014583	0.014095	0.003279	9.7693...	4.1169...	yes	no	44,45,4...
518		1.029017	2.007525	20	18,19,2...	0.003670	0.009479	0.005053	2.8162...	31.418...	yes	no	18,19,2...
801		1.495241	2.000133	29	29,30,36	n/a	n/a	n/a	5.5644...	n/a	yes	no	29,30,36
941		1.465802	1.947799	39	38,39,4...	0.006439	0.005259	0.004626	0.001037	18.952...	yes	no	38,39,4...
1477		1.328652	1.947619	56	56,57,59	0.002526	0.004854	0.016627	9.9169...	13.517...	yes	no	56,57,59
1188		1.354999	1.942827	50	50,52,5...	0.001922	0.002686	0.010591	0.001151	35.950...	yes	no	50,52,5...
1415		1.131979	1.840196	57	53,54,5...	0.001995	0.003129	0.006370	9.0709...	29.056...	yes	no	53,54,5...
383		1.158683	1.789515	18	11,12,1...	0.006002	0.003283	0.003259	0.001218	53.919...	yes	no	11,12,1...
1107		1.220270	1.789380	51	47,49,5...	0.001460	0.002098	0.006918	0.001101	78.148...	yes	no	47,49,5...
429		0.911457	1.764415	20	17,18,1...	0.004538	0.011436	0.004389	1.6217...	14.970...	yes	no	17,18,1...
109		0.802849	1.752233	13	5,6,8,9,...	0.001678	0.003071	0.001824	6.9386...	87.178...	yes	no	5,6,8,9,...

Figure 6.11: Point table Quality in PhotoModeler application

In addition, bottom right, the application tells us from what time we can try to process the data, or to orient the photos selecting *Process.* We continued in the same way by adding more photos and other points obtaining a final error of 0,70 pixels.
The values of the orientation could be evaluated seeing the window *Create/Edit Tables* and after *Point table Quality.* There, are reported all the information concerning the points: identification of the points (id), order number, root mean squared errors (in pixels), once again error in pixel of how far, according with the previous values, is the point from the value considered by the calculation model (Figure 6.11). The latter is a three-dimensional vector visible on the desktop if the option *Residual* was activated in the tab *Visibility of photos*. In this window, it is also possible to see the photo where there is that *Large Residual*, the photos containing points and the precisions on the x and y-axis obtained.
In the case studied we used 138 points to orientate the pictures and after the *Process* phase we corrected the major errors (Max residual) in order to have the maximum value of 2,90 pixel.
Once the desired value is obtained, it was possible to proceed with the generation of geometry. First of all we created new layers in order to differentiate the new points that we inserted and which did not be considered on the orientation of the photos (do not check the option uses in processing); they are *Oriented; Geometry* and *Arch.*
The points thus identified served, therefore, for the definition of straight lines (*Mark Lines Mode*) or curves (*Curves through points*) useful for the generation of surfaces (*Path Mode*). From this moment, it was possible to open the 3D space selecting *3D Viewer*. As shown in the figure 6.12 the points and surfaces previous identified were

Figure 6.12: PhotoModeler model from Fujifilm XF1 photos

placed in the space, in order to project the texture we had to open the option tab *display style* and check *quality texture;* the others choose are *shaded*, *wire frame*, *dots*, *fast textures*.
The generated model, being a photogrammetric process, does not present the true form and greatness; therefore, we proceed to scale it. To done this, the application only need one distance. In the option *Project* we opened the window *Scale/Rotate,* initially it is necessary to indicate the unit of measure that we used and continually to introduce the measure selecting two points or the line to scale.
The same procedure is used to insert the reference system; that is, selecting two points or the line and after the corresponding axis.

Figure 6.13: Ortophoto of the South-Est elevation of Torre di Vietri with Photo Modeller

Once the model was created, scaled and oriented it was possible to proceed with the exportation of the orthophoto: open the command *File*, select *Export Ortho Photo* and check the several alternatives. In our case, we chose *all photo textured surface* as source data, the *3 points* to identify the projection plane and image size 897x1026.[6]

[1] García Fernández, J.,Álvaro Tordesillas, A.,Barba, S. (2015) An approach to 3D digital modeling of surfaces with poor texture by range imaging techniques. 'shape from stereo' vs. 'shape from silhouette' in digitizing Jorge Oteiza's sculptures. In: *The International Archives of the Photogrammetry, Remote Sensing and Spatial Information Sciences*, Volume XL-5/W4, 2015.

[2] Agisoft PhotoScan User Manual. Professional Edition, Version 1.2 (http://www.agisoft.com/pdf/photoscan-pro_1_2_en.pdf).

[3] Autodesk ReCap Photo Getting Staerted Guide (https://adsk-recap-public.s3.amazonaws.com/Getting_Started_Guide_ReCap_Photo.pdf).

[4] Manual of Reality Capture.

[5] García Fernández, J.,Álvaro Tordesillas, A.,Barba, S., op. cit.

[6] Cueli Lopez J. T., (2011). *Fotogrametría práctica. Tutorial Photomodeler.* Cantabria (Spain), Tantin , 2011.

7. Methodological verification

7.1 The purpose

This chapter provides an original research about the analysis and comparison of different methodologies used in this study. This evaluation will take place throughout the development of the *error theory* in order to estimate reliability and precision of the results. Subsequently, the method used to ascertain the results obtained was been validated with *predictive value of tests*. In particular, this analysis will be focused on the Torre della Marina, a building of the 16th century and located in Vietri sul Mare; it will be organized in two parts. The first one provides for the data collection and processing phase of data in order to manage the metric information in different ways. Later, the research focuses on some different comparison (on two-dimensional and three-dimensional model) and on the validation of what has been done.

7.2 Comparison of the orthophotos

In this part of the chapter, we proceed with an analytic analysis of the orthophto obtained so far with the compact camera. The elements available for comparison are the elevations (in raster) resulting from the four software shown previously, so each of these drawings is a product of a treatment of the data.
In summary, four software has been used: the PhotoModeler application, which foresees the manual identification of homologous points for the generation of the 3D model, and three SfM (Structure for Motion) applications that allow to extract the spatial information from the images through the automated processes; we worked with PhotoScan, Reality Capture and Recap Photo software.
In both cases, the starting data are the same 69 shots obtained from the Fujifilm XF1 and we attempted working with a GSD less than 1cm. Commonly, whenever a measure of size is carried out, the purpose of the operation is to associate a number

to it; therefore, size and measure must correspond unequivocally; to each size must correspond to one and only one measure. The determination of a physical quantity, however, is always subject to a series of errors that depend partly on the methodology used and partly on the operator performing the operation. As known, when we performer a measurement this can be altered from three types of errors: *gross*, *systematic* and *random* errors.
The latter, in particular, are due to causes that cannot be determined and so that cannot be controlled; they are inevitable and not eliminable errors. This means that multiple measures of the same size performed by one operator with the same instrument could have different values for each measurement. However, although they cannot be avoided and eliminated completely, they can be considerably attenuated and limited within a tolerance desired by means of *error theory*.
In our case, the application of error theory consisted of a punctual analysis: the difference were calculated in terms of coordinates between "type points" present in the four orthophotos extracted from the 3D models.
In the specific case 73 points have been identified for each image, differentiating clearly visible points in red (*real points*), while in yellow those not easily identifiable (*hypothesized points*) as visible in the figure 7.1.
Therefore, the exported images of the different software were imported into AutoCAD, aligned respect the same reference system and, subsequently detected the various coordinate values of the homologous points (*type points*).
The initial data at our disposal are represented by the coordinates x and y of 73 coincident points in the four images:
$x_{i,PS}$ values of the x coordinate of the points relative to the PhotoScan software,
$y_{i,RC}$ values of the y coordinate of the points relative to the PhotoScan software;
$x_{i,RC}$ values of the x coordinate of the points relative to the Reality Capture software,
$y_{i,RP}$ values of the y coordinate of the points relative to the Reality Capture software;
$x_{i,RP}$ values of the x coordinate of the points relative to the Recap software,
$y_{i,PS}$ values of the y coordinate of the points relative to the Recap software;
$x_{i,PM}$ values of the x coordinate of the points relative to the PhotoModeler software,
$y_{i,PM}$ values of the y coordinate of the points relative to the PhotoModeler software.

For each of these points we proceeded to calculate two most effective statistical parameters for our objectives either the *arithmetic mean* of the data and the *variance* or the *standard deviation* calculated respectively for the variables x and y:

$$x_m = \frac{x_{i,PS} + x_{i,RC} + x_{i,RP} + x_{i,PM}}{n}$$

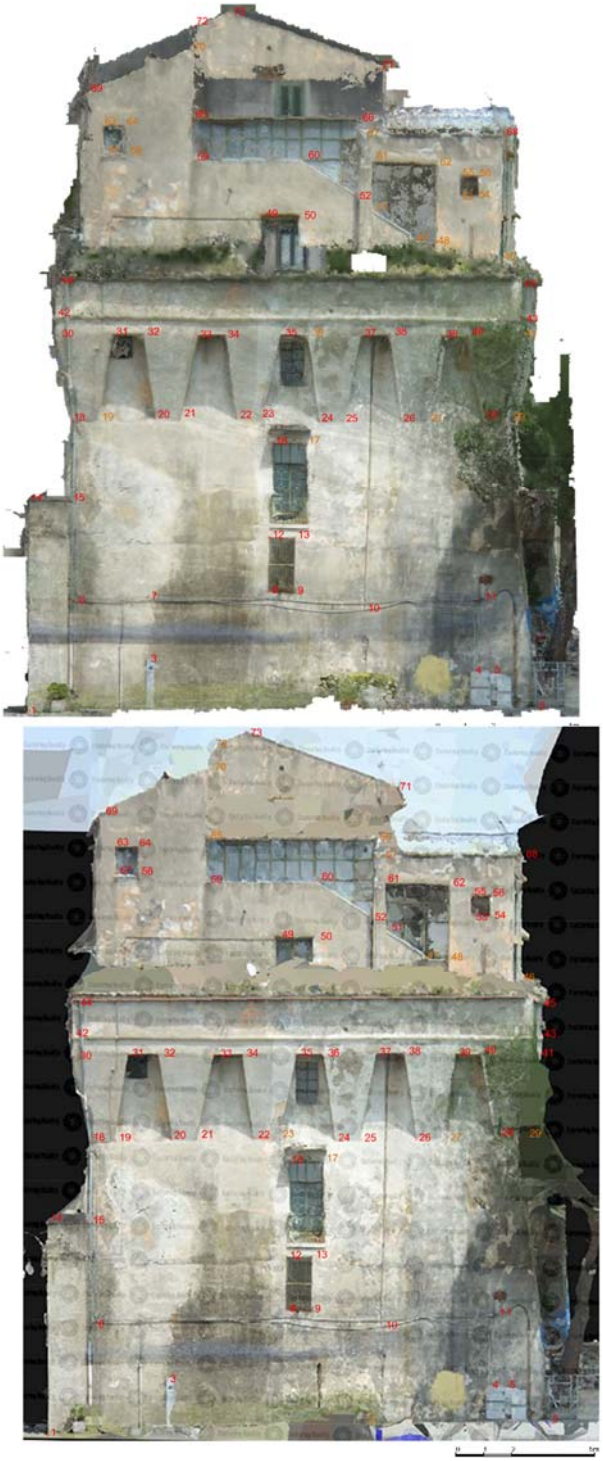

Figure 7.1: 73 points identified on the orthophoto exported from PhotoScan and Reality Capture; in red points clearly visible, in yellow hypothesized ones

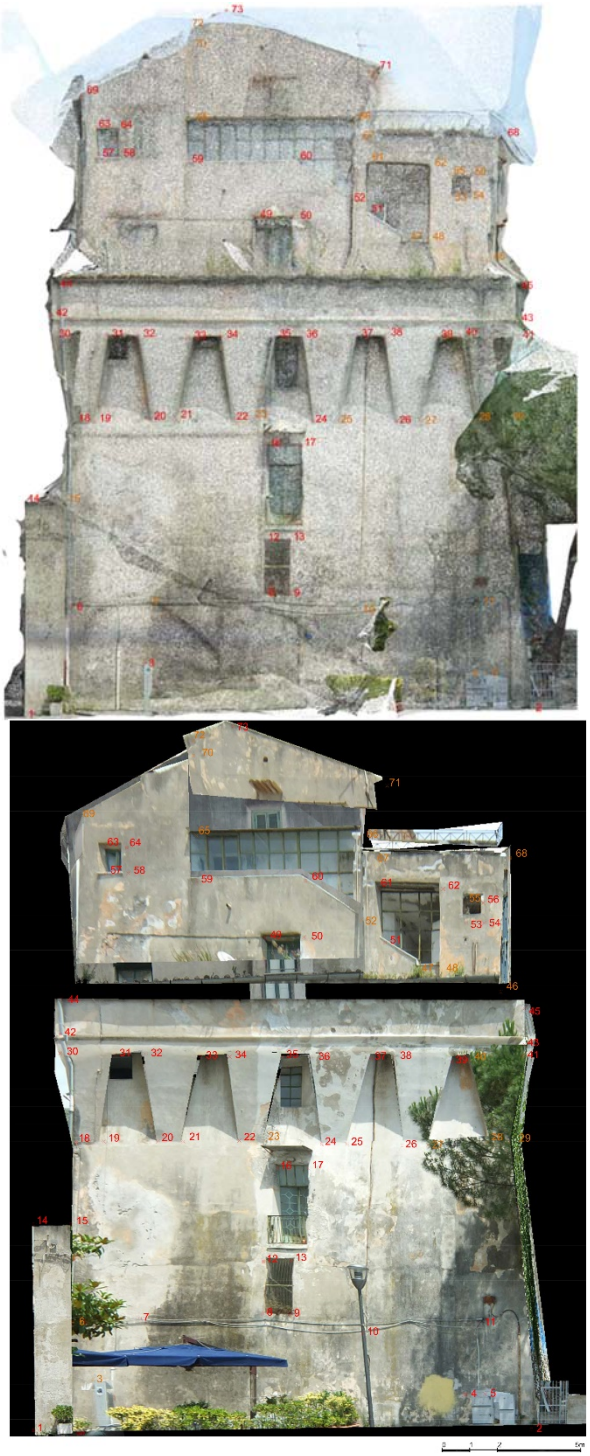

Figure 7.2: 73 points identified on the orthophoto exported from PhotoScan and Reality Capture; in red points clearly visible, in yellow hypothesized ones

$$y_m = \frac{y_{i,PS} + y_{i,RC} + y_{i,RP} + y_{i,PM}}{n}$$

$$\sigma = \sqrt{\frac{\sum_{i=1}^{n} s_i^2}{n-1}}$$

where

$$s_{x,i} = x_i - x_m$$

$$s_{y,i} = y_i - y_m$$

Smaller the values obtained more precise the measurement will be; in fact, it allows to determine the maximum limit beyond which the errors of a set of measures cannot be accepted as *random errors*.
Experience shows that 70% of errors do not exceed the absolute value of σ; 95% of errors do not exceeds the double of σ; and finally 99,7%-100% of the errors does not exceed the triple of σ. It follows that the possibility that a measure contains an error greater than triple of σ is very difficult, so that this same value is taken as a maximum permissible error, called *tolerance*:

$$T = \pm 3\sigma$$

It is possible to notice that in our case for all the points, the errors are tolerable and so we can deduce that in all the measurements carried out we did not commit *gross errors* but only *systematic* or *random* ones.
Among the variation it was interesting to evaluate the values that where included in the σ; in the table 7.1 and 7.2 in fact, in addition to highlighting in yellow the hypothesized points, we proceeded to colour in green the values below the standard deviation and in red those that exceed it. Of the 73 measurements the points exceeding *standard deviation* along the *x-axis* are:
- n. 10 for PhotoScan;
- n. 30 for Reality Capture;
- n. 10 for Recap Photo;
- n. 41 for PhotoModeler.

The points exceeding *standard deviation* along the *y-axis*:
- n. 5 for PhotoScan;
- n. 16 for Reality Capture;
- n. 6 for Recap Photo;
- n. 61 for PhotoModeler.

	PhotoScan		Reality Capture		Recap Photo		PhotoModeler									
n	x_{PS} [m]	y_{PS} [m]	x_{RC} [m]	y_{RC} [m]	x_{RP} [m]	y_{RP} [m]	x_{PM} [m]	y_{PM} [m]	x_m [m]	y_m [m]	$s_{x,PS}$ [m]	$s_{x,RC}$ [m]	$s_{x,R}$ [m]	$s_{x,PM}$ [m]	σ_x [m]	T_x [m]
1	0,89	0,17	0,89	0,23	0,89	0,18	0,86	0,23	0,88	0,20	0,01	0,01	0,01	-0,02	0,01	0,04
2	19,15	0,51	18,90	0,78	19,10	0,46	18,83	0,27	19,00	0,51	0,15	-0,10	0,10	-0,16	0,15	0,46
3	5,25	2,15	5,17	2,23	5,19	2,07	3,0057	2,0549	4,66	2,13	0,60	0,52	0,54	-1,65	1,10	3,30
4	16,84	1,67	16,73	2,00	16,79	1,71	16,45	1,52	16,70	1,73	0,14	0,02	0,09	-0,25	0,17	0,52
5	17,53	1,80	17,35	2,00	17,49	1,72	17,17	1,53	17,39	1,76	0,15	-0,03	0,11	-0,22	0,17	0,50
6	2,52	4,21	2,50	4,20	2,53	4,12	2,2861	4,1334	2,46	4,16	0,06	0,04	0,07	-0,18	0,12	0,35
7	5,24	4,37	5,25	4,30	5,37	4,30	4,72	4,28	5,15	4,31	0,10	0,11	0,22	-0,43	0,29	0,87
8	9,53	4,59	9,50	4,72	9,51	4,59	9,14	4,43	9,42	4,58	0,11	0,08	0,09	-0,28	0,19	0,56
9	10,47	4,57	10,36	4,73	10,42	4,58	10,10	4,41	10,34	4,57	0,13	0,03	0,08	-0,23	0,16	0,49
10	13,01	3,89	12,94	4,10	12,91	3,96	12,75	3,72	12,90	3,92	0,11	0,03	0,01	-0,15	0,11	0,32
11	17,13	4,36	16,95	4,55	17,16	4,25	16,91	4,05	17,04	4,30	0,09	-0,09	0,12	-0,13	0,13	0,38
12	9,54	6,60	9,53	6,07	9,53	6,54	9,17	6,31	9,44	6,38	0,10	0,09	0,09	-0,27	0,18	0,55
13	10,51	6,59	10,42	6,60	10,40	6,54	10,17	6,34	10,38	6,52	0,14	0,04	0,03	-0,21	0,15	0,45
14	0,91	7,82	0,90	7,92	0,89	7,91	0,88	7,67	0,90	7,83	0,01	0,01	0,00	-0,01	0,01	0,03
15	2,33	7,84	2,33	7,85	2,38	7,94	2,21	7,67	2,31	7,82	0,02	0,01	0,07	-0,10	0,07	0,21
16	9,68	9,98	9,60	10,07	9,61	9,95	9,68	9,69	9,64	9,92	0,04	-0,04	-0,04	0,04	0,04	0,13
17	10,90	9,98	10,82	10,08	10,82	9,94	10,78	9,68	10,83	9,92	0,07	-0,01	-0,01	-0,04	0,05	0,14
18	2,49	10,74	2,47	10,80	2,58	10,81	2,42	10,60	2,49	10,74	0,00	-0,02	0,09	-0,07	0,07	0,21
19	3,38	10,76	3,32	10,83	3,40	10,81	3,40	10,65	3,38	10,76	0,01	-0,06	0,03	0,02	0,04	0,12
20	5,43	10,84	5,33	10,89	5,42	10,87	5,37	10,65	5,39	10,81	0,04	-0,06	0,03	-0,02	0,04	0,13
21	6,33	10,81	6,23	10,89	6,32	10,86	6,27	10,65	6,29	10,81	0,04	-0,06	0,04	-0,02	0,05	0,14
22	8,35	10,85	8,33	10,92	8,35	10,88	8,30	10,68	8,33	10,83	0,02	-0,01	0,02	-0,03	0,02	0,07
23	9,28	10,84	9,27	10,92	9,10	10,88	9,2442	10,6904	9,22	10,83	0,05	0,05	-0,12	0,02	0,08	0,25
24	11,32	10,78	11,26	10,84	11,24	10,80	11,27	10,54	11,27	10,74	0,05	-0,01	-0,03	0,00	0,03	0,10
25	12,22	10,75	12,17	10,85	12,11	10,81	12,19	10,55	12,17	10,74	0,05	0,00	-0,06	0,01	0,04	0,13
26	14,32	10,81	14,17	10,89	14,26	10,83	14,16	10,50	14,23	10,76	0,09	-0,06	0,03	-0,06	0,07	0,22
27	15,31	10,82	15,27	10,93	15,17	10,82	15,1134	10,519	15,22	10,77	0,09	0,05	-0,04	-0,10	0,09	0,26
28	17,22	10,79	17,10	10,94	17,07	10,80	17,2266	10,6197	17,15	10,79	0,07	-0,06	-0,09	0,07	0,08	0,25
29	18,05	10,77	17,92	10,95	18,18	10,82	18,0484	10,6287	18,05	10,79	0,00	-0,13	0,13	0,00	0,11	0,32
30	1,85	13,85	1,83	13,83	1,88	13,90	1,834	13,8295	1,85	13,85	0,00	-0,02	0,03	-0,02	0,02	0,07
31	3,94	13,91	3,80	13,92	3,88	13,89	3,8251	13,7659	3,86	13,87	0,08	-0,06	0,02	-0,04	0,06	0,19
32	4,99	13,91	4,91	13,95	4,99	13,93	4,9333	13,7997	4,96	13,90	0,04	-0,04	0,03	-0,02	0,04	0,12
33	6,94	13,90	6,91	13,93	6,78	13,86	6,8744	13,71	6,88	13,85	0,06	0,03	-0,09	0,00	0,07	0,20
34	7,97	13,87	7,88	13,92	7,96	13,87	7,9493	13,7078	7,94	13,84	0,03	-0,06	0,02	0,01	0,04	0,12
35	9,94	13,93	9,87	13,92	9,89	13,88	9,8364	13,7032	9,88	13,86	0,06	-0,02	0,01	-0,05	0,04	0,13
36	10,92	13,91	10,82	13,93	10,84	13,89	10,90	13,67	10,87	13,85	0,05	-0,05	-0,03	0,03	0,05	0,14
37	12,86	13,91	12,74	13,96	12,88	13,91	13,05	13,65	12,88	13,86	-0,02	-0,15	0,00	0,17	0,13	0,39
38	13,93	13,89	13,71	13,97	13,85	13,92	13,88	13,66	13,84	13,86	0,08	-0,13	0,01	0,04	0,09	0,28
39	15,72	13,89	15,59	13,94	15,74	13,86	15,97	13,51	15,75	13,80	-0,04	-0,16	-0,01	0,21	0,16	0,47
40	16,64	13,88	16,49	13,94	16,60	13,86	16,62	13,54	16,59	13,81	0,05	-0,10	0,01	0,04	0,07	0,21
41	18,65	13,89	18,56	13,97	18,65	13,89	18,52	13,74	18,60	13,87	0,06	-0,04	0,06	-0,07	0,07	0,20
42	1,86	14,63	1,80	14,63	1,87	14,63	1,84	14,50	1,84	14,60	0,02	-0,04	0,03	0,00	0,03	0,10
43	18,67	14,46	18,70	14,61	18,58	14,54	18,59	14,14	18,64	14,44	0,04	0,06	-0,06	-0,05	0,06	0,18
44	1,86	15,84	1,82	15,82	1,90	15,76	1,86	15,77	1,86	15,80	0,00	-0,04	0,04	-0,01	0,03	0,10
45	18,65	15,82	18,64	15,90	18,62	15,80	18,59	15,45	18,63	15,74	0,03	0,02	-0,01	-0,03	0,03	0,08
46	17,85	16,51	17,82	16,53	17,56	16,56	17,73	16,05	17,74	16,41	0,11	0,08	-0,18	-0,01	0,13	0,39
47	14,62	17,28	14,49	17,42	14,58	17,38	14,83	16,80	14,63	17,22	-0,01	-0,14	-0,05	0,20	0,15	0,44
48	15,49	17,32	15,25	17,42	15,38	17,39	15,57	16,83	15,42	17,24	0,07	-0,17	-0,04	0,15	0,14	0,41
49	9,20	18,23	9,19	18,20	9,21	18,16	9,25	17,99	9,21	18,14	-0,01	-0,02	0,00	0,04	0,03	0,08
50	10,52	18,12	10,46	18,20	10,54	18,20	10,62	18,02	10,53	18,14	-0,02	-0,07	0,00	0,09	0,07	0,20
51	13,30	18,40	13,12	18,48	13,19	18,39	13,55	17,83	13,29	18,27	0,01	-0,17	-0,10	0,26	0,19	0,57
52	12,64	18,93	12,56	18,98	12,60	18,91	12,71	18,65	12,63	18,87	0,01	-0,07	-0,02	0,08	0,06	0,19
53	16,38	18,94	16,20	19,00	16,27	18,95	16,48	18,53	16,33	18,85	0,04	-0,13	-0,06	0,15	0,12	0,37
54	17,01	18,95	16,83	19,00	16,86	18,95	17,14	18,53	16,96	18,86	0,05	-0,13	-0,10	0,18	0,14	0,43
55	16,38	19,68	16,18	19,69	16,26	19,67	16,49	19,26	16,33	19,57	0,06	-0,15	-0,07	0,16	0,14	0,41
56	16,99	19,67	16,79	19,68	16,89	18,95	17,10	19,25	16,94	19,39	0,05	-0,15	-0,06	0,16	0,13	0,40
57	3,49	20,38	3,36	20,51	3,53	20,35	3,49	20,32	3,47	20,39	0,02	-0,11	0,06	0,02	0,07	0,22
58	4,28	20,05	4,08	20,49	4,24	20,37	4,28	20,32	4,22	20,31	0,06	-0,14	0,02	0,06	0,10	0,29
59	6,77	20,25	6,64	20,24	6,76	20,20	6,78	20,06	6,74	20,19	0,03	-0,10	0,03	0,04	0,07	0,20
60	10,61	20,29	10,55	20,24	10,52	20,22	10,69	20,05	10,59	20,20	0,02	-0,05	-0,07	0,09	0,07	0,22
61	13,21	20,10	13,10	20,12	13,26	20,04	13,34	19,77	13,23	20,01	-0,02	-0,13	0,03	0,11	0,10	0,31
62	15,57	19,99	15,34	20,06	15,43	20,03	15,65	19,76	15,50	19,96	0,08	-0,16	-0,07	0,15	0,14	0,41
63	3,47	21,40	3,36	21,44	3,50	21,33	3,50	21,25	3,46	21,36	0,01	-0,09	0,05	0,04	0,06	0,19
64	4,26	21,42	4,11	21,44	4,25	21,32	4,24	21,25	4,21	21,36	0,04	-0,10	0,04	0,03	0,07	0,21
65	6,71	21,68	6,70	21,71	6,71	21,65	6,74	21,68	6,72	21,68	0,00	-0,02	-0,01	0,03	0,02	0,05
66	12,71	21,67	12,62	21,72	12,68	21,69	12,65	21,61	12,66	21,67	0,04	-0,05	0,02	-0,02	0,04	0,12
67	12,79	21,22	12,77	21,13	12,81	21,12	12,9608	20,8102	12,83	21,07	-0,04	-0,07	-0,02	0,13	0,09	0,26
68	17,92	21,04	17,94	21,04	17,86	21,04	18,06	20,87	17,94	21,00	-0,03	-0,01	-0,08	0,12	0,08	0,25
69	2,89	22,59	2,79	22,55	2,90	22,53	2,46	22,25	2,76	22,48	0,13	0,03	0,14	-0,30	0,21	0,62
70	6,76	24,16	6,61	24,24	6,70	24,31	6,64	24,56	6,68	24,32	0,08	-0,07	0,02	-0,04	0,07	0,20
71	13,60	23,53	13,53	23,54	13,60	23,53	13,63	23,48	13,59	23,52	0,01	-0,07	0,01	0,04	0,05	0,14
72	6,75	24,99	6,95	24,99	6,90	24,95	6,64	25,10	6,81	25,01	-0,06	0,14	0,09	-0,17	0,14	0,43
73	8,04	25,57	8,01	25,63	8,15	25,64	8,07	25,63	8,07	25,62	-0,02	-0,06	0,08	0,00	0,06	0,18

Table 7.1: 73 coordinates of the points and those that exceeding standard deviation along the x-axis

	PhotoScan		Reality Capture		Recap Photo		PhotoModeler									
n	x_{PS} [m]	y_{PS} [m]	x_{RC} [m]	y_{RC} [m]	x_{RP} [m]	y_{RP} [m]	x_{PM} [m]	y_{PM} [m]	x_m [m]	y_m [m]	$s_{y,PS}$ [m]	$s_{y,RC}$ [m]	$s_{y,R}$ [m]	$s_{y,PM}$ [m]	σ_y [m]	T_y [m]
1	0,89	0,17	0,89	0,23	0,89	0,18	0,86	0,23	0,88	0,20	-0,03	0,03	-0,02	0,03	0,03	0,10
2	19,15	0,51	18,90	0,78	19,10	0,46	18,83	0,27	19,00	0,51	0,01	0,27	-0,04	-0,24	0,21	0,63
3	5,25	2,15	5,17	2,23	5,19	2,07	3,0057	2,0549	4,66	2,13	0,02	0,10	-0,05	-0,07	0,08	0,23
4	16,84	1,67	16,73	2,00	16,79	1,71	16,45	1,52	16,70	1,73	-0,05	0,28	-0,02	-0,21	0,20	0,60
5	17,53	1,80	17,35	2,00	17,49	1,72	17,17	1,53	17,39	1,76	0,03	0,24	-0,04	-0,23	0,19	0,58
6	2,52	4,21	2,50	4,20	2,53	4,12	2,2861	4,1334	2,46	4,16	0,05	0,03	-0,05	-0,03	0,05	0,14
7	5,24	4,37	5,25	4,30	5,37	4,30	4,72	4,28	5,15	4,31	0,06	-0,01	-0,01	-0,03	0,04	0,11
8	9,53	4,59	9,50	4,72	9,51	4,59	9,14	4,43	9,42	4,58	0,01	0,14	0,00	-0,15	0,12	0,36
9	10,47	4,57	10,36	4,73	10,42	4,58	10,10	4,41	10,34	4,57	0,00	0,15	0,01	-0,16	0,13	0,39
10	13,01	3,89	12,94	4,10	12,91	3,96	12,75	3,72	12,90	3,92	-0,03	0,19	0,04	-0,19	0,16	0,47
11	17,13	4,36	16,95	4,55	17,16	4,25	16,91	4,05	17,04	4,30	0,06	0,25	-0,05	-0,26	0,21	0,63
12	9,54	6,60	9,53	6,07	9,53	6,54	9,17	6,31	9,44	6,38	0,22	-0,31	0,16	-0,07	0,24	0,73
13	10,51	6,59	10,42	6,60	10,40	6,54	10,17	6,34	10,38	6,52	0,07	0,08	0,02	-0,18	0,12	0,37
14	0,91	7,82	0,90	7,92	0,89	7,91	0,88	7,67	0,90	7,83	-0,01	0,09	0,08	-0,16	0,11	0,34
15	2,33	7,84	2,33	7,85	2,38	7,94	2,21	7,67	2,31	7,82	0,02	0,03	0,11	-0,16	0,11	0,34
16	9,68	9,98	9,60	10,07	9,61	9,95	9,68	9,69	9,64	9,92	0,05	0,15	0,03	-0,23	0,16	0,49
17	10,90	9,98	10,82	10,08	10,82	9,94	10,78	9,68	10,83	9,92	0,06	0,16	0,02	-0,24	0,17	0,51
18	2,49	10,74	2,47	10,80	2,58	10,81	2,42	10,60	2,49	10,74	0,00	0,06	0,07	-0,14	0,10	0,29
19	3,38	10,76	3,32	10,83	3,40	10,81	3,40	10,65	3,38	10,76	0,00	0,07	0,05	-0,11	0,08	0,24
20	5,43	10,84	5,33	10,89	5,42	10,87	5,37	10,65	5,39	10,81	0,03	0,07	0,06	-0,16	0,11	0,33
21	6,33	10,81	6,23	10,89	6,32	10,86	6,27	10,65	6,29	10,81	0,01	0,09	0,06	-0,16	0,11	0,33
22	8,35	10,85	8,33	10,92	8,35	10,88	8,30	10,68	8,33	10,83	0,02	0,09	0,05	-0,15	0,11	0,32
23	9,28	10,84	9,27	10,92	9,10	10,88	9,2442	10,6904	9,22	10,83	0,01	0,09	0,05	-0,14	0,10	0,30
24	11,32	10,78	11,26	10,84	11,24	10,80	11,27	10,54	11,27	10,74	0,04	0,10	0,06	-0,20	0,13	0,40
25	12,22	10,75	12,17	10,85	12,11	10,81	12,19	10,55	12,17	10,74	0,01	0,10	0,07	-0,19	0,13	0,39
26	14,32	10,81	14,17	10,89	14,26	10,83	14,16	10,50	14,23	10,76	0,05	0,14	0,07	-0,25	0,17	0,52
27	15,31	10,82	15,27	10,93	15,17	10,82	15,1134	10,519	15,22	10,77	0,05	0,16	0,05	-0,26	0,18	0,54
28	17,22	10,79	17,10	10,94	17,07	10,80	17,2266	10,6197	17,15	10,79	0,01	0,15	0,01	-0,17	0,13	0,39
29	18,05	10,77	17,92	10,95	18,18	10,82	18,0484	10,6287	18,05	10,79	-0,02	0,16	0,03	-0,16	0,13	0,40
30	1,85	13,85	1,83	13,83	1,88	13,90	1,834	13,8295	1,85	13,85	0,00	-0,02	0,04	-0,02	0,03	0,09
31	3,94	13,91	3,80	13,92	3,88	13,89	3,8251	13,7659	3,86	13,87	0,04	0,05	0,02	-0,10	0,07	0,21
32	4,99	13,91	4,91	13,95	4,99	13,93	4,9333	13,7997	4,96	13,90	0,01	0,05	0,03	-0,10	0,07	0,20
33	6,94	13,90	6,91	13,93	6,78	13,86	6,8744	13,71	6,88	13,85	0,05	0,08	0,01	-0,14	0,10	0,30
34	7,97	13,87	7,88	13,92	7,96	13,87	7,9493	13,7078	7,94	13,84	0,03	0,08	0,03	-0,13	0,09	0,28
35	9,94	13,93	9,87	13,92	9,89	13,88	9,8364	13,7032	9,88	13,86	0,07	0,07	0,02	-0,16	0,11	0,32
36	10,92	13,91	10,82	13,93	10,84	13,89	10,90	13,67	10,87	13,85	0,06	0,08	0,04	-0,18	0,12	0,36
37	12,86	13,91	12,74	13,96	12,88	13,91	13,05	13,65	12,88	13,86	0,05	0,10	0,05	-0,21	0,14	0,42
38	13,93	13,89	13,71	13,97	13,85	13,92	13,88	13,66	13,84	13,86	0,03	0,11	0,06	-0,20	0,14	0,42
39	15,72	13,89	15,59	13,94	15,74	13,86	15,97	13,51	15,75	13,80	0,09	0,14	0,06	-0,29	0,20	0,59
40	16,64	13,88	16,49	13,94	16,60	13,86	16,62	13,54	16,59	13,81	0,08	0,14	0,05	-0,27	0,18	0,54
41	18,65	13,89	18,56	13,97	18,65	13,89	18,52	13,74	18,60	13,87	0,02	0,10	0,02	-0,13	0,09	0,28
42	1,86	14,63	1,80	14,63	1,87	14,63	1,84	14,50	1,84	14,60	0,03	0,03	0,04	-0,10	0,06	0,19
43	18,67	14,46	18,70	14,61	18,58	14,54	18,59	14,14	18,64	14,44	0,02	0,18	0,10	-0,30	0,21	0,63
44	1,86	15,84	1,82	15,82	1,90	15,76	1,86	15,77	1,86	15,80	0,04	0,02	-0,04	-0,02	0,04	0,11
45	18,65	15,82	18,64	15,90	18,62	15,80	18,59	15,45	18,63	15,74	0,08	0,16	0,06	-0,29	0,20	0,60
46	17,85	16,51	17,82	16,53	17,56	16,56	17,73	16,05	17,74	16,41	0,10	0,12	0,14	-0,36	0,24	0,73
47	14,62	17,28	14,49	17,42	14,58	17,38	14,83	16,80	14,63	17,22	0,06	0,20	0,16	-0,42	0,29	0,86
48	15,49	17,32	15,25	17,42	15,38	17,39	15,57	16,83	15,42	17,24	0,08	0,18	0,15	-0,41	0,28	0,83
49	9,20	18,23	9,19	18,20	9,21	18,16	9,25	17,99	9,21	18,14	0,09	0,05	0,02	-0,16	0,11	0,33
50	10,52	18,12	10,46	18,20	10,54	18,20	10,62	18,02	10,53	18,14	-0,01	0,07	0,06	-0,11	0,08	0,25
51	13,30	18,40	13,12	18,48	13,19	18,39	13,55	17,83	13,29	18,27	0,12	0,21	0,12	-0,45	0,30	0,90
52	12,64	18,93	12,56	18,98	12,60	18,91	12,71	18,65	12,63	18,87	0,06	0,11	0,04	-0,21	0,15	0,44
53	16,38	18,94	16,20	19,00	16,27	18,95	16,48	18,53	16,33	18,85	0,08	0,15	0,09	-0,32	0,22	0,65
54	17,01	18,95	16,83	19,00	16,86	18,95	17,14	18,53	16,96	18,86	0,09	0,14	0,09	-0,32	0,22	0,65
55	16,38	19,68	16,18	19,69	16,26	19,67	16,49	19,26	16,33	19,57	0,11	0,11	0,10	-0,32	0,21	0,64
56	16,99	19,67	16,79	19,68	16,89	18,95	17,10	19,25	16,94	19,39	0,29	0,29	-0,44	-0,14	0,36	1,07
57	3,49	20,38	3,36	20,51	3,53	20,35	3,49	20,32	3,47	20,39	-0,01	0,12	-0,04	-0,07	0,08	0,25
58	4,28	20,05	4,08	20,49	4,24	20,37	4,28	20,32	4,22	20,31	-0,26	0,19	0,06	0,02	0,19	0,56
59	6,77	20,25	6,64	20,24	6,76	20,20	6,78	20,06	6,74	20,19	0,06	0,05	0,01	-0,13	0,09	0,27
60	10,61	20,29	10,55	20,24	10,52	20,22	10,69	20,05	10,59	20,20	0,09	0,04	0,02	-0,15	0,10	0,30
61	13,21	20,10	13,10	20,12	13,26	20,04	13,34	19,77	13,23	20,01	0,09	0,11	0,03	-0,24	0,16	0,48
62	15,57	19,99	15,34	20,06	15,43	20,03	15,65	19,76	15,50	19,96	0,03	0,10	0,07	-0,20	0,14	0,41
63	3,47	21,40	3,36	21,44	3,50	21,33	3,50	21,25	3,46	21,36	0,05	0,09	-0,03	-0,11	0,08	0,25
64	4,26	21,42	4,11	21,44	4,25	21,32	4,24	21,25	4,21	21,36	0,06	0,08	-0,03	-0,11	0,09	0,27
65	6,71	21,68	6,70	21,71	6,71	21,65	6,74	21,68	6,72	21,68	0,00	0,03	-0,03	0,00	0,02	0,07
66	12,71	21,67	12,62	21,72	12,68	21,69	12,65	21,61	12,66	21,67	0,00	0,05	0,01	-0,06	0,05	0,14
67	12,79	21,22	12,77	21,13	12,81	21,12	12,9608	20,8102	12,83	21,07	0,15	0,06	0,05	-0,26	0,18	0,54
68	17,92	21,04	17,94	21,04	17,86	21,04	18,06	20,87	17,94	21,00	0,04	0,04	0,04	-0,13	0,08	0,25
69	2,89	22,59	2,79	22,55	2,90	22,53	2,46	22,25	2,76	22,48	0,11	0,07	0,04	-0,23	0,15	0,46
70	6,76	24,16	6,61	24,24	6,70	24,31	6,64	24,56	6,68	24,32	-0,16	-0,08	-0,01	0,25	0,17	0,52
71	13,60	23,53	13,53	23,54	13,60	23,53	13,63	23,48	13,59	23,52	0,01	0,02	0,01	-0,04	0,03	0,08
72	6,75	24,99	6,95	24,99	6,90	24,95	6,64	25,10	6,81	25,01	-0,02	-0,02	-0,06	0,09	0,06	0,19
73	8,04	25,57	8,01	25,63	8,15	25,64	8,07	25,63	8,07	25,62	-0,05	0,01	0,02	0,01	0,03	0,10

Table 7.2: 73 coordinates of the points and those that exceeding standard deviation along the y-axis

In summary, total points exceeding *standard deviation*:
- n. 15 for PhotoScan;
- n. 46 for Reality Capture;
- n. 16 for Recap Photo;
- n. 102 for PhotoModeler.

The analysis point out a significant number of deviations in the average that exceeding the deviation standard in relation to PhotoModeler software, which allows us to assert that in this case, maybe for the particular geometry of the tower, the manual detection of homologous points for the generation of the three dimensional model involve a greater quantity of errors than the automated processes. A further interesting result is the little difference between PhotoScan and Recap Photo; being the second a free and *cloud compare* software increases even more the idea and possibility of safeguarding of historical heritage also using low cost technologies.

7.2.1 Validation of results

In order to validate the previously implemented comparison methodology, we proceeded with the *predictive value of test*, which is a dichotomous qualitative test necessary to evaluate the quality of a comparison and not its amplitude.
Before proceeding, however, it is necessary to establish a threshold value, called *cut-off*, indicative of the positive or not of the result: in our case, this value coincide with the standard deviation previously calculated. It is worth pointing out that there are no validation sure at 100%, so if we must see it as an indication of probability.
The points before located can be divided in two types of data: *real point* (R) and *hypothesized point* (H). The former, in red, are those pixels clearly visible on the orthophotos obtained and on which great errors would not be expected; the other ones, vice versa, are points that are not easily identifiable and, consequently, we suppose that they are more subject to error.
We proceeded to generate matrixes

	H	**R**	
T+	a	b	(a+b)
T-	c	d	(c+d)
	(a+c)	(b+d)	

with:

a: hypothesized points and test-positive;
b: real points and test-positive;
c: hypothesized points and test-negative;
d: real points and test-negative;
(a+c). tot points assumed;
(b+d): tot real points;
(a+b): tot test-positive;
(c+d): tot test-negative.

Whose columns indicate the type of data and the rows the result obtained (if it exceeds or not the *cut-off* value); therefore with the *test-positive* definition (T+) is indicated that they have a value exceeding the standard deviation, while with *test-negative* (T-) no.
Once the data at our disposal are identified and classified, we can proceed to the calculation of interesting values to establish the quality of the method used in the identification of errors.
The *sensitivity* (Se) is used to identify the ability of the test to correctly recognize the hypothesized points, so it is the probability that an H data is T+. The hypothesized points are represented in the matrix from (a + c) and, among these, the positive tests are represented by (a); therefore, the sensitivity is calculated with the proportion

$$\frac{a}{(a+c)}$$

The *specificity* (Sp), different to the previous one, recognises the ability of the method to correctly identify the points R; that is, the probability that a real point is test-negative (T-). In this case, the real values are (b + d) and, among these, the negative tests are (d); it follows that the specificity is calculated

$$\frac{d}{(b+d)}$$

In both cases, it is a proportion that can take values between 0 and 1, which can also be expressed with percentage values. Moreover, these indexes are calculated on a limited number of values, data samples selected from a statistical population, and therefore often subject to the problem of variability due to chance.
To overcome this problem, it is appropriate to calculate the *confidence interval* necessary to quantify the accuracy of the estimate obtained; in case you want to calculate the 95% confidence interval (as in our case), the formulas respectively of sensitivity and specificity are:

$$\mathrm{IC95\%} = \pm 1{,}96 \sqrt{\frac{\mathrm{Se} \cdot (1 - \mathrm{Se})}{\mathrm{n}}}$$

$$\mathrm{IC95\%} = \pm 1{,}96 \sqrt{\frac{\mathrm{Sp} \cdot (1 - \mathrm{Sp})}{\mathrm{n}}}$$

and n is the total of real and hypothetical data. The amplitude of this interval depends on the number n of points that we examine, the confident interval is more restricted if we have many data, this is because increases the accuracy of the estimate.
Other interesting values to consider are the *Positive Predictive Value* (PPV), and the *Negative Predictive Value* (NPV). The first is the probability that the resulting test-positive point (T+) is a hypothesized point (H), while the second one is the probability that the resulting test-negative point (T-) is a real point (R). This indexes are different from the previous ones because Se and Sp are proper characters of the test and are related to its intimate functioning (pre-test probability). Once the test is performed, Sf and Sp lose importance and to interpret the result, the following two post-test probably become important.

$$\mathrm{PPV} = \frac{\mathrm{a}}{(\mathrm{a} + \mathrm{b})}$$

$$\mathrm{NPV} = \frac{\mathrm{d}}{(\mathrm{c} + \mathrm{d})}$$

Once again, the result will be given in terms of probability. As in the other case, also for these indexes is possible to calculate the confidence interval to evaluate the accuracy:

$$\mathrm{IC95\%} = \mathrm{PPV} \pm \sqrt{\frac{\mathrm{PPV} \cdot (1 - \mathrm{PPV})}{\mathrm{n}}}$$

$$\mathrm{IC95\%} = \mathrm{NPV} \pm \sqrt{\frac{\mathrm{NPV} \cdot (1 - \mathrm{NPV})}{\mathrm{n}}}$$

where

(1-PPP) = probability of the event that the positive test-point (T+) is a real point (R);

(1-PPN) = probability of the event that the test-negative point (T-) is a hypothetical point (I). These last values are obtained by applying the *Bayes Theorem*:

$$1 - \mathrm{NPV} = \frac{\mathrm{P} \cdot (1 - \mathrm{Se})}{\mathrm{P} \cdot (1 - \mathrm{Se}) + [(1 + \mathrm{P}) \cdot \mathrm{Sp}}$$

with
P = prevalence, that is the percentage of points exceeding the standard deviation.
The two values that contribute to verify the quality of a test, PPV and NPV, can be assembled into a single parameter, the *Validity*. This parameter could correctly classify both the correct and incorrect points and consequently, this value will assume higher value more the test is true.

$$V = \frac{(\mathrm{a} + \mathrm{d})}{(\mathrm{a} + \mathrm{b} + \mathrm{c} + \mathrm{d})}$$

Based on the foregoing, therefore, we proceeded to realize the matrixes related to each software both for the *x-axis* and for the *y-axis*. In particular, referring to the theory of errors previously applied, visible in the tables 7.1 and 7.2, we could differentiate between the hypothetical points (highline in yellow) and the real points. In the same figure, in addition, we could identify the point that exceed the values of standard deviation (highline in pink) and which no (highline in green). Known this it is possible distinguish the points resulted test-positive (T+) from which ones test-negative (T-); in particular when a hypothetical point do not exceed the standard deviation it will be test-negative, otherwise it will be test-positive. The same applies to the case of real points; but in this case, we expect fewer points test-positive.
The purpose, therefore, is to identify which of these software allows to make fewer errors in the identification of points on the exported orthophotos.
In summary, with PhotoScan application:

	H(x)	**R(x)**	
T+	5	5	10
T-	14	49	63
	19	54	

PPV:50%; **NPV:**78%; **Se:**26%; **Sp:**91%

	H(y)	**R(y)**	
T+	2	3	5
T-	17	51	68
	19	54	

PPV:40%; **NPV:**75%; **Se:**11%; **Sp:**94%

with Reality Capture:

	H(x)	**R(x)**	
T+	2	28	30
T-	11	32	43
	13	60	

PPV:10%; **NPV:**77%; **Se:**23%; **Sp:**55%

	H(y)	**R(y)**	
T+	2	14	16
T-	11	46	57
	13	60	

PPV:40%; **NPV:**75%; **Se:**11%; **Sp:**94%

with Recap Photo:

	H(x)	**R(x)**	
T+	6	4	10
T-	19	44	63
	25	48	

PPV:60%; **NPV:**70%; **Se:**24%; **Sp:**92%

	H(y)	**R(y)**	
T+	1	5	6
T-	24	43	67
	25	48	

PPV:17%; **NPV:**64%; **Se:**4%; **Sp:**90%

and with PhotoModeler:

	H(x)	R(x)	
T+	11	30	41
T-	9	64	73
	20	94	

PPV:27%; **NPV:**88%; **Se:**55%; **Sp:**68%

	H(y)	R(y)	
T+	16	45	61
T-	4	69	73
	20	114	

PPV:26%; **NPV:**95%; **Se:**80%; **Sp:**61%

Analysing these values and remembering the previously test (paragraph 7.2), we could see that the best results have been obtained on PhotoScan application where there are less number of errors and it is also possible to deduced that using the *theory of errors* the probability of identify real point in right way is 78% on the *x-axis* and 75% on the *y-axis*. The same analysis was made for the overall methodology:

	H(x)	R(x)	
T+	25	66	91
T-	54	190	244
	79	256	

PPV:27%; **NPV:**78%; **Se:**32% **Sp:**74%

	H(y)	R(y)	
T+	21	22	43
T-	56	209	265
	77	231	

PPV:49%; **NPV:**79%; **Se:**27%; **Sp:**90%

where it is deduced that the probability of making mistakes with the hypothetical points is 23% on the *x-axis* and 29% on the *y-axis*

$$\frac{P \cdot (1 - Se)}{P \cdot (1 - Se) + [(1 - P) \cdot Sp]}$$

7.3 Comparison of 3D models

7.3.1 PhotoScan vs Recap Photo

This section was relevant for the evaluation of the distribution of errors in three-dimensional space, in particular we proceeded to analyse the difference between the software in which we found the best values in the previous analysis.
The application selected to compare the two models was Cloud Compare. They, as we know, were made from the same photos but elaborated in different software; so the first step has been to align them respect the same reference system (identifying three pairs of homologous points: 3,4 and 5) and then submitting it to a comparative analysis.
In the figure 7.3 is possible to notice how the Recap model, compared to PhotoScan (the one chosen as reference), presents 2,5% of the points with a distance, in absolute value, greater than 0,08m, while, 45% of the points are included in a distance not higher, always in absolute value, at 0,024m.
Moreover, in the other figure 7.4, is visible as the irregular deformations between the two models are more in the limit areas where the greater deviation is observed; this probably due to the impossibility in Recap Photo to create masks to eliminate parts of the scene that should not be computed by the algorithm of matching. However, on global level the Gauss curve presents a mean of 0,024m and a standard deviation of 0,087m.
In addition, a metric comparison was made; once again, using the *error theory* we evaluated the differences existing between the linear distances detected on the respective models and those acquired by the total station TopCon GPT 3002.
The same distances then have been evaluated on the Recap model and PhotoScan model; in this way it was possible to calculate the absolute difference existent between the latter and those measured with total station (where the best precision is expected). The admissible error considered in this analysis was 1cm as request by

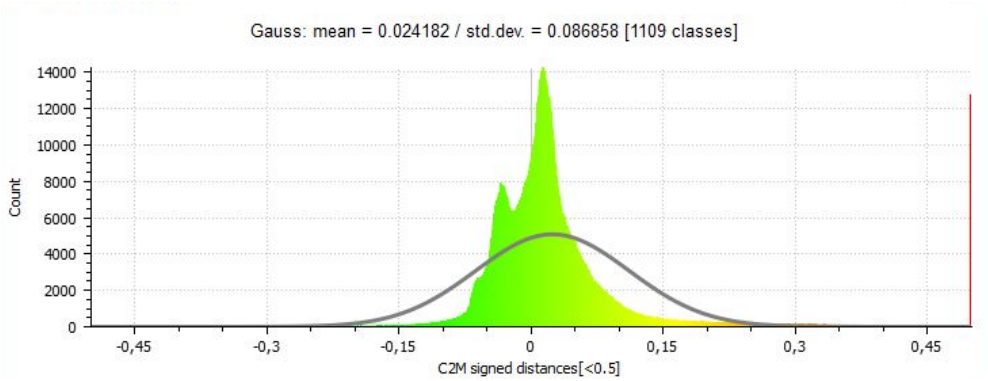

Figure 7.3: Curve of Gauss representative of the distance between the PhotoScan and Recap Photo models

graphic accuracy for technical drawing 1:50 scale; the absence of some measures in the table 7.3 is due to the difficulty in collimating some points on the mesh model. As visible, once again the best results have been obtained with PhotoScan application where five values exceeding the admissible error has been detected.
It was also interesting to evaluate the *trendlines* for each of them in order to compare them more easily. On the *x-axis* there is the id-number of the measure (from 1 until 25) while the *y*- axis is represented by the distance observed which increases as the id-number increases.
However, it is interesting to note how, despite quantitatively the Recap errors are more, only three of them are greater than tolerance (T= ±3σ) like the Photoscan application. Based on the experimental evidence, it is concluded that for PhotoScan 76% of the resulting values is less than σ, 10% upper the deviation standard and 14% upper to tolerance. In the case of Recap Photo, while, we obtained that 50% is upper than σ of which 15% upper than tolerance.
Generally, from the comparative study developed it can be concluded that although the model generated by the application PhotoScan allows to guarantee better metric information, with Recap Photo it is possible detected dimensions roughly corrected, with more errors in the highest part of the buildings and in the details.
However, the latter compared to commercial software such as PhotoScan is cheaper because it is free and it works in cloud compare, so, not need a workstation for the post-processing phase, as well as having complete automation of the process as previously descripted.

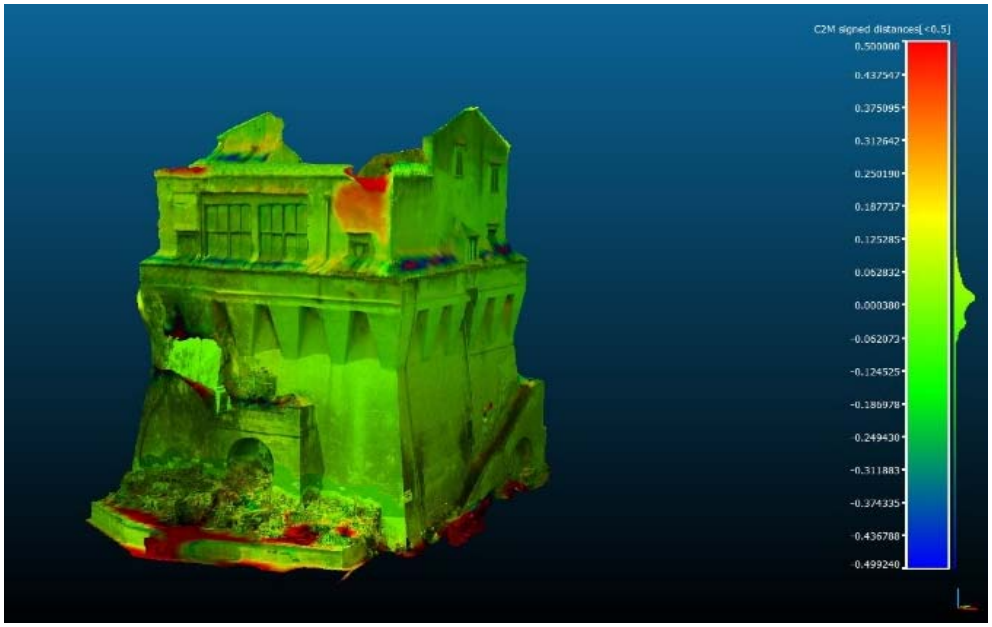

Figure 7.4: DEM analysis between PhotoScan and Recap Photo models

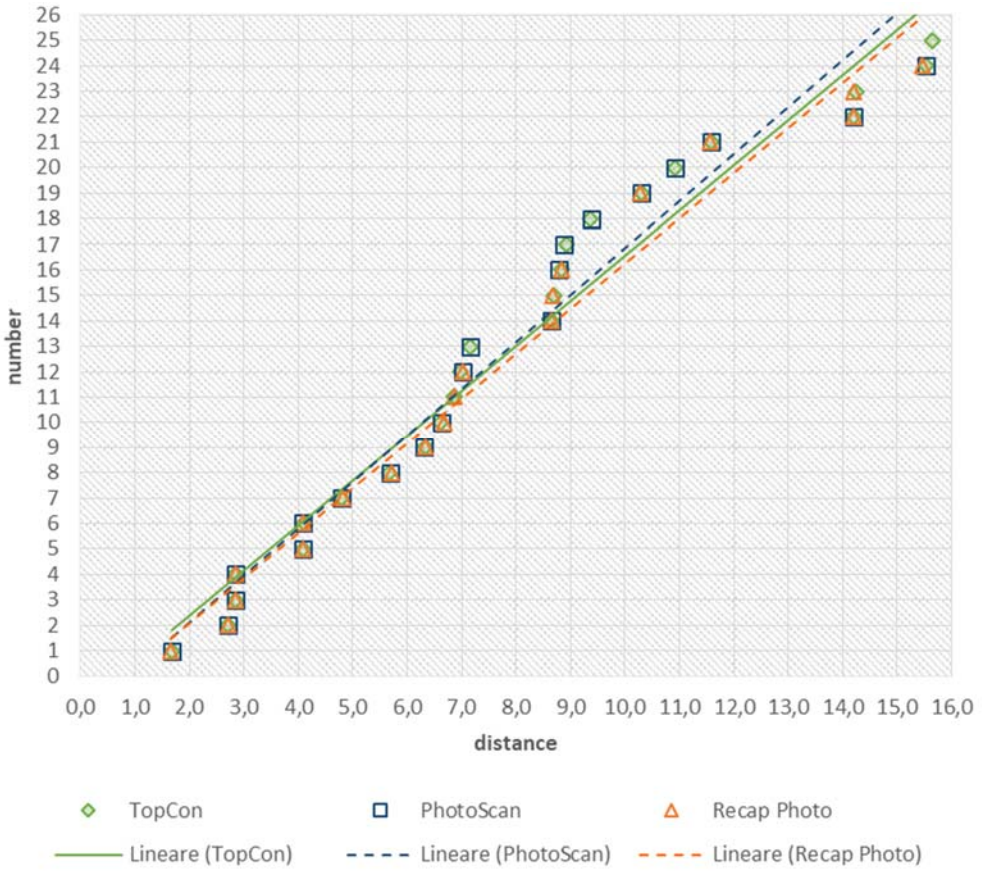

n	point	TopCon d_{TC} [m]	PhotoScan d_{PS} [m]	Recap d_{RP} [m]	s_{TC-PS} [m]	s_{TC-R} [m]
1	5-6	1,67	1,67	1,65	0,00	-0,03
2	3-5	2,71	2,71	2,72	0,00	0,01
3	7-9	2,84	2,85	2,85	0,01	0,01
4	9-8	2,84	2,84	2,85	0,00	0,01
5	6-4	4,09	4,08	4,08	-0,01	0,00
6	16-15	4,11	4,09	4,08	-0,01	-0,03
7	21-24	4,80	4,80	4,82	0,01	0,03
8	8-7	5,68	5,69	5,71	0,02	0,03
9	4-3	6,33	6,32	6,33	-0,01	0,00
10	12-13	6,62	6,62	6,67	0,01	0,06
11	14-16	6,87		6,85		-0,02
12	7-10	6,98	7,02	7,01	0,05	0,04

n	point	TopCon d_{TC} [m]	PhotoScan d_{PS} [m]	Recap d_{RP} [m]	s_{TC-PS} [m]	s_{TC-R} [m]
14	15-12	8,65	8,65	8,65	0,00	0,00
15	14-12	8,68		8,68		-0,01
16	3-7	8,83	8,79	8,82	-0,04	0,00
17	22-24	8,91	8,87		-0,04	
18	18-20	9,35	9,38		0,03	
19	23-21	10,30	10,30	10,27	0,00	-0,03
20	17-18	10,92	10,92		0,00	
21	24-25	11,59	11,58	11,56	-0,01	-0,03
22	11-8	14,20	14,20	14,20	0,00	0,00
23	13-14	14,24		14,21		-0,03
24	19-17	15,54	15,54	15,46	0,00	-0,08
25	25-22	15,64				

Figure 7.5: Trendline and absolute difference existent between the Photoscan and Recap phot models with those measured with total station TopCon GPT 3002

7.3.2 Compact vs Reflex camera

The last analysis offers a comparison between the different tools used during the survey: digital compact camera Fujifilm XF1 and Canon EOS 600D Digital Reflex. In this case, therefore, what change are the starting data and not the software used for data processing; we opted for PhotoScan because it was the one that always gave the best results. As already known, the dissimilar hardware features of the cameras involve in different GSD values (respectively 0,34cm/pixel and 0,17cm/pixel) and also the final results will be influenced.
Another substantial difference to consider is the number of photos used, in the case of the compact camera the work was completed with the creation of 69 photos, while with the SLR were taken about 247 pictures of which only 224 were chosen for the process.
Furthermore, the surveys were been realized in different days and different condition; in particular during the first field work with the Canon EOS 600D some shadows of the surrounding buildings were projected on the tower, so it was necessary a second field work session in order to take the necessary photos and to improve the model.
As a result of data processing, performed as explained earlier in paragraph 6.4 we have obtained two different models, that with the compact camera that presents 12320950 faces and the one of the reflex that has a mesh with 13467263 faces.
Once again, the three-dimensional models were compared to the Cloud Compare application. In the same way as the previous analysis, three pairs of homologous points have been identified to align the 3D models respect to the same coordinate system. The reflex model was chosen as reference model, the Gauss curve in figure 7.6 shows how the mean of the comparison is 0,0013m, while the standard deviation is 0,074m. In addition, in the figure 7.7 is possible to notice how the compact model presents about 14% of the points with a distance, in absolute value, greater than deviation standard 0,074m, 56% of the points present, always in absolute value, a

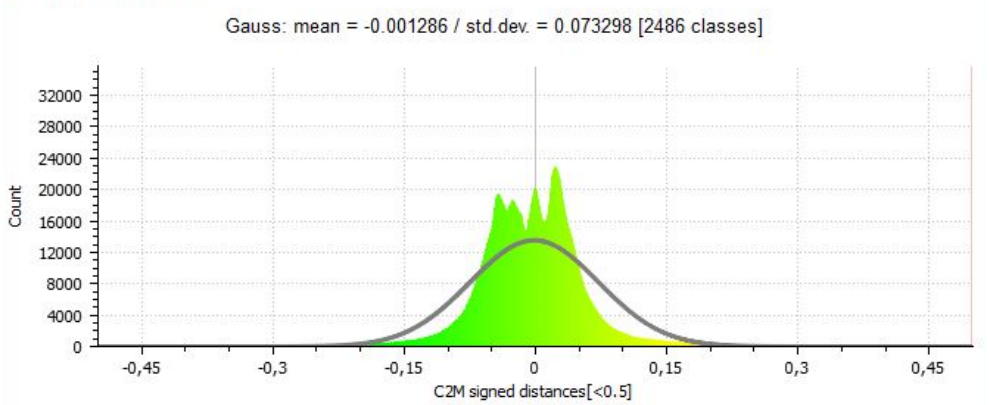

Figure 7.6: Curve of Gauss representative of the distance between the DEM analysis between PhotoScan and Recap Photo models

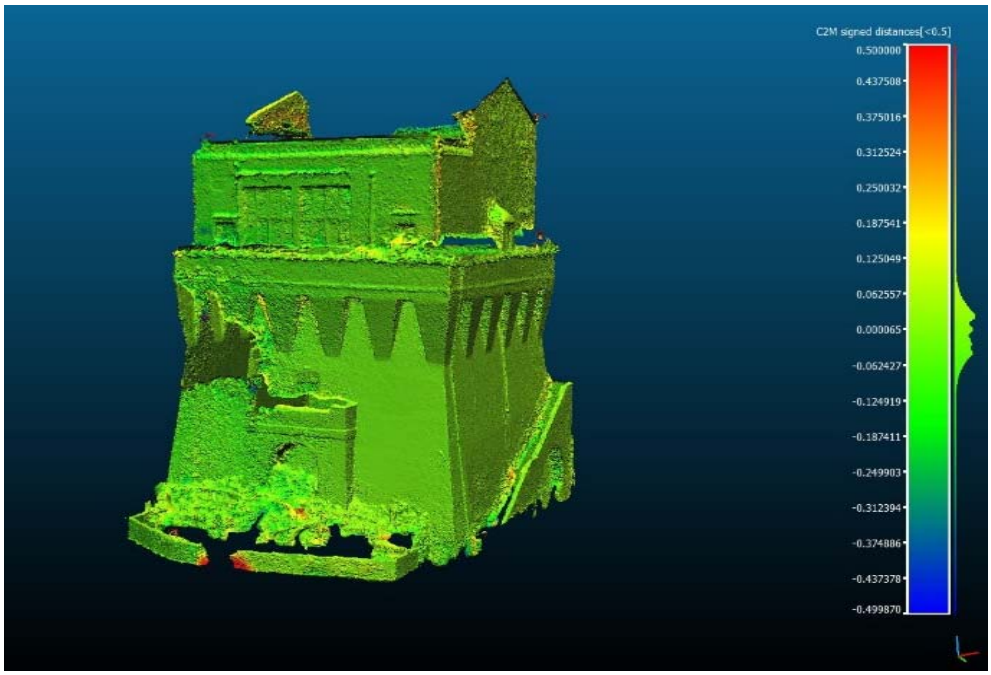

Figure 7.7: DEM analysis between the models realized with photos taken with reflex and compact cameras

distance less of 0,03m and the other 42% are between these two values; the bigger problem, as always, are in the margin of the buildings. It is important to consider also that despite the model realize with the Canon camera is better, it was necessary more time for post processing as well as a better performing computer.
Hence, differently from the previous case, the models generated by the use of two different instruments do not present very high deviations, which underlines the improvements made in recent years in the interaction between low cost technologies and software on the market today; a process, hopefully, in constant evolution.

Conclusion and possible future developments

Aware of the numerous and high-level patrimony of which we are heirs, it is fundamental to identify an innovative system to preserve, divulge and pass our "tangible" and "intangible" heritage.
The role of photogrammetry in the field of Cultural Heritage, for a long time now, is undisputed; its enormous flexibility, given the vast variety of cases where it could be used, certainly decrees its great success.
Investing in culture does not only mean increasing the quantity of investments but also aiming for quality. Hence also directing attention to search an innovative system of use, as well as, greater digitization of assets.
As examined in this thesis, the use of panoramic photogrammetry could be used in the field of tangible and intangible heritage. The sharing on internet of the virtual tour allows to transmit information and to live experiences in any part of the world as well as to increase the interest to the fascinating places of our territory often unknown. Working in this way the level of accessibility of documents would increase intensely: ancient manuscripts difficult to consult because stored in archives or located in place not open to the public; architectural or archaeological assets that are difficult to reach because of inaccessible places or regions of the world that are politically unstable. Hence, the generation of virtual tours, as in the case studied, allows us to explore, navigate and interrogate in a personal way and according to own interests.
This is a new method of communication, a tool to deepen and at the same time communicate information of various kinds (historical or technical) and at different levels of accessibility (experts or just tourists). Obviously, these systems will never be a replacement of the on-site visit, but they will certainly increase their understanding and stimulate the curiosity. The achievement of these objectives also include the multidisciplinary approach where the scientific aspect dialogues and enters into harmony with the humanistic aspect in order to be able to pass on not only tangible information such as volumes or technical drawings but also information difficult to transmit with the classic representations.
Another aspect analysed, on the possibilities offered by photogrammetry, is the use of low-cost technologies for the acquisition of infographics models with a certain scientific rigor. In particular, the focus was on close-range photogrammetry

applied to the survey of a single tower.
Through the application of *error theory* it was, in fact, possible to evaluate the accuracy achievable in the implementation of some software on the market today and of two different types of hardware (reflex and compact cameras). The results thus obtained were then further substantiated with the *predictive value of tests*. As already anticipated in the overview, this is an innovative methodology for the field of architecture survey of nominal dichotomous qualitative type. The implementation of this test has proved to be very useful in order to calculate and evaluate in probabilistic terms the possible errors committed in the comparison and therefore in evaluating the goodness of what has been achieved.
The results obtained showed the great potential of such technologies in terms of data obtained, for its relative inexpensiveness and flexibility of use.
During the experimentation, different software and tools were used with the purpose to validate the use of economic technologies for architectural survey. In the case of the applications used, the results have shown that the great progress of the software on the market today allows to reach more and more acceptable results. However, with the implementation of the free cloud compare software Recap Photo, despite its complete automation in the process, it is not yet possible to export models useful for scientific purposes. The data obtained, in fact, are more suitable for the generation of visual and sharing models on the web; also due to their lesser weight and better manageability.
The number of points exceeding the *standard deviation* – calculated on the *x* and *y* coordinates of 73 points identified on the different orthophotos generated and more detailed in Chapter 7 – is congruent with that of Photoscan. However, the validation of the test underlined a *Negative Predictive Value* (both for the *x* and *y* axes) lower than those of the reference software, about 70% and 64% of the possibility of not obtaining errors compared to 78% and 75% of Photoscan. On a three-dimensional level the DEM comparison of the two models returns a Gauss curve with an average value of distance of about 0,024 m and a *standard deviation* of 0,087 m.
Different is the case of the use of compact camera in the field of architectural survey. In fact, despite the same levels of precision of a reflex camera are not guaranteed, they allow to obtain competitive results, with minimum deviations from instruments with better technical characteristics. In the case in question, for example, the Gauss curve obtained from the new comparison, returns an average value of distance of 0,0013 m with 14% of the points having a distance, in absolute value, greater than the standard *deviation* (equal to 0,074 m).
At more general level, in order to guarantee better results from the photogrammetric paradigm, as is well known, it would be advisable to proceed by

integrating the currently available techniques; being able to pursue this objective, with not excessive costs, would represent an excellent goal for the protection of heritage and, above all, for those 'hidden' architectures of which our territories are rich.

In order to guarantee excellent results, as known, it would be convenient to proceed with the integration of several techniques currently present in the field of survey (like drone and laser scanners) to ensure greater accuracy, lack of information gaps and products with greater readability. In fact, one of the main purpose of the survey applied to cultural heritage is the generation of models that would represent the basis for subsequent studies of documentation and representation as well as of recovery, restoration and diagnostics. Being able to pursue this objective with not expensive costs would represent an excellent goal for the protection of the heritage and especially for those "hidden" architectures of which the territories are rich.

The case studied of the defensive system, in fact, despite the extensive historical studies previously conducted by various scholars, pours into a state without technical information: absence of precise surveys and graphic documentation. Furthermore, the use of these new and low-cost technologies could restore the interest, both public and private, to possible refurbish interventions. Only a multi-disciplinary and multi-technical approach, therefore, represents the right path to pursue in order to paying attention to these structures. The restoration and conservation of these artefacts, as well as other less-known architectures in the country, would restore not only the physical aspect but also the identification of our culture, history and territory.

Conclusioni e possibili sviluppi futuri

Consapevoli del Cultural Heritage di cui siamo eredi – quantitativo e qualitativo – risulta abbastanza doveroso identificare un sistema innovativo per preservare, divulgare e trasmettere il nostro patrimonio "tangibile" e "intangibile".
Il ruolo della fotogrammetria nel campo dei Beni Culturali è da molto tempo indiscusso; la sua flessibilità, per la varietà di casi in cui può essere applicata, ne ha decretato un indiscutibile successo. Investire nel campo della cultura, tuttavia, non implica solo incrementare la quantità di risorse finanziare ma anche una ricerca della qualità; da qui l'attenzione di tale lavoro orientato verso nuovi approcci di fruizione.
Come analizzato, l'uso della fotografia panoramica riscontra una grande utilità nel campo del patrimonio materiale e immateriale. La condivisione su internet di *virtual tour*, infatti, consente di trasmettere informazioni e di vivere esperienze di fruizione da remoto con la possibilità di ampliare anche l'interesse nei confronti di luoghi affascinanti ma troppo spesso sconosciuti. Operando in questo modo, infatti, il livello di accessibilità di documenti e siti aumenterebbe a dismisura; basti pensare a manoscritti antichi difficili da consultare perché conservati in archivi o collocati in luoghi non aperti al pubblico o a beni architettonici-archeologici difficili da raggiungere perché localizzati in luoghi inaccessibili o in regioni del mondo politicamente instabili. La generazione di tour virtuali, quindi, permette di esplorare, navigare e interrogare in modo personale e secondo i propri interessi i luoghi di interesse. Trattasi di un modello relativamente innovativo di comunicazione, uno strumento per approfondire e allo stesso tempo comunicare informazioni di vario genere (storico o tecnico), a diversi livelli di accessibilità (esperti o anche solo a turisti).
Ovviamente, questi strumenti, non si pongono come sostituti di una visita in loco, ma sicuramente ne aumentano la loro stessa comprensione così come stimolano la curiosità. Risulta pertanto sempre più necessario un approccio di tipo multidisciplinare in cui l'aspetto scientifico dialoghi ed entri in armonia con l'aspetto umanistico, con la finalità di trasmettere non solo dati metrici ma anche informazioni complesse (spesso difficili da trasferire con le classiche rappresentazioni grafiche). Un altro aspetto analizzato, frutto delle nuove possibilità offerte dalla fotogrammetria, è l'uso di tecnologie low-cost per

l'acquisizione di modelli infografici caratterizzati sempre da affidabilità certa. In particolare, l'attenzione è stata rivolta alla close range photogrammetry applicata al rilievo di una singola torre.
Attraverso l'applicazione della *teoria degli errori* è stato, infatti, possibile valutare l'accuratezza raggiungibile nell'implementazione di alcuni principali software oggi presenti sul mercato e di due differenti tipologie di hardware (fotocamera reflex e compatta). I risultati così ottenuti sono stati poi ulteriormente comprovati con il *test dei valori predittivi*. Come già anticipato nell'overview, si tratta di una metodologia innovativa per il campo del rilievo dell'architettura di tipo nominale qualitativo dicotomico. L'implementazione di tale test si è dimostrato di notevole utilità al fine di calcolare e valutare in termini probabilistici i possibili errori commessi nel confronto e quindi nel valutare la bontà di quanto realizzato.
Le osservazioni scaturite dall'analisi delle diverse applicazioni utilizzate, hanno permesso di validare i risultati che si caratterizzano per una sempre maggior 'accettabilità': segnaliamo, ad esempio, il software gratuito Recap Photo, con una completa automazione nel processo che però ad oggi non assicura la possibilità di esportare modelli utili per successivi approfondimenti. I dati così ottenuti, infatti, sono adatti maggiormente per la generazione di modelli con finalità di visualizzazione e di condivisione sul web, ciò anche per la minore dimensione in termini di occupazione di massa dei dati e migliore gestibilità.
Il numero dei punti eccedenti la deviazioni standard – calcolato sulle coordinate *x* e *y* di 73 punti individuati sulle diverse ortofoto generate e maggiormente approfondito nel Capitolo 7 – risulta congruente con PhotoScan. Tuttavia la validazione del test ha sottolineato un *Valore Predittivo Negativo* (sia per gli assi *x* che *y*) minore rispetto a quelli nell'ambiente software assunto come riferimento, ovvero rispettivamente il 70% e 64% circa di possibilità di non restituire errori, quando gli analoghi valori di PhotoScan si attestano al 78% e 75%. A livello tridimensionale il confronto DEM dei due modelli restituisce una curva di Gauss con un valore medio di scostamento di circa 0,024 m e una *deviazione standard* di 0,087 m.
Diversamente, quando l'implementazione ha riguardato un hardware low-cost, come il caso dell'uso di fotocamera compatta applicata al rilievo architettonico, i risultati perseguiti sono risultati competitivi, con scostamenti minimi rispetto a quando ottenibile con il ricorso a strumenti specifici e dedicati. Nel caso in esame, ad esempio, la curva di Gauss ottenuta da questo nuovo confronto, restituisce un valore medio di scostamento di 0,0013 m con il 14% dei punti aventi una distanza, in valore assoluto, maggiore della deviazione standard (pari a 0,074 m).
A livello più generale, al fine di garantire risultati migliori dal paradigma fotogrammetrico, come risaputo, sarebbe opportuno procedere attraverso

l'integrazione delle tecniche attualmente disponibili; essere in grado di perseguire questo obiettivo, con costi non eccessivi, rappresenterebbe un ottimo traguardo per la protezione del patrimonio e, soprattutto, per quelle architetture 'nascoste' di cui i nostri territori sono ricchi.

Nel caso delle torri oggetto di studio, infatti, nonostante i vasti studi storici già condotti da molti studiosi, le stesse continuano a versare in uno stato che potremmo definire di abbandono grafico, ovvero con pochissime informazioni tecniche e in assenza di rilievi precisi. L'uso delle tecnologie low-cost potrebbe ripristinare l'interesse, sia pubblico sia privato, verso possibili e auspicabili interventi di restauro, da progettare e mettere in essere con un rigoroso approccio multidisciplinare. Così la storia dell'architettura, il disegno e il restauro architettonico, ristabilirebbero non solo l'aspetto tangibile – di questi manufatti, così come di altri meno noti –, ma anche l'identificazione della nostra cultura, storia e territorio.

Essential bibliography

Arnaud F., (2007). *Panoramic Photography: from Composition and Exposure to Final Exhibition*. Taylor & Francis, 2007.

Baltsavias E.P., (1999). A comparison between photogrammetry and laser scanning. In: *ISPRS Journal of Photogrammetry and Remote Sensing*, Vol.54, pp.83-94.

Barba S., (2008). *Tecniche digitali per il rilievo di contatto*. Salerno (italy) CUES, 2008.

Barba S., Fiorillo F., Sánchez Rivera J.I., (2010). La propagazione dell'errore medio della media nei fotopiani. In: *Nuevos medios gráficos, nueva arquitectura. XIII international conference of Expresión Gráfica Arquitectónica*. Valencia (Spain), Universitat Politècnica de València, 2010, pp. 71-75.

Barba S., Fiorillo F., Morena S., Giordano M., (2014). National & International UID Portfolio. In: *P. Giandebiaggi, A. Zerbi (Eds) AA.VV. Italian Survey. Roma: ARACNE EDITRICE SRL*, 2014.

Barba S., Lomónaco P., (2016). Introducción al relevamiento digital. In A&P CONTINUIDAD, Vol. 4, 2016, pp. 79-91.

Barba S.; M. A. Mage, (2014). Evaluación ex-ante y ex-post de la precisión de un proyecto fotogramétrico. In: *Lomonaco H. C. (Eds) V Congreso Internacional de Expresión Gráfica en Ingeniería, Arquitectura y Carreras afines, EGraFIA 2014*. Rosario (Argentine), 2014, pp. 548-557.

Barbato D., Morena S., (2016). Infographic techniques for the representation of marginal buildings of Salerno coast. In: *Bertocci S. (Eds) The reasons of drawing. Thought, Shape and Model in the Complexity Management. XIII Congresso UID, Firenze (Italia)*. Rome (Italy), Gangemi Ed, 2016, pp. 69-73.

Barbato D., Morena S., (2017). BIM and low-cost survey techniques for the preservation of building heritage, In: *Convegno Internazionale e Interdisciplinare IMG2017*. Bressanone (Italy), MDPI AG, 2017.

Bitelli G., (2002). Moderne tecniche e strumentazioni per il rilievo dei Beni Culturali. In: *VI Conferenza Nazionale ASITA, IX-XXIV*, Perugia (Italy), 2002, Vol. I, pp. 9-24.

Bixio A., (2008). *Torri di mare ed osservatori di paesaggi costieri*, Potenza (Italy), Grafie, 2008.

Boehler W., Marbs A., (2004). 3D scanning and photogrammetry for Heritage recording: a comparison. In: *XXII international conference on Geoinformatics - Geospatial Information Research: Bridging the Pacific and Atlantic*. Sweden, 2004.

Cardaci A., Versaci A., (2013). L'innovazione nel rilievo fotografico per la conoscenza, la documentazione e la fruizione dei beni culturali. In *Rodríguez Navarro P., Disegnare con la fotografia digitale* Vol. 6, n. 12, 2013, pp.1-10.

Cardone V., (1993). Tipologia e morfologia delle torri in Campania. Studio puntuale sul riuso delle emergenze fortificate. In: *Tipologia e morfologia delle torri in Campania. Studio puntuale sul riuso delle emergenze fortificate. Colloqui internazionali castelli e città fortificate, Palmanova*. Udine (Italy) Università degli Studi di Udine, 1993, pp.361-371.

Cardone V., (1998). Sul disegno delle torri costiere del Regno di Napoli. In: *De' castelli di pietra e di ... cristallo, Colloqui internazionali castelli e città fortificate, Tricesimo*. Udine (Italy), Università degli Studi di Udine, 1998, pp.107-113.

Cardone V.; Carluccio C., (1999). Il rilievo delle torri costiere del salernitano. In: *AA.VV. Emergenza Rilievo*. Rome (Italy), Edizioni Kappa, 1999, pp.169-193.

Cisternino R., (1977). *Torri costiere e torrieri del Regno di Napoli: 1521-1806*. Rome (Italy), Istituto italiano dei castelli, 1977.

Cueli Lopez J. T., (2011). *Fotogrametría práctica. Tutorial Photomodeler.* Cantabria (Spain), Tantin , 2011.

Faglia V., Mazzon L., (1986). *24 Restauri di Torri Costiere: pianificazione interregionale per il recupero delle torri costiere del Regno di Napoli - Catalogo automatico di valutazione degli oneri di restauro per il riuso*. Rome (Italy), Istituto italiano dei castelli, 1986.

Fangi G., (2017). *The book of sfherical photogrammetry*. Berlin (Germany), Ediz. Accademiche Italiane, 2017.

Fino L. (1995). *La Costa d'Amalfi e il Golfo di Salerno (da Scafati a Cava da Amalfi a Vietri da Salerno a Paestum) disegni acquarelli stampe e ricordi di viaggio di tre secoli*. Naples (Italy), Grimaldi & C. Editori, 1995.

Fiorillo F., Morena S., (2014). Aplicación en 123D Catch para un nuevo enfoque a la fotogrametría low-cost. In: *Tordesillas A. A. (Eds), LDL-C: Levantamiento Digital Low-Cost, Valladolid (Spagna)*. Ediciones Universidad De Valladolid, 2014.

Filangieri G., (1883). *Documenti per la storia, le arti e le industrie delle provincia napoletane.* Naples (Italy), Tipografia dell'accademia reale delle scienze, 1883.

Giribet J., (2011). La fotografia de molt alta resolució aplicada a la pintura mural, In *Revista cultural de l'Urgell*, 2011, pp. 200-207.

Hogg I. V., (1982). *Storia delle fortificazioni*. Novara (Italy), Istituto geografico De Agostini, 1982.

Iennaco G. *Le 99 Torri delle Coste Salernitane. I Principi e le loro monetazioni. La lotta contro i Saraceni*. Fisciano (Italy), Edizioni Sessa.

Inzerillo L., Santagati C., Di Paola F., (2013). Image-based modeling techniques for architectural heritage 3d digitalization: limits and potentialities. In: *XIV international CIPA symposium*. Strasbourg (French), 2013, pp. 555-560.

Jacobs C., (2004). *Interactive Panoramas: Techniques for Digital Panoramic Photography*. Berlin (Germany), Springer, 2004.

Kraus K., (1998). *Fotogrammetria vol.1 – Teoria ed applicazioni. Traduzione ed ampliamenti di Sergio Dequal*. Torino (Italy), Levrotto & Bella, 1998.

Lowe D. G., (2004). Distinctive Image Features from Scale-Invariant Keypoints. In: *Iternational Journal of Computer Vision*. Vol. 60, Issue 2. Netherlands, Kluwer Academic Publishers, 2004, pp. 91-110.

Luhmann T., Robson S., Kyle S., Harley I., (2006). *Close Range Photogrammetry. Principles, Methods and Applications*. Caithness (Scotland), Whittles Publishing, 2006.

McGlone J. C. (Eds), (2013). *Manual of Photogrammetry*. ASPRS, 2013

Miccio G., (1991). Alcune considerazioni sul sistema di difesa costiera di Camerota. In: *Castelli e città fortificate. Storia recupero valorizzazione*. Udine (Italy) Coacem, 1991.

Morena S., (2015). The virtual reconstruction of the minaret of Mansourah mosque (Algeria). In: *Digital Heritage International Congress 2015*. Granada (Spain) IEEE, 2015, pp. 131-134.

Morena S., Barba S., Tordesillas A.A., (2014). Fotogrammetria e tecnologia IR per un rilievo digitale low-cost della scultura "Torso", di Eduardo Chillida. In: *AA.VV. LDL-C: Levantamiento Digital Low-Cost*, Valladolid (Spain) Ediciones Universidad De Valladolid, 2014, pp. 67-80.

Morena S., Fiorillo F., (2014). Un corretto approccio alle tecniche di fotogrammetria low-cost: il caso di 123D Catch, In: *Lomonaco H. C. (Eds) EGraFIA 2014. V Congreso Internacional De Expresión Gráfica, XI Congreso Nacional de Profesores de Expresión Gráfica en Ingeniería, Arquitectura y Áreas afines.* Rosario (Argentine). Salerno (Italy) CUES, 2014, pp. 580-584.

Morena S., Barba S., Merino Gómez E., Sánchez Rivera J. I., 2017. The technologies of architectural survey: a new comparison based on the tower of Sotillo de la Ribera, Burgos (Spagna). In: *Amoruso G. (Eds) Putting Tradition into Practice: Heritage, Place and Design, INTBAU.* Milan (Italy), Spriger, 2017, pp. 475-484.

Pasanini O., (1926). Costruzione generale delle torri marittime ordinata dalla R. Cort di Napoli nel sec. XVI. In: *AA.VV. Studi di storia napoletana in onore di Michelangelo Schipa*. Naples (Italy), I.T.E.A., 1926.

Pignatelli G., Programmi difensivi vicereali e architetture fortificate sulla costa amalfitana. In: *Gambardella A. e Jacazzi D. (Eds) Archihitettura del classicismo tra Quattrocento e Cinquecento. Campania Ricerche*. Rome (Italy), Gangemi, 2007.

Remondino F., (2011). *Heritage Recording and 3D Modeling with Photogrammetry and 3D Scanning*. Remote Sensing, Vol 3, 2011, pp. 1104-1138.

Ricciardi M., (1998). *La costa d'Amalfi nella pittura dell'ottocento*. Salerno (Italy), De Luca Editore, 1998.

Russo F., (2001). *Le torri anticorsare vicereali. Con particolare riferimento a quelli della costa campana. S.l.* Caserta (Italy), Istituto Italiano dei Castelli, 2001

Russo F., (2002). *Le torri vicereali anticorsare della costa d'Amalfi. Immagini e suggestioni della guerra di corsa.* Naples (Italy), Centro di cultura Amalfitana, 2002

Russo F., (2009). *Le torri costiere del regno di Napoli. La frontiera marittima e le incursioni corsare tra il XVI ed il XIX secolo*. Naples (Italy), Edizioni Scientifiche e Artistiche, 2009.

Russo M., Remondino F., Guidi G., (2011). *Principali tecniche e strumenti. per il rilievo tridimensionale in ambito archeologico*. Archeologia e Calcolatori, 2011.

Santoro L., (2012). *Le torri costiere della Provincia di Salerno: paesaggio, storia e conservazione*. Salerno (Italy), Paparo edizioni, 2012.

Santoro L., *Fortificazioni della Campania Antica. Contributo alla conoscenza dei Beni Culturali della Regione*

Sánchez Rivera J.I., (2004). La emocionante evolución de la fotografía. In: *La audiencia imaginaria 3*. Valladolid (Spain) Universidad de Valladolid, 2004.

Sánchez Rivera J. I., Merino Gómez E., Morena S., Barba S., 2014. Documentación gráfica de la iglesia de Santa Águeda en Sotillo de la Ribera (Spagna). In: *Bertocci S., Van Riel S. (Eds) REUSO. La cultura del restauro e della valorizzazione. Temi e problemi per un percorso internazionale di conoscenza. ReUSO 2014, II Convegno Internazionale sulla documentazione, conservazione e recupero del patrimonio architettonico e sulla tutela paesaggistica. La cultura del restauro e della valorizzazione, temi e problemi per un percorso internazionale di conoscenza.* Firenze (Italy). Alinea Editrice, 2014, pp. 1247-1252.

Sebastiano V., (2006). *L'architettura fortificata nel Cilento e nel Vallo di Diano*. Salerno (Italy) Minima menabò, 2006.

Soprintendenza ai beni ambientali, architettonici, artistici e storici delle province di Avellino e Salerno. Assessorato ai beni culturali, (1994). T*ra il Castello e il Mare: l'immagine di Salerno capoluogo del Principato*. Naples (Italy), Fausto Fiorentino, 1994.

Talenti S., Morena S., (2016). Da Positano a Sapri: la rete di "sguardi" del sistema difensivo costiero. In: *Verdiani G. (Eds), Defensive Architecture of the Mediterranean XV to XVIII Centuries. International Conference on Modern*

Age fortifications of the Mediterranean coast, FORTMED. Florence (Italy), Didapress, 2016, pp. 169-176.

Triggs B., McLauchlan P. F., Hartley R. I., Fitzgibbon A. W., (1999). Bundle Adjustment – A Modern Synthesis. In: B. Triggs, A. Zisserman, R. Szeliski (Eds) *Vision Algorithms: Theory and Practice.* Corfu (Greece)*,* Springer, 2000, pp. 298-372

Vassalluzzo M., (1969). *Castelli torri e borghi della costa cilentana*. Salerno (Italy), Pepe, 1969.

Verhoeven Geert, (2016). Basics of photography for cultural heritage imaging. In: *Remondino F., Efstratios S. 3D Recording, Documentation and Management of Cultural Heritage*. Whittles Publishing, 2016, pp.127-251.

Acknowledgment

I am grateful to all the people who have helped and supported me during these three years of research in particular I want to thank:
Carla Ferreyra
Davide Barbato,
Domenico Federico,
Elvira Scibelli,
Fausta Fiorillo,
Ida Maria Morena,
Lucas Fabian Olivero,
Marco Limongiello,
Michele Calandriello,
Michele Morena,
Photis Patonis,
Santoro Lorenzo,
Tomas Martinez Chao,
and all the staff of the State Archive of Salerno, National Library of Naples, Multimedia Library Arturo Loria of Carpi and Library delle Arti of Reggio Emilia.